

Appendix A

Sample Calculations

Rock D50 on the South Top, Side , and Apron

Scour Depth on the South

Size side slope riprap using the Abt and Johnson Method (1991)
 For the PMP, the requirement is that the safety factor, S, be greater than 1.
 The top slope RipRap is sized with the safety factor method.
 Only marginal exceedance is required for safety factor.

Enter Data Here		Then	
Maximum Flow Length on Top (ft)	1292		
Slope on the Top of Cell (ft/ft)	0.02		
Length of the Side Slope (ft)	176		
Side Slope (ft/ft)	0.2		

Results are Below

Don't enter any data below this point !!!

Maximum Flow Length on Top (ft)	1292	Length of the Side Slope (ft)	176	Tc(minutes)		
	Slope on the Top of Cell (ft/ft)		0.02	Side Slope (ft/ft)	0.2	Top
				Kirpich	8.75	0.78
				SCS	8.76	0.78
				B&O	9.87	2.36
				Mean	9.12	1.30
				Top + Side	10.43	
				q Top(cf/ft-sec)	0.982	x3 2.95
				q Side(cf/ft-sec)	1.016	x3 3.05

Use Angular Riprap with a D50 of **1.8** inches on the top slope
 Use Angular Riprap with a D50 of **5.8** inches on the side slope
 Use Angular Riprap with a D50 of **11.6** inches on the apron.
 Minimum apron rock depth is **34.7** inches
 and minimum width of apron is **9.6** feet

For flow in cfs/ft width use with i(inches/hr), L(ft) is the flow path length
 This is almost the rational formula but is more theoretically based.

$$q = \frac{CiL}{43,200}$$

Find the time of concentration using three formulas and take the mean.

	Tc for Top of Cell		Tc for Side Slope	
	Feet	Miles	Feet	Miles
Maximum Flow Length	1292	0.2447	176	0.0333
Slope of watershed =	0.02		0.2	
Delta H =	25.8 feet		35.2 feet	

Kirpich(1940) $T_c = \frac{0.0078L^{0.377}}{S^{0.385}}$ 8.75 minutes 0.78 minutes

SCS $T_c = \left[\frac{11.9L^3}{H} \right]^{0.85}$ 8.76 minutes 0.78 minutes

Brant & Oberman $T_c = C \left[\frac{L}{S_i^2} \right]^{(X)}$ 9.87 minutes 2.36 minutes

Mean Tc 9.12 minutes 1.30 minutes

Combined Tc Top and Side 10.43 minutes

Unit Weight of Water 62.4
 Specific Gravity of Rock 2.65

1 Hour PMP = 8.2 inches for 1 square mile watershed

9.12 minute PMP = 60.9% of 1 hour = 4.99 inches
 10.43 minute PMP = 64.6% of 1 hour = 5.30 inches

Set up Solver

D ₅₀	1.8 inches	0.1468 feet
S _s	2.65 specific gravity	
Gamma	62.4 lb/cf	
Safety Factor	1.01	
Alpha	1.146 degrees	
Phi	37 degrees	
n	0.0268 manning	
y	0.556 ft	
q	2.95 cfs	
Tau ₀	0.6934406	
Slope	0.02 ft/ft	
Eta	0.9634	
Velocity (fps)	5.30	

For Rock on top Slope
 Rainfall Intensity = 32.84 inches/hour

Max Q/ft width = 0.982 cfs/ft
 Multiply by Concentration Factor of 3 2.95 cfs/ft

Rock size on top slope by Safety Factor Method

$$S = \frac{\cos \alpha \tan \phi}{\eta \tan \phi + \sin \alpha}$$

where $\eta = \frac{21\tau_o}{(S_s - 1)\gamma D}$ and $\tau_o = \gamma S'$

For Rock on Side Slope
 Rainfall Intensity = 30.48 inches/hour

Max Q/ft width = 1.016 cfs/ft
 Multiply by Concentration Factor of 3 3.05 cfs/ft
 Multiply by stone movement to stone failure ratio = 1.35 4.11 cfs/ft

For side Slope D50 = 5.8 inches

Appendix B

Reference Material

Safety Factors Method

Overtopping Flow

Toe of Embankments

Culvert Scour

Interstitial Flow

JOURNAL OF THE HYDRAULICS DIVISION

SAFETY FACTORS FOR RIPRAP PROTECTION^a

By Michael A. Stevens,¹ Daryl B. Simons,² F. ASCE,
and Gary L. Lewis,³ A. M. ASCE

INTRODUCTION

The safety factor for rock riprap is defined as the ratio of the moments of forces resisting rotation of the rock particle out of the riprap blanket to the moments tending to dislodge the particle out of the riprap layer into the flow. The critical condition is the flow for which incipient motion occurs. At the critical condition, the riprap particles have a safety factor of unity. If the safety factor is greater than one, the riprap is considered safe from failure; if the safety factor is less than one, rocks are washed from the riprap layer and failure of the protection may occur. The safety factor for riprap protection is analogous to the safety factor employed in structural design. Incipient motion conditions for rock riprap correspond to yield stress conditions in structural members.

The equations describing safety factors for riprap protection are based on theoretical considerations and existing empirical information. Shield's criteria for incipient particle motion as modified by Gessler (9) is employed. Hydrodynamic drag of the fluid on the rock is considered in the same manner as employed by Lane (12). The hydrodynamic lift of the fluid on the rock (5,8) is included in the analysis. The magnitude of the lift force is proportional to the magnitude of the drag force, but the lift force acts normal to the drag force. This difference in direction of force is important in analyzing stability of particles on side slopes (6). The stability of the particle is obtained from its submerged weight and the angle of repose. The particle stability analysis is similar to that made by Campbell (3) except that herein, the safety factor term is added.

Safety factors in riprap protection design are employed for two purposes:

Note.—Discussion open until October 1, 1976. To extend the closing date one month, a written request must be filed with the Editor of Technical Publications, ASCE. This paper is part of the copyrighted Journal of the Hydraulics Division, Proceedings of the American Society of Civil Engineers, Vol. 102, No. HY5, May, 1976. Manuscript was submitted for review for possible publication on November 26, 1974.

^a Presented at the July 15-19, 1974, ASCE/EIC/RTAC Joint Transportation Engineering Meeting, held at Montreal, Canada.

¹ Assoc. Prof., Dept. of Civ. Engrg., Colorado State Univ., Fort Collins, Colo.

² Assoc. Dean for Research and Prof. of Civ. Engrg., Colorado State Univ., Fort Collins, Colo.

³ Assoc. Prof., Dept. of Civ. Engrg., Univ. of Nebraska, Lincoln, Neb.

(1) The safety factor can be used to assess the merits of a particular riprap design; and (2) the safety factor can be used to evaluate different riprap design methods that have been recommended in the technical literature. Illustrations of riprap design and comparisons with recommended design methods are presented.

RIPRAP STABILITY ANALYSIS

In the absence of waves and seepage, the stability of rock riprap particles on a side slope is a function of: (1) The magnitude and direction of the stream velocity in the vicinity of the particles; (2) the angle of the side slope; and (3) the characteristics of the rock including the geometry, angularity, and density.

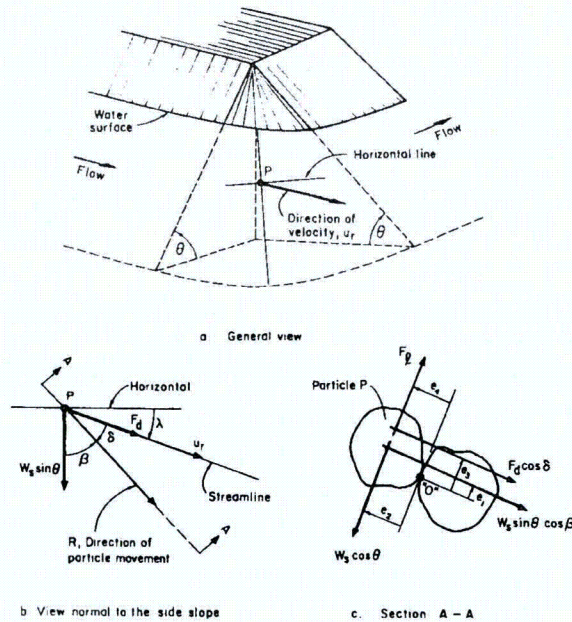


FIG. 1.—Diagrams for Riprap Stability Analysis

The functional relations between the variables are developed subsequently. This development closely follows those given by Stevens and Simons (20) and Lewis (13).

Oblique Flow on Side Slope.—Consider flow along an embankment as shown in Fig. 1. The fluid forces on a rock particle identified as *P* in Fig. (1a) result primarily from fluid pressures around the surface of the particles. Lift force, F_l , is defined herein as the fluid force normal to the plane of the bank. The lift force is zero when the fluid velocity is zero. Drag force, F_d , is defined as the fluid force acting on the particle in the direction of the velocity field in the vicinity of the particle. The drag force is normal to the lift force and

is zero when the fluid velocity is zero. The remaining force is the submerged weight of the rock particle, W_s .

Rock particles on side slopes tend to roll rather than slide, so it is appropriate to consider the stability of rock particles in terms of moments about the point of rotation. In Fig. 1(b) the direction of movement is defined by vector **R**. The point of contact about which rotation in the **R** direction occurs is identified as point "0" in Fig. 1(c).

Forces acting in the plane of the side slope are F_d and $W_s \sin \theta$ as shown in Fig. 1(b). The angle θ is the side slope angle. The lift force acts normal to the side slope and the component of submerged weight $W_s \cos \theta$ acts in the direction as shown in Fig. 1(c).

At incipient motion, there is a balance of moments about the contact point "0" such that

$$e_2 W_s \cos \theta = e_1 W_s \sin \theta \cos \beta + e_3 F_d \cos \delta + e_4 F_l \dots \dots \dots (1)$$

Moment arms $e_1, e_2, e_3,$ and e_4 are defined in Fig. 1(c) and angles δ and β are defined in Fig. 1(b).

The factor of safety, *S*, of particle *P* against rotation is defined as the ratio of the moments resisting particle rotation out of the bank to the submerged weight and fluid force moments tending to rotate the particle out of its resting position. Accordingly

$$S = \frac{e_2 W_s \cos \theta}{e_1 W_s \sin \theta \cos \beta + e_3 F_d \cos \delta + e_4 F_l} \dots \dots \dots (2)$$

If there is no flow and the side slope angle is increased to the angle of repose ϕ for the rock particles, the safety factor becomes unity. Then, $S = 1.0$; $\theta = \phi$; $\beta = 0^\circ$; $\lambda = 0^\circ$; and $\delta = 90 - \lambda - \beta = 90^\circ$ [see Fig. 1(b)]. With these values, Eq. 2 reduces to

$$\tan \phi = \frac{e_2}{e_1} \dots \dots \dots (3)$$

that is, the ratio of the moment arms, e_2/e_1 , is characterized by the natural angle of repose, ϕ . Further, it is assumed that the ratio, e_2/e_1 , is invariant to the direction of particle motion indicated by angle β .

Dividing both numerator and denominator by $e_1 W_s$, Eq. 2 is transformed to

$$S = \frac{\cos \theta \tan \phi}{\eta' \tan \phi + \sin \theta \cos \beta} \dots \dots \dots (4)$$

in which $\eta' = \frac{e_3 F_d \cos \delta + e_4 F_l}{e_2 W_s} \dots \dots \dots (5)$

The variable η' is called the stability number for particles on the embankment side slope.

The angle λ shown in Fig. 1(b) is the angle between the horizontal and the velocity vector (or drag force) measured in the plane of the side slope. Then

$$\delta = 90 - \lambda - \beta \dots \dots \dots (6)$$

It is assumed that moments of the drag force, F_d , and the component of

submerged weight, $W_s \sin \theta$, normal to path R are balanced so that the direction of particle motion will be along R . Thus

$$e_3 F_d \sin \delta = e_1 W_s \sin \theta \sin \beta \dots\dots\dots (7)$$

It follows then from Eqs. 6 and 7 that

$$\sin \beta = \frac{e_3 F_d \sin \delta}{e_1 W_s \sin \theta} = \frac{e_3 F_d (\cos \lambda \cos \beta - \sin \lambda \sin \beta)}{e_1 W_s \sin \theta} \dots\dots\dots (8)$$

$$\text{or } \tan \beta = \frac{\cos \lambda}{\frac{e_1 W_s}{e_3 F_d} \sin \theta + \sin \lambda} \dots\dots\dots (9)$$

The stability number η for particles on a plane bed ($\theta = 0$) with $\delta = 0$ would be

$$\eta = \frac{e_3 F_d}{e_2 W_s} + \frac{e_4 F_l}{e_2 W_s} \dots\dots\dots (10)$$

according to Eq. 5. Also, Eq. 4 becomes

$$S = \frac{1}{\eta} \dots\dots\dots (11)$$

for flow over a plane flat bed.

Both the hydrodynamic drag and lift on the particle are related to the square of the fluid velocity in the vicinity of the particle and to the exposed area of the particle (8,20). The tractive force on the bed is also directly related to the square of the fluid velocity, or

$$F_l = c_1 k^2 \tau_s \dots\dots\dots (12)$$

$$\text{and } F_d = c_2 k^2 \tau_s \dots\dots\dots (13)$$

in which τ_s = the average tractive force on the plane containing the particle, P ; and k = the diameter of the rock particle. Coefficients c_1 and c_2 are dependent on the exposed area of the particle, the coefficients of drag and lift, and the relation between velocity and tractive force.

The submerged weight of the particle can be written (20) as

$$W_s = c_3 (S_s - 1) \gamma k^3 \dots\dots\dots (14)$$

in which c_3 is a coefficient depending only on the shape of the particle; P ; S_s = the specific weight of the rock; and γ is the unit weight of water.

Substitution of Eqs. 12, 13 and 14 into Eq. 10 we obtain

$$\eta = \frac{c_1 e_4 + c_2 e_3}{c_3 e_2} \frac{\tau_s}{(S_s - 1) \gamma k} \dots\dots\dots (15)$$

The term $\tau_s / (S_s - 1) \gamma k$ is known as Shield's parameter.

Incipient motion conditions for flow over a plane flat bed give $S = 1.0$ by definition so from Eq. 11, $\eta = 1.0$. When flow along the bed is fully turbulent, Shield's parameter for incipient motion has the value 0.047 according to Gessler

(9). It follows then that

$$\frac{c_1 e_4 + c_2 e_3}{c_3 e_2} = \frac{1}{0.047} = 21 \dots\dots\dots (16)$$

For flow conditions other than incipient Eq. 15 becomes

$$\eta = \frac{21 \tau_s}{(S_s - 1) \gamma k} \dots\dots\dots (17)$$

For convenience, let

$$M = \frac{e_4 F_l}{e_2 W_s} \dots\dots\dots (18)$$

$$\text{and } N = \frac{e_3 F_d}{e_2 W_s} \dots\dots\dots (19)$$

In terms of these new variables, Eq. 5 becomes

$$\eta' = M + N \cos \delta \dots\dots\dots (20)$$

and Eq. 10 becomes

$$\eta = M + N \dots\dots\dots (21)$$

Thus η' and η are related by

$$\frac{\eta'}{\eta} = \frac{\frac{M}{N} + \cos \delta}{\frac{M}{N} + 1} \dots\dots\dots (22)$$

The problem is to select the proper value of the ratio M/N so that the stability factor on a slide slope η' can be related to the stability factor on a plane horizontal bed, η , which in turn is related to the Shield's parameter. The assumption that the drag force, F_d , is zero means M/N is infinite. β is zero, and $\eta' = \eta$. The assumption of zero lift force F_l means M/N is zero and $\eta'/\eta = \cos \delta$. For finite values of lift and drag forces, stability factor ratios are between the limits 0 and $\cos \delta$.

In considering incipient motion of riprap particles, the ratios, F_l/F_d and e_4/e_3 , depend on the turbulent conditions of the flow and the interlocking arrangement of the rock particles. To facilitate the analysis, the product of F_l/F_d and e_4/e_3 is assumed to be

$$\frac{M}{N} = \frac{e_4 F_l}{e_3 F_d} = 1 \dots\dots\dots (23)$$

This value was chosen by Stevens and Simons (20) after considering the range of possible values for F_l/F_d and e_4/e_3 and the effect of M/N on the value of the safety factor, S . The safety factor, S , depends on the value of M/N only for flow on side slopes. Otherwise, the value of S is independent of the value chosen for M/N . With $M/N = 1$, Eq. 22 becomes

$$\frac{\eta'}{\eta} = \frac{1 + \cos \delta}{2} \dots \dots \dots (24)$$

or by using Eq. 6

$$\frac{\eta'}{\eta} = \frac{1 + \sin(\lambda + \beta)}{2} \dots \dots \dots (25)$$

In Eq. 9, the term $e_1 W_s / e_3 F_d$ can be written

$$\frac{e_1 W_s}{e_3 F_d} = \frac{e_2 W_s e_1}{e_3 F_d e_2} = \frac{1}{N \tan \phi} \dots \dots \dots (26)$$

according to Eqs. 3 and 19. For $M/N = 1$, Eq. 21 becomes

$$N = \frac{\eta}{2} \dots \dots \dots (27)$$

If we substitute Eqs. 26 and 27 into Eq. 9, the expression for β becomes

$$\beta = \tan^{-1} \left(\frac{\cos \lambda}{\frac{2 \sin \theta}{\eta \tan \phi} + \sin \lambda} \right) \dots \dots \dots (28)$$

In summary, the safety factor for rock riprap on side slopes where flow has a nonhorizontal velocity vector is related to properties of the rock, side slope, and flow by Eqs. 4, 17, 25, and 28.

Given a rock size k of specific weight S_s and angle of repose ϕ and given a velocity field at an angle λ to the horizontal producing a tractive force τ_s on the side slope of angle θ , the set of four equations (Eqs. 4, 17, 25, and 28) can be solved to obtain the safety factor, S . If S is greater than unity, the riprap is safe from failure; if S is unity, the rock is at the condition of incipient motion; and if S is less than unity, the riprap will fail.

Horizontal Flow on Side Slope.—In many circumstances, the flow angularity with the horizontal is small, i.e., $\lambda = 0$. Then Eqs. 25 and 28 reduce to

$$\beta = \tan^{-1} \left(\frac{\eta \tan \phi}{2 \sin \theta} \right) \dots \dots \dots (29)$$

$$\text{and } \eta' = \left(\frac{1 + \sin \beta}{2} \right) \dots \dots \dots (30)$$

When Eqs. 29 and 30 are substituted into Eq. 4, the expression for the safety factor for horizontal flow along a side slope is

$$S = \frac{S_m}{2} [(\xi^2 + 4)^{1/2} - \xi] \dots \dots \dots (31)$$

$$\text{in which } \xi = S_m \eta \sec \theta \dots \dots \dots (32)$$

$$\text{and } S_m = \frac{\tan \phi}{\tan \theta} \dots \dots \dots (33)$$

Department of Energy - Rev 1 - Feb 2008 Final Remedial Action Plan - DOE-EM/GJ1547 - Addendum D - C02 - Page 25

If we solve Eqs. 32 and 33 for η , then

$$\eta = \left(\frac{S_m^2 - S^2}{SS_m^2} \right) \cos \theta \dots \dots \dots (34)$$

The term, S_m , is the safety factor for riprap on a side slope with no flow. Unless flow is up the slope, the safety factor for the riprap cannot be greater than S_m .

Flow on Plane Sloping Bed.—Flow over a plane bed at a slope of α degrees in the downstream direction is equivalent to oblique flow on a side slope with $\theta = \alpha$ and $\lambda = 90^\circ$.

Then, according to Eq. 28, $\beta = 0^\circ$ and from Eq. 25, $\eta' = \eta$. It follows from Eq. 4 that

$$S = \frac{\cos \alpha \tan \phi}{\eta \tan \phi + \sin \alpha} \dots \dots \dots (35)$$

for flow on a plane bed sloping α degrees to the horizontal. Alternatively, solving for η in Eq. 35, we obtain

$$\eta = \cos \alpha \left(\frac{1}{S} - \frac{\tan \alpha}{\tan \phi} \right) \dots \dots \dots (36)$$

Flow on Horizontal Bed.—For fully developed rough turbulent flow over a plane horizontal bed ($\alpha = 0$) of rock riprap, Eq. 35 reduces to

$$S = \frac{1}{\eta} \dots \dots \dots (37)$$

If the riprap particles are at the condition of incipient motion, $S = 1$ so $\eta = 1$ and we revert back to Shield's expression for incipient motion (Eq. 17 with $\eta = 1$).

Relation Between Shear and Velocity.—In order to compare the equations previously developed with those employed by others to design riprap, it is necessary to relate tractive forces acting on the riprap bed or bank to fluid velocities in the vicinity of the riprap. For fully turbulent flow, the relation between the local velocity, u , at distance y above the bed is

$$u = 2.5 u_* \ln \left(30.2 \frac{y}{k} \right) \dots \dots \dots (38)$$

in which u_* is the shear velocity defined as

$$u_* = \left(\frac{\tau_s}{\rho} \right)^{1/2} \dots \dots \dots (39)$$

This velocity distribution equation was derived by Keulegan (11) and was employed by Einstein (7) in his bed-load function research.

If we select the velocity at a distance $y = k$ above the bed as a reference velocity, u_r , then

$$u_r = 2.5 u_* \ln 30.2 = 8.5 u_* \dots \dots \dots (40)$$

Calculation C-02 Project 35DJ2600 Appendix B Page B-5 of 37

The value of the reference velocity, u_r , given by Eq. 40 is the same as that employed by Campbell (3) in the Corps of Engineers' studies of the hydraulic design of rock riprap.

From Eqs. 39 and 40, the relation between u_r and τ_s is

$$\rho u_r^2 = 72 \tau_s \dots \dots \dots (41)$$

This relation is strictly valid only for uniform flow in wide prismatic channels in which flow is fully turbulent. For purposes of riprap design, Eq. 41 can be employed when flow is accelerating, e.g., on the nose of a spur dike. **The equation should not be used in areas where the flow is decelerating or below energy dissipating structures.** In these areas, the shear stress is larger than would be calculated by Eq. 41 because of turbulence in the flow.

Substitution of Eq. 41 into Eq. 17 gives the stability factor

$$\eta = \frac{0.30 u_r^2}{(S_s - 1)gk} \dots \dots \dots (42)$$

The average velocity in the vertical U is given by

$$U = 2.5 u_r \ln \left(12.3 \frac{y_0}{k} \right) \dots \dots \dots (43)$$

in which y_0 = the depth of flow. This equation is the companion to Eq. 38 and was also obtained by Keulegan (11). The ratio of the reference velocity, u_r , to the depth-averaged velocity is

$$\frac{u_r}{U} = \frac{2.5 u_r \ln (30.2)}{2.5 u_r \ln \left(12.3 \frac{y_0}{k} \right)} = \frac{3.4}{\ln \left(12.3 \frac{y_0}{k} \right)} \dots \dots \dots (44)$$

Now the expression for the stability factor, η , can be written in terms of the depth-averaged velocity. From Eqs. 42 and 44

$$\eta = \frac{\epsilon U^2}{(S_s - 1)gk} \dots \dots \dots (45)$$

$$\text{in which } \epsilon = 0.30 \left[\frac{3.4}{\ln \left(12.3 \frac{y_0}{k} \right)} \right]^2 \dots \dots \dots (46)$$

In his study, Search (16) gives the expression

$$\frac{v_s}{V} = \frac{1}{0.958 \log \left(\frac{y_0}{k} \right) + 1} \dots \dots \dots (47)$$

in which v_s = the velocity against the stone; and V = the mean velocity in the channel. This equation can be closely approximated by dividing Eq. 38 by Eq. 43, using the assumption that $u = v_s$ when $y = 0.39k$. The velocity against the stone can, therefore, be considered as the velocity from Eq. 38 at a distance $y = 0.39k$ above the bed.

In wide channels, the depth-averaged velocity and the mean velocity in the channel are nearly equal, i.e., $U \approx V$. Then the velocity against the stone is related to the reference velocity by the expression

$$\frac{u_r}{v_s} = \frac{u_r U}{U v_s} = \frac{3.4 \left[0.958 \log \left(\frac{y_0}{k} \right) + 1 \right]}{\ln \left(12.3 \frac{y_0}{k} \right)} \dots \dots \dots (48)$$

according to Eqs. 44 and 47. For values of y_0/k between 1×10^0 and 1×10^6 , the value of the u_r/v_s is nearly 1.4. Finally, by letting $u_r/v_s = 1.4$ the expression for the stability factor η (Eq. 42) becomes

$$\eta = \frac{0.60 v_s^2}{(S_s - 1)gk} \dots \dots \dots (49)$$

Representative Grain Size.—In studies of scour below culvert outlets, Stevens (21) was able to consolidate a wide range of scour data by employing the expression

$$k = \left(\frac{\sum_{i=1}^{10} d_i^3}{10} \right)^{1/3} \dots \dots \dots (50)$$

for the effective or representative grain size of graded materials. Here: d_i ($i = 1$) = $(d_0 + d_{10})/2$; d_i ($i = 2$) = $(d_{10} + d_{20})/2$; ... d_i ($i = 10$) = $(d_{90} + d_{100})/2$. The terms, $d_0, d_{10}, \dots, d_{100}$, are sieve diameters of the riprap for which 0%, 10%, ..., 100% of the material (by weight) is finer. Eq. 50 is equivalent to determining the arithmetic average of the sum of weights of individual particles. In Stevens' studies (21), the ratio k/d_{50} varied from 1.005–2.25, but normally $k \leq d_{67}$.

SAFETY FACTORS FOR EXISTING DESIGN METHODS

Many methods of designing riprap are available. The developed equations are compared subsequently with methods developed by the Bureau of Public Roads, the Corps of Engineers, the California Division of Highways, the ASCE Task Committee on Sedimentation, the Bureau of Reclamation, and Lane's and Campbell's methods.

Bureau of Public Roads.—Searcy (16) used the 1948 ASCE Subcommittee's summary on slope protection (15) to adopt Fig. 2. The relations shown in Fig. 2 require the velocity against the stone given by Eq. 47 and the median spherical diameter of the rock. Searcy recommended a gradation specification for riprap patterned after gradations recommended by Murphy and Grace (14). These gradations were called the A-rock for which $k/d_{50} = 1.08$ and the B-rock for which $k/d_{50} = 1.36$. Searcy chose the A-rock gradation in formulating his specifications.

Safety factors for the curves in Fig. 2 can be determined in the following manner. The recommended equivalent spherical diameter of the d_{50} rock is 3.75 ft (1.14 m) for $v_s = 24$ fps (7.3 m/s) on a horizontal bed. This diameter

corresponds to $k = 5.1$ ft (1.56 m) if we use the B-rock gradation. The stability factor for this rock and velocity is given by Eq. 49 or $\eta = 1.28$ and from Eq. 37, the safety factor is $S = 0.78$.

If Searcy's recommended gradation (A-rock) is used, $k = 4.1$ ft (1.25 m)

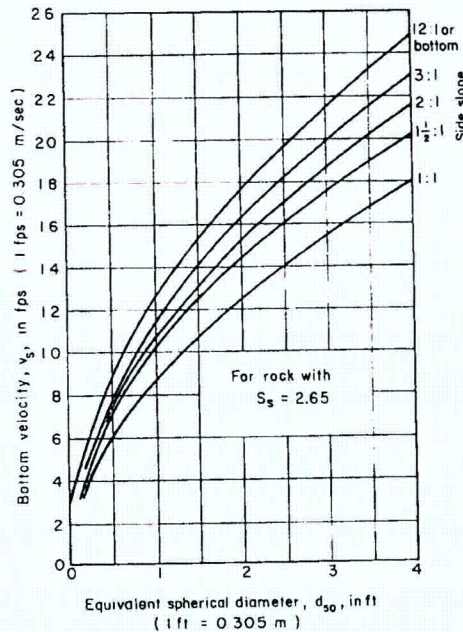


FIG. 2.—Rock Size for Bureau of Public Roads Design

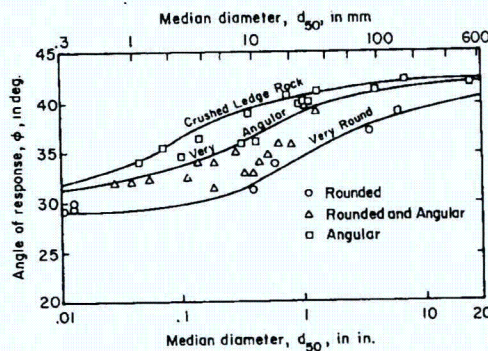


FIG. 3.—Angle of Repose for Dumped Riprap (15)

and $S = 0.63$. For either gradation, the rock sizes obtained from Fig. 2 for flow on a horizontal bed are considered "unsafe" according to the equations presented herein.

On a 2:1 side slope, the B-rock gradation has a safety factor of 0.76 which is obtained in the following manner. For a velocity v_o of 20 fps (6.1 m/s). Fig. 2 specifies a rock size d_{50} of 3.4 ft (1.04 m). With the B-rock gradation $k = 4.6$ ft (1.40 m) and from Eq. 49, $\eta = 0.98$. On a 2:1 side slope with horizontal flows ($\lambda = 0^\circ$), the safety factor is given by Eq. 31. An estimate of the angle of repose can be made by extrapolating information obtained by Simons (18) and given in Fig. 3. With $\phi = 42^\circ$, from Eq. 33 $S_m = 1.80$, from Eq. 32 $\xi = 1.97$, and from Eq. 31 $S = 0.76$. Again, the safety factor is less than unity indicating that rock selected from Fig. 2 is undersized.

In order to have a safety factor greater than unity for the 1:1 side slope curve shown in Fig. 2, the angle of repose for the riprap must be very large. From the 1:1 curve in Fig. 2, a 2.5-ft (0.76-m) diam rock should withstand a bottom velocity of 14 fps (4.3 m/s) on a 1:1 side slope. With the B-rock gradation $k = 3.4$ ft (1.04 m). From Eq. 34, $\eta = 0.65$, and by solving Eq. 34 with $S = 1.0$ we obtain $S_m = 3.52$. As $\tan \phi = S_m \tan \theta$ (from Eq. 33), $\phi = 74^\circ$. To obtain a ϕ this large, the riprap would have to be placed piece by piece by crane or by some other mechanical means. An alternative would be to grout the riprap or to place smaller rock in baskets.

In conclusion, safety factors for the design curves in Fig. 2 are less than unity.

U.S. Army Corps of Engineers Waterways Experiment Station.—The riprap design criteria adopted by the Corps of Engineers (22) is based on Isbash's equation for the movement of stone in flowing water. The equation can be written

$$\frac{U^2}{(S_s - 1)gd_{50}} = 2C^2 \dots \dots \dots (51)$$

and is applicable for flow on plane flat beds. Here C is Isbash's turbulence coefficient.

By comparing this expression with Eq. 45, it is found that

$$\eta = 2\epsilon C^2 \frac{d_{50}}{k} \dots \dots \dots (52)$$

According to the gradation criteria recommended by the Corps of Engineers (22), the representative grain size, k , is not more than 5% greater than d_{50} . Therefore, $k \approx d_{50}$ and $S = 1/2\epsilon C^2$.

The Corps of Engineers uses $C = 1.20$ for applications in which the turbulence level is low. Accordingly, $S = 0.347/\epsilon$. The coefficient ϵ is a function of y_o/k (Eq. 46), and the relation between S and y_o/k for the design equation recommended by the Corps of Engineers is shown in Fig. 4. The safety factor is less than unity for very shallow flows and increases to unity when $y_o/k = 1.92$. For relative depths greater than 1.92, the safety factor is greater than unity.

California Division of Highways.—The California expression (1) for sizing riprap is

$$W = \frac{2 \times 10^{-5} S_s V^6}{(S_s - 1)^3 \sin^3(70^\circ - \theta)} \dots \dots \dots (53)$$

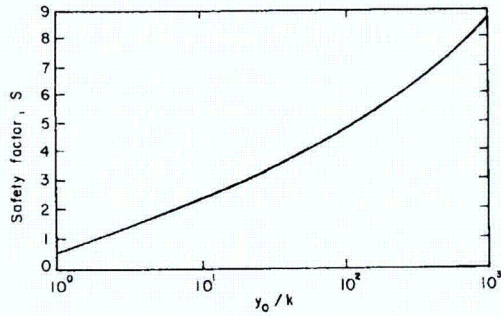


FIG. 4.—Safety Factors for Corps of Engineer's Riprap Design

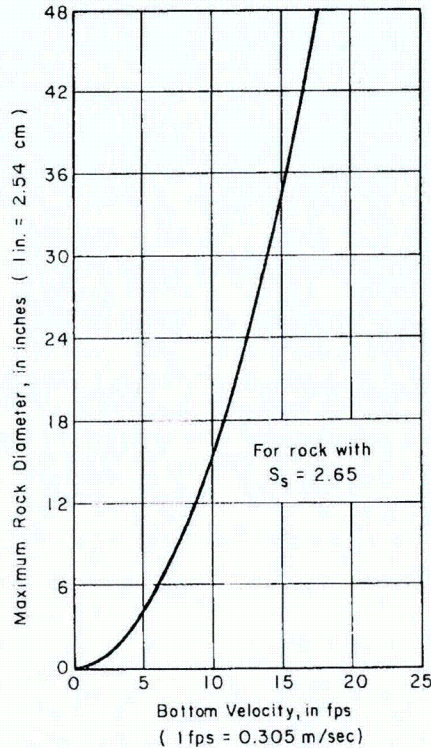


FIG. 5.—Rock Size for Bureau of Reclamation Design

in which W = the minimum weight, in pounds, of the outside stone; and V = the average stream velocity, in feet per second. If we assume $S_s = 2.65$ and that the particles are spheres with diameter d_{50} , then Eq. 53 reduces to

$$\frac{0.27 V^2}{(S_s - 1)gd_{50}} = \sin(70^\circ - \theta) \dots \dots \dots (54)$$

Department of Energy - Rev 1 - Feb 2008 Final Remedial Action Plan - DOE-EM/GJ1547 - Addendum D - C02 - Page 28

for horizontal flow on side slopes. For flow on level beds, Eq. 54 reduces to

$$\frac{0.29 V^2}{(S_s - 1)gd_{50}} = 1 \dots \dots \dots (55)$$

Eq. 55 can be compared directly with Eq. 45 if it is assumed the channel is wide so that $V \approx U$. Then

$$\eta = 3.45\epsilon \frac{d_{50}}{k} \dots \dots \dots (56)$$

$$\text{so } S = \frac{0.29 k}{\epsilon d_{50}} \dots \dots \dots (57)$$

For comparison purposes, if we make $k = 1.2 d_{50}$, then $S = 0.347/\epsilon$ which is the same expression as was obtained in the analysis of the Corps of Engineers' method. The safety factors are given in Fig. 4.

For horizontal flows on side slopes, the comparison is more difficult. The relation between the mean channel velocity and the shear stress or velocity on the side slopes must be established to obtain a safety factor. This relation has been established by Lane (12) and others and depends on the geometry of the channel. As Eq. 54 is based on an average stream velocity, some simplifying assumptions must have been made about the ratio of side slope shear to average shear. The analysis of these assumptions are outside the scope of this paper.

ASCE Task Committee on Preparation of Sedimentation Manual.—This committee (17) has recommended Isbash's formula

$$W_{50} = \frac{4.1 \times 10^{-5} S_s V^6}{(S_s - 1)^3 \cos^3 \theta} \dots \dots \dots (58)$$

for riprap design. Here W_{50} is the weight of the rock with an equivalent spherical diameter d_{50} . Eq. 58 reduces to

$$\frac{0.347 V^2}{(S_s - 1)gd_{50}} = \cos \theta \dots \dots \dots (59)$$

For flow on a horizontal bed ($\theta = 0^\circ$), Eq. 59 becomes

$$\frac{0.347 V^2}{(S_s - 1)gd_{50}} = 1 \dots \dots \dots (60)$$

Eq. 60 can be compared directly with Eq. 45, if it is assumed the channel is wide so that $V \approx U$. Accordingly

$$\eta = 2.88\epsilon \frac{d_{50}}{k} \dots \dots \dots (61)$$

$$\text{so } S = \frac{0.347 k}{\epsilon d_{50}} \dots \dots \dots (62)$$

For comparison purposes, if we make $k = 1.2 d_{50}$, then $S = 0.416/\epsilon$. This

Calculation C-02 Project 35DJ2600 Appendix B Page B-8 of 37

Department of Energy - Rev 1 - Feb 2008 Final Remedial Action Plan - DOE-EM/GJ1547 - Addendum D - C02 - Page 29

safety factor for Isbash's formula is 20% greater for flow on a horizontal bed than that obtained by the California Division of Highways method (1).

Bureau of Reclamation.—The Bureau of Reclamation (10) developed Fig. 5 to determine the maximum stone size in a riprap mixture downstream from stilling basins. If the bottom velocity is assumed equal to the velocity against the stone, v_s , the curve in Fig. 5 can be closely approximated by

$$V_s^2 = 49.1 (S_s - 1) d_{100} \quad (63)$$

The stability factor for the curve in Fig. 5 is determined from Eq. 49 or

$$\eta = 0.915 \frac{d_{100}}{k} \quad (64)$$

and from Eq. 37, the corresponding safety factor for particles on a horizontal bed is

$$S = 1.09 \frac{k}{d_{100}} \quad (65)$$

For comparison purposes, if we make $k = 1.2 d_{50}$, then

$$S = 1.31 \frac{d_{50}}{d_{100}} \quad (66)$$

resulting in the conclusion that the Bureau of Reclamation curve in Fig. 5 provides stable d_{100} riprap sizes on horizontal beds whenever the gradation is selected such that the d_{50} size is greater than $0.76 d_{100}$. For cases other than $k = 1.2 d_{50}$, the riprap is stable when k is greater than $0.92 d_{100}$. Riprap designed from Fig. 5 with a uniform gradation ($k = d_{100}$) would have a safety factor of 1.09.

Lane's Design of Stable Channels.—In his method for designing stable channels in noncohesive materials, Lane (12) employed the expression

$$K = \left(1 - \frac{\tan^2 \theta}{\tan^2 \theta} \right)^{1/2} \cos \theta \quad (67)$$

to relate the stability of materials on a side slope to those on a horizontal bed. The factor K was defined as ". . . the ratio of the tractive force required to start motion on the sloping sides to that force required, in the same material, to start motion on a level surface." Eq. 67 was developed earlier by Carter, Carlson, and Lane (4).

Because $S_m = \tan \phi / \tan \theta$ the expression for K can be written

$$K = \left(1 - \frac{1}{S_m^2}\right)^{1/2} \cos \theta \quad (68)$$

Eq. 68 can be obtained in the foregoing theoretical analysis by assuming that the lift force is zero. In other words, Lane's method does not consider fluid lift forces on the particles. With lift forces included, the equation corresponding to Eq. 67 is obtained from Eq. 34 with $S = 1$, i.e.

$$\eta = \left(1 - \frac{1}{S_m^2}\right) \cos \theta \quad (69)$$

The ratio η/K then reflects the consequence of ignoring lift in a riprap stability analysis. From Eqs. 68 and 69, the ratio is

$$\frac{\eta}{K} = \left(1 - \frac{1}{S_m^2}\right)^{1/2} \quad (70)$$

for the initiation of motion condition and is

$$\frac{\eta}{K} = \left(\frac{S_m^2 - S^2}{S_m^2}\right)^{1/2} \quad (71)$$

for other conditions of horizontal flow along a side slope.

For a given rock material on a given side slope, the ratio, η/K , is the ratio of the computed incipient motion tractive force, τ_s , including lift, to the computed incipient motion shear stress, τ'_s , ignoring lift or, from Eq. 70

$$\frac{\tau_s}{\tau'_s} = \left(1 - \frac{1}{S_m^2}\right)^{1/2} \quad (72)$$

Eq. 72 indicates that neglecting the lift force for flow along a horizontal bed is of no consequence. On a horizontal bed, $S_m = \infty$ and $\tau_s = \tau'_s$. On steep side slopes, S_m is small and Eq. 72 shows that the allowable shear stress would be much lower when lift is included than when lift is ignored.

The conclusion is that lift is an important factor in the stability analysis of particles on steep side slopes. For flow on a level bed, Lane (12) recommended an allowable shear stress

$$\tau_s = 4.8 d_{75} \quad (73)$$

in which d_{75} = the rock size, in feet, for which 75% of the material (by weight) is finer. The units of shear stress are pound per square foot. Eq. 73 was recommended for rock with $S_s = 2.56$, but can be written

$$\tau_s = 0.049 (S_s - 1) \gamma d_{75} \quad (74)$$

for rock with any specific weight. Substitution of Eq. 74 into Eq. 32, the stability number becomes $\eta = 1.03 d_{75}/k$. Using Lane's recommended shear stress, the safety factor on a level bed becomes $S = 0.97 k/d_{75}$. As k is usually slightly less than d_{75} , the safety factor is slightly less than unity. For horizontal flow along a side slope, the safety factor for Lane's design criteria is given by

$$S = \frac{S_m}{2} [(\Omega^2 + 4)^{1/2} - \Omega] \quad (75)$$

$$\text{in which } \Omega = 1.03 \frac{d_{75}}{k} (S_m^2 - 1)^{1/2} \quad (76)$$

The value of the safety factor as determined by Eq. 75 is generally less than unity.

According to the stability analysis presented herein, Lane's design criteria for stable channels yields designs in which particle motion would likely occur on the banks.

Campbell's Analysis.—Campbell (3) employed a reference velocity $u_r = 8.5u_s$ and Isbash's equation to develop the relation

$$\frac{u_r^2}{(S_s - 1)gd_{50}} = 2.94 \dots \dots \dots (77)$$

for stable rock sizes. Eq. 77 corresponds to $\eta = 0.882 d_{50}/k$ and the safety factor for flow on a plane flat bed becomes $S = 1.13 k/d_{50}$. As $k \geq d_{50}$, Campbell's safety factor is always greater than unity for flow on a plane flat bed.

Campbell (3) also derived a method of sizing riprap for side slopes. The derivation is similar to that employed herein. His relations are complex so that no direct comparison can be made. However, according to his example calculation a 1.25-ft (0.38-m) diam riprap size is required on a 6:1 side slope in which $u_r = 14.4$ fps (4.39 m/s). Assuming that flow velocity along the bankline is horizontal, then from Eq. 42, $\eta = 0.937$. The angle of repose for dumped riprap of diameter 1.25 ft (0.38 m) is approx 42° (from Fig. 3). Therefore, from Eqs. 31, 32, and 33, $S_m = 5.40$, $\xi = 5.13$, and $S = 1.015$. That is, the 1.25-ft (0.38-m) diam rock is at the condition of incipient motion.

RIPRAP DESIGN WITH SAFETY FACTORS

The set of equations describing stability of rock riprap permits the use of four possible design options for a fixed set of flow conditions on a side slope or on a plane bed. The options are: (1) For a given rock size and side slope or bed slope, the safety factor can be computed and the design accepted or rejected on the basis of the value of the safety factor; (2) for a given rock size, the side slope or bed slope can be chosen so as to provide a preselected safety factor; (3) for a given side slope or bed slope, the rock size which gives a preselected safety factor can be computed; and (4) for a given safety factor, the proper combinations of rock size and side slope or bed slope can be computed.

Suppose for Option 1 that the flow at point P on the nose of the embankment in Fig. 1 has a velocity $u_r = 6$ fps (1.8 m/s) and is directed down the slope so that $\lambda = 20^\circ$. The embankment side slope is 3:1 or $\theta = 18.4^\circ$. If the embankment is covered with dumped rock having a specific weight, $S_s = 2.65$, and an effective rock size, $k = 1.0$ ft (0.3 m), the safety factor is determined in the following manner.

From Eq. 42, $\eta = 0.203$, and according to Fig. 3 this dumped rock has an angle of repose of approx 35°. Therefore, from Eq. 28, $\beta = 11^\circ$ and from Eq. 25, $\eta' = 0.154$. The safety factor for the rock is given by Eq. 4 or $S = 1.59$. Thus, this rock is more than adequate to withstand the flow velocity.

Because it is easier to compute the safety factor given rock size and side slope, Option 3 is best accomplished by repeating Option 1 over the range of interest for k . The results of such computations (with $\phi = 35^\circ$) are given in Fig. 6 which shows that the incipient motion rock size is approx 0.35 ft (0.11 m) and that the maximum safety factor is less than 2.0 on the 3:2 side slope.

The safety factor of a particular side slope riprap design can be increased by decreasing the side slope angle, θ . If the side slope angle is decreased to

RIPRAP PROTECTION

0°, then Eq. 37 is applicable and $S = 4.93$. The curve in Fig. 7 relates the safety factor and side slope angle of the embankment shown in Fig. 1 [for $\lambda = 20^\circ$, $k = 1.0$ ft (0.305 m) and $u_r = 6.0$ fps (1.8 m/s)]. The curve can be employed to obtain Option 2.

Design Option 4 is difficult to use for oblique flow on side slopes and is,

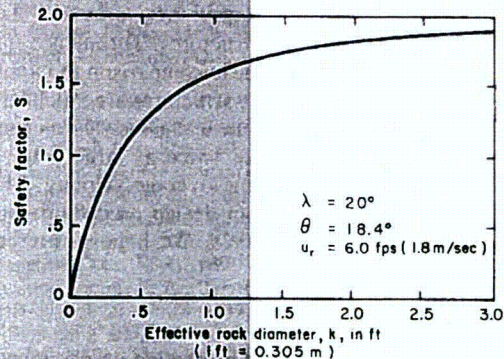


FIG. 6.—Safety Factors for Various Rock Sizes on Side Slope

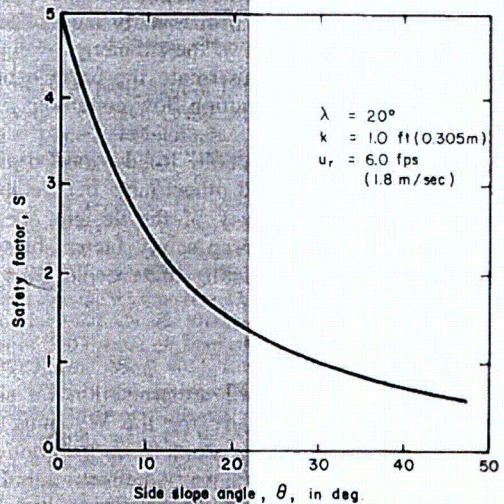


FIG. 7.—Safety Factors for Various Side Slopes

therefore, recommended only if the flow velocity vector on the side slope is nearly horizontal.

The developed equations deal with average values of shear stress and local velocity. Instantaneous values of the shear stress, τ_s , or local velocity, u_r , may be as much as two or three times greater or less than the average value. The fact that instantaneous shear stress at the bed could be varying greatly

is accounted for in Shield's criteria for incipient motion if turbulence is generated at the channel boundary. However, if turbulence is being generated in some other manner (e.g., by a hydraulic jump), then the average boundary shear stress is more closely related to the turbulence intensity of the flow than to the velocity gradients.

As there are very few measurements of turbulence intensities in flow fields over riprap below energy dissipators, riprap in these areas are sized from model studies and from experience with field structures. Turbulence intensities below energy dissipating structures are very large in comparison to intensities in normal channels. Rock sizes required below these structures are much larger than would be needed for the same mean velocity in a channel. For example, the U.S. Army Engineers (22) specify a rock size twice as large below stilling basins as in normal turbulent flow with the same average velocity. The writers have had the opportunity to confirm the riprap design procedures presented herein by experimentation with large-scale models. We hope to present these model data in the future.

SUMMARY AND CONCLUSIONS

Stability equations for design of riprap protection on plane beds, side slopes, and embankment slopes have been formulated from theoretical considerations and existing empirical information. The relative importance of the magnitude and direction of the velocity vector, the angle of side slope, and the size and angle of repose for riprap, are reflected in the safety factor. The safety factor is formulated as the ratio of the moment of the submerged weight of a particle to the lift and drag moments tending to rotate the particle out of the bed. The safety factor is unity for incipient-motion flow conditions over riprap, and is greater than unity for stable riprap.

The design criteria of the Bureau of Public Roads, the Corps of Engineers, the California Highway Department, and others have been compared with the developed stability criteria. The adequacy of the designs are judged on the basis of the computed values of the riprap safety factor. In some cases, the safety factors are less than unity indicating there could be a loss of riprap material when the design flows are obtained.

ACKNOWLEDGMENTS

The problem of safety factors for riprap protection on side slopes was investigated by Colorado State University for the Wyoming State Highway Department, Planning and Research Division, in cooperation with the U.S. Department of Transportation, Federal Highway Administration, Bureau of Public Roads. The writers wish to acknowledge the support of the Wyoming State Highway Department and the Federal Highway Administration and the technical help of Mainard Wacker and his staff in the Hydraulic Design Office of the Wyoming Highway Department. The opinions, findings, and conclusions in this publication are those of the writers and not necessarily those of the State Highway Commission of Wyoming or the Federal Highway Administration.

APPENDIX.—REFERENCES

1. "Bank and Shore Protection in California Highway Practice," California Division

- of Highways, Department of Public Works, Sacramento, Calif., Nov., 1970.
2. Brooks, N. H., discussion of "Boundary Shear Stresses in Curves Trapezoidal Channels," By A. T. Ippen and P. A. Drinker, *Journal of the Hydraulics Division, ASCE*, Vol. 89, No. HY3, Proc. Paper 3529, May, 1963, pp. 327-333.
3. Campbell, F. B., "Hydraulic Design of Rock Riprap," *Miscellaneous Paper No. 2-777*, Office, Chief of Engineers, U.S. Army, Waterways Experiment Station, Vicksburg, Miss., Feb., 1966.
4. Carter, A. C., Carlson, E. J., and Lane, E. W., "Critical Tractive Forces on Channel Side Slopes in Coarse Noncohesive Material," *Hydraulic Laboratory Report No. Hyd.-366*, Bureau of Reclamation, U.S. Department of the Interior, Washington, D.C., 1953.
5. Cheng, E. D. H., and Clyde, C. G., "Instantaneous Hydrodynamic Lift and Drag Forces on Large Roughness Elements in Turbulent Open Channel Flow," *Sedimentation*, published by Hsieh Wen Shen, ed., Fort Collins, Colo., 1972, pp. 3-1 to 3-20.
6. Christensen, B. A., "Incipient Motion on Cohesionless Channel Banks," *Sedimentation*, published by Hsieh Wen Shen, ed., Fort Collins, Colo., 1972, pp. 4-1 to 4-22.
7. Einstein, H. A., "The Bed-Load Function for Sediment Transportation in Open Channel Flows," *Technical Bulletin No. 1026*, U.S. Department of Agriculture, Soil Conservation Service, Washington, D.C., Sept., 1950.
8. Einstein, H. A., and Samni, E. A., "Hydrodynamic Forces on a Rough Wall," *Review of Modern Physics*, Vol. 21, No. 3, 1949, pp. 520-524.
9. Gessler, J., "Beginning and Ceasing of Sediment Motion," *River Mechanics*, Vol. 1, published by Hsieh Wen Shen, ed., Fort Collins, Colo., 1971, pp. 7-1 to 7-22.
10. "Hydraulic Design of Stilling Basins and Energy Dissipators," *Engineering Monograph No. 25*, U.S. Bureau of Reclamation, Technical Information Branch, Denver Federal Center, Denver, Colo., 1958.
11. Keulegan, G. H., "Laws of Turbulent Flow in Open Channels," *Journal of Research*, Vol. 21, National Bureau of Standards, Washington, D.C., 1938, pp. 701-741.
12. Lane, E. W., "Design of Stable Channels," *Transactions, ASCE*, Vol. 120, Paper No. 2776, pp. 1234-1260.
13. Lewis, G. L., "Riprap Protection of Bridge Footings," thesis presented to Colorado State University, at Fort Collins, Colo., in 1972, in partial fulfillment of the requirements for the degree of Doctor of Philosophy.
14. Murphy, T. E., and Grace, J. L., "Riprap Requirements for Overflow Embankments," *Highway Research Board Record*, No. 30, Washington, D.C., 1963, pp. 47-55.
15. "Review of Slope Protection Methods," by the ASCE Subcommittee on Slope Protection, *Transactions, ASCE*, Vol. 74, 1948, pp. 845-866.
16. Searcy, J. K., "Use of Riprap for Bank Protection," *Hydraulic Engineering Circular No. 11*, Hydraulics Branch, Bridge Division, Office of Engineering and Operations, Bureau of Public Roads, Washington, D.C., June, 1967.
17. "Sediment Control Methods: B. Stream Channels," by the ASCE Task Committee on Preparation of Sedimentation Manual, *Journal of the Hydraulics Division, ASCE*, Vol. 98, No. HY7, Proc. Paper 9071, July, 1972, pp. 1295-1326.
18. Simons, D. B., "Theory and Design of Stable Channels in Alluvial Materials," thesis presented to Colorado State University, at Fort Collins, Colo., in 1957, in partial fulfillment of the requirements for the degree of Doctor of Philosophy.
19. Simons, D. B., and Lewis, G. L., "Flood Protection at Bridge Crossings," *CER71-72DBS-GLL10*, Colorado State University, Fort Collins, Colo., 1971.
20. Simons, D. B., and Stevens, M. A., "Stability Analysis for Coarse Granular Material on Slopes," *River Mechanics*, Vol. 1, published by Hsieh Wen Shen, ed., Fort Collins, Colo., 1971, pp. 17-1 to 17-27.
21. Stevens, M. A., "Scour in Riprap at Culvert Outlets," thesis presented to Colorado State University, at Fort Collins, Colo., in 1968, in partial fulfillment of the requirements of the degree of Doctor of Philosophy.
22. "Stone Stability—Velocity vs Stone Diameter," Sheet 712-1, Civil Works Investigations, *Hydraulic Design Criteria*, U.S. Army Engineers, Waterways Experiment Station, Vicksburg, Miss., Revised, Aug., 1970.

Estimating Probabilities of Extreme Rainfalls. Thomas A. Fontaine and Kenneth W. Potter.
By George A. Harper. Closure by authors1092

RIPRAP DESIGN FOR OVERTOPPING FLOW

By Steven R. Abt¹ and Terry L. Johnson,² Members, ASCE

ABSTRACT: Near-prototype flume studies were conducted in which riprap-protected embankments were subjected to overtopping flows. Embankment slopes of 1, 2, 8, 10, and 20% were covered with riprap layers with median stone sizes of 1, 2, 4, 5, and/or 6 in. Each riprap layer was tested by slowly increasing the discharge to failure. Riprap design criteria for overtopping flows were developed for estimating incipient stone movement and riprap layer failure as a function of the unit discharge, stone shape, median stone size, and embankment slope. Incipient stone movement occurred at approximately 74% of the riprap layer failure unit discharge. It was determined that rounded shape stone should be oversized approximately 40% to provide comparable protection of an angular shape stone. Flow channelization was observed to occur at approximately 88% of the unit discharge at failure. A flow concentration factor of approximately 1 to 3 was introduced for sizing stone.

INTRODUCTION

The erosion potential of dams, levees, roadways, and other embankment structures resulting from overflows during flood events has become an important aspect of assessing structure stability and safety. The technology and procedures developed for evaluating embankment safety have also been applied to the capping and sealing of waste disposal impoundments that have been legislated to be stable for periods of up to 1,000 years. Therefore, understanding the mechanics of erosion due to overtopping and providing alternative design measures for preventing erosion are vital steps in providing the engineer the tools to insure embankment stability.

The mechanics of erosion on embankments due to overtopping were reviewed by Powledge et al. (1989b), in which information was presented based on research and case studies of embankment overtopping. In addition, alternative methods for embankment protection systems were summarized to include vegetation, geotextiles, mat and block systems, gabions, and riprap. Powledge et al. evaluated the various embankment protective systems by relating the flow depth over the embankment, flow duration, and soil composition, where applicable, to the extent of erosive damage to the embankment.

One embankment protective system investigated and reported by Powledge et al. was the placement of a riprap layer over the embankment downstream face. It was indicated that riprap can provide suitable overtopping protection. However, undersizing of the riprap or layer thickness may result in a fluidizing of the protective layer subjecting the embankment to severe erosive processes. Powledge et al. did not specifically present a method(s) of sizing riprap for preventing fluidizing of the riprap layer.

The objective of this investigation is to develop riprap design criteria ap-

¹Prof. and Dir., Hydr. Lab., Dept. of Civ. Engrg., Colorado State Univ., Fort Collins, CO 80523.

²Sr. Hydr. Engr., U.S. Nuclear Regulatory Commission, Washington, DC 20555.

Note. Discussion open until January 1, 1992. To extend the closing date one month, a written request must be filed with the ASCE Manager of Journals. The manuscript for this paper was submitted for review and possible publication on December 28, 1989. This paper is part of the *Journal of Hydraulic Engineering*, Vol. 117, No. 8, August, 1991. ©ASCE, ISSN 0733-9429/91/0008-0959/\$1.00 + \$.15 per page. Paper No. 26038.

plicable to overtopping flow conditions to prevent fluidization of the protective riprap layer. If riprap is to be a viable, long-term alternative for protecting embankments from erosion, engineering design criteria must be formulated to prevent stone movement and riprap layer failure.

BACKGROUND

One of the classic studies of rockfill design and placement was conducted by Isbash (1935). Isbash investigated the construction of dams by dumping rounded stones into flowing rivers. His investigation focused on:

1. Sizing individual stones located on the downstream dam slope to resist displacement due to overtopping flow and percolation through the dam body.
2. Estimating spillway discharge coefficients of the dam for various stages of completion.
3. Characterizing percolated flow through the coarse-grained material from the dam.

Isbash also conducted a series of experiments that yielded an expression indicating the critical transport velocity for displacing rounded stones as:

$$V = Y\psi(d)^{1/2} \dots\dots\dots (1)$$

where

$$\psi = \left[2g \left(\frac{\Delta_s - \Delta_w}{\Delta_s} \right) \right]^{1/2} \dots\dots\dots (2)$$

and V = the velocity acting against the individual stones, d = the stone size reduced to the equivalent sphere, Δ_s = the unit weight of the stone, Δ_w = the unit weight of water, Y = a coefficient, and g = the acceleration of gravity. Further, he expressed the percolation velocity, V_p , through the rock layer as:

$$V_p = C_0 P(dI)^{1/2} \dots\dots\dots (3)$$

where I = the average hydraulic gradient, P = the natural porosity or void ratio of rockfill, and C_0 = a coefficient. Based upon these relationships, Isbash formulated a procedure for dumping and stabilizing stones in flowing water.

A comprehensive investigation was conducted by Olivier (1967) on the flow through and over rockfill dams. A series of laboratory experiments were performed to evaluate how rockfill could be safely overtopped by floods both during and after construction without risk of failure. Olivier carried out his experiments in flumes 22-in. (56-cm) wide and 5-ft (152-cm) long on slopes ranging from 8 to 45%. Median stone sizes ranged from 0.51 in. (1.3 cm) to 2.33 in. (6 cm) for crushed granite and from 0.63 in. (1.6 cm) to 1.01 in. (2.6 cm) for pebbles and gravel.

Olivier observed two distinct stages during each test, threshold flow, and collapse flow. Threshold flow was defined when incipient stone movement occurs. Collapse flow is the final stage where stone failure results. Olivier was the first to recognize that channelization occurred between the threshold and collapsing stages.

Olivier empirically derived an expression for overtopping flow linking the design parameters of unit flow, slope, and median rock size for crushed or rough stones to threshold flow. The unit discharge at stone movement is:

$$q_{or} = 0.423 d_s^{3/2} \left[\frac{(w_s - w)}{w} \right]^{5/3} i^{-7/6} \dots\dots\dots (4)$$

where q_{or} = the unit discharge in cfs per foot, d_s = the median stone size in feet, w_s = the unit weight of the stone, w = the unit weight of water, and i = the embankment gradient.

Hartung and Scheuerlein (1970) performed a series of overflow tests in a steep flume simulating steep open channels with natural roughness. They determined that the maximum unit discharge, q_{max} , that would resist stone movement can be expressed as:

$$q_{max} = T \cdot Y_m \cdot V_c \dots\dots\dots (5)$$

where

$$V_c = 1.2 \left[\frac{2g(\gamma_s - \gamma_w)}{T \cdot \gamma_w} \right]^{1/2} (d_s \cos \phi)^{1/2} \dots\dots\dots (6)$$

and

$$T = \frac{\gamma_{wl}}{\gamma_w} \dots\dots\dots (7)$$

or

$$T = 1 - 1.3 \sin \phi + 0.08 \frac{Y_m}{\theta_m} \dots\dots\dots (8)$$

where Y_m = the mean water depth, θ_m = the mean roughness height ($\sim d_s/3$), d_s = the equivalent diameter of the stones, ϕ = the angle of slope, T = the aeration factor, V_c = the critical velocity at which the stone begins to move, γ_w = the specific weight of water, γ_{wl} = the specific weight of the air-water mixture, γ_s = the specific weight of the stone, and g = the acceleration of gravity.

Stephenson (1979) performed a stability analysis for stones placed on the downstream face of a rockfilled embankment subjected to overtopping. His analysis of the hydraulic reaction on the resisting stones related the stone size to the slope angle and flow rate. Stephenson derived an equation to determine median stone size, d , for the threshold flow expressed as:

$$d = \left[\frac{q (\tan \theta)^{7/6} n^{1/6}}{Cg^{1/2} [(1 - n)(S - 1) \cos \theta (\tan \phi - \tan \theta)]^{2/3}} \right]^{2/3} \dots\dots\dots (9)$$

where q = the threshold unit discharge, n = the porosity, s = the relative density of the stone, C = a coefficient, θ = the slope angle, ϕ = the angle of friction, and g = the gravitational acceleration. The coefficient, C , is derived from Olivier (1967) and reported to be 0.22 for gravel and pebbles, and 0.27 for crushed stone. Complete collapse of the riprap will occur when the unit discharge is increased 120% for gravel and 108% for crushed stone.

Knauss (1979) performed a comparison of the Olivier expression, (4), and

the Hartung and Scheuerlein expression, (5), for overtopping flow conditions. He determined that both equations were valid for crushed stone with angular shapes. However, Knauss recommended the Hartung and Scheuerlein equation for the design of overflowed rockfill dams with steep downstream slopes ranging from 20 to 67%.

Powledge and Dodge (1985) conducted a series of small-scale overtopping tests using riprap as embankment protection on the downstream face. Since the tests were to evaluate embankment protection and not to provide riprap design criteria, the riprap fluidized and eroded the embankment. Powledge and Dodge determined that improperly designed riprap did not provide erosive protection to the embankment from overtopping flow.

It is evident that riprap design to resist overtopping flow is a function of the representative stone size, the hydraulic gradient, and the discharge. Further, riprap design should be directed toward preventing stone movement and to insure the riprap layer does not fail or collapse.

TESTING FACILITIES

An experimental program (Abt et al. 1987, 1988) was conducted in two flume facilities located at the Engineering Research Center of Colorado State University (CSU). An outdoor flume was utilized for simulating steep embankment slopes (≥ 0.10) while an indoor laboratory flume was used for simulating flatter slopes (≤ 0.10). Each flume was modified to enable prototype testing of stone-covered embankments in order to evaluate flow conditions and stone movement.

The outdoor facility is a concrete flume that is 180-ft (54.9-m) long, 20-ft (6.1-m) wide, and 8-ft (2.4-m) deep. The flume was modified to where the upper 20 ft (6.1 m) served as a holding basin and inlet to the test section. A headwall was constructed 20 ft (6.1 m) downstream of the inlet. The embankment was constructed downstream of the headwall. The throat of the test section containing the embankment was 12-ft (3.7-m) wide to concentrate flow onto the slope. Fig. 1 depicts the outdoor facility.

The test embankment was constructed of a moistened, compacted sand in the throat of the test section. The initial 15 ft (4.6 m) of embankment, downstream of the headwall, was horizontally placed to simulate the embankment crest and to fully develop flow approaching the slope. The embankment transitioned to a designated slope. A geofabric covered and stabilized the sand. The geofabric allowed the embankment face to be saturated and flex under a variety of loading conditions. However, the geofabric prevented the sand from massive failure, thereby minimizing turn-around time between experiments. A 6-in. (0.15-m) thick sand/gravel bedding was placed on top of the geofabric as specified by the bedding design criteria suggested by Sherard et al. (1984). Riprap was placed on top of the bedding material.

The indoor facility, located in the CSU Hydraulics Laboratory, is a steel, tilting flume that is 200-ft (61-m) long, 8-ft (2.4-m) wide, and 4-ft (1.2-m) deep. The flume was modified to enable the embankment slope to vary from 0.01 to 0.10. The flume inlet was modified to where flows entered the head box, discharged through a diffuser, and transitioned into the flow development section. Rock was placed in the upstream 80 ft of the flume to establish uniform approach flow conditions. A 20-ft (6.1-m) transition section was constructed linking the approach to the riprap test section. The riprap test

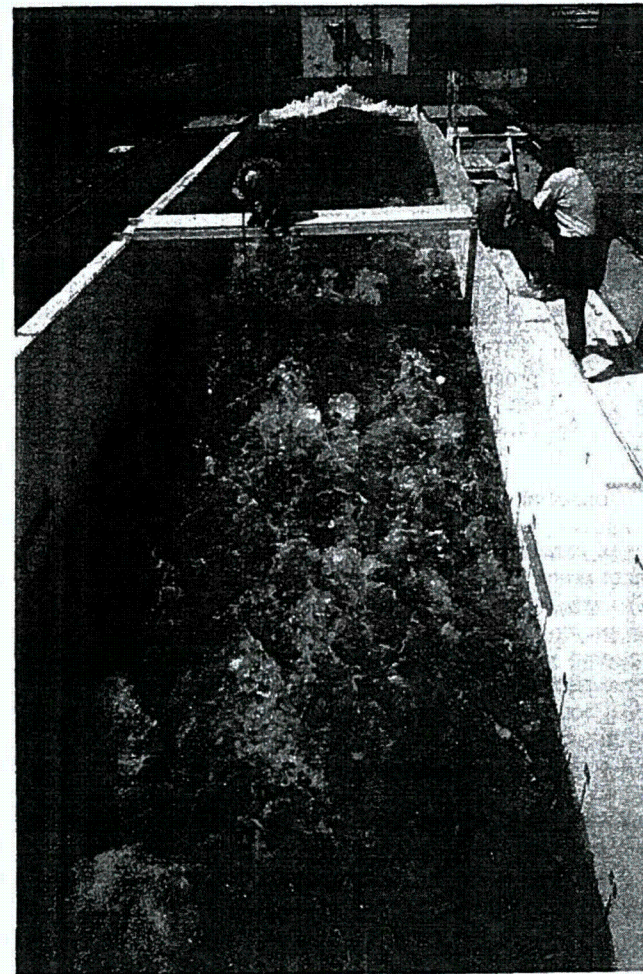


FIG. 1. Test Facility with Riprap-Protected Embankment

section extended 50 ft (15.2 m). The remainder of the flume served as the tailwater control and material recovery basin. The test embankment consisted of a moistened, compacted 4-in. (0.10-m) sand layer. A geofabric covered and stabilized the sand bed. An appropriately sized sand/gravel bedding was placed on the geofabric to a thickness of approximately 6 in. (0.15 m). Riprap was placed on top of the bedding material.

The instrumentation used in both facilities consisted of the equipment and materials necessary to monitor the discharge, water surface elevation, and flow velocity over the riprap layer. Surface velocities were recorded using a Marsh-McBirney® magnetic flowmeter and discharges were measured with a sonic flowmeter in the outdoor flume. A pitot tube was used to determine

the velocity profiles and orifice plates measured discharges entering the headbox in the indoor flume.

Water-surface elevations were monitored using manometer taps installed beneath the bedding of the embankment of both flumes. The manometer taps were placed at sections near the transition, at the upper one-third point of the slope, and at the lower one-third point of the slope. The taps were equally spaced across the embankment at the quarter points of each section to monitor potential differences in the flow distribution.

RIPRAP PROPERTIES

The riprap was derived from a limestone quarry. Median stone sizes, D_{50} , tested ranged from 1.02 in. (2.59 cm) to 6.2 in. (15.75 cm) as summarized in Table 1. Rock properties of gradation, unit weight, γ , specific gravity, G_s , porosity, n_p , void ratio, e , and friction angle, ϕ , were determined using procedures outlined by the American Society for Testing Materials (ASTM).

TESTING PROCEDURE

A series of experiments were conducted in which riprap was placed as an embankment protective material and subjected to an overtopping flow until failure. The experimental variables encompassed the median stone diameter, channel slope, unit surface discharge, surface flow velocity, and water surface elevation.

The riprap testing and failure procedures were similar for all experiments conducted in both indoor and outdoor facilities. The riprap was dump-placed. However, the stone surface was leveled to avoid the occurrence of man-made flow concentrations. Once the riprap was placed and the instrumentation set and checked, the flume inlet valves were opened, initiating flow. The riprap was inundated and the bed was allowed to adjust and/or settle. The flow was increased until flow over the riprap surface was observed. Once the flow stabilized, the discharge was determined and localized velocities and water surface elevations were obtained through the upper third and lower third of the embankment when and where possible. Since the depth of surface flow could not be directly measured due to cascading flow conditions, the depth of flow along the slope was determined by monitoring

TABLE 1. Riprap Properties

Shape (1)	D_{50} (in.) (2)	D_{50} (cm) (3)	$C_u (d_{80}/d_{10})$ (4)	$\sigma (d_{84}/d_{16})$ (5)	γ (6)	G_s (7)	n_p (8)	ϕ (9)
Subangular	1.02	2.59	1.75	1.79	94	2.72	0.44	40
Angular	2.2	5.59	2.09	2.09	92	2.72	0.45	41
Angular	4.1	10.41	2.15	2.16	92	2.65	0.44	42
Angular	5.1	12.95	1.62	1.87	90	2.65	0.46	42
Angular	6.2	15.75	1.69	1.86	90	2.65	0.46	42
Angular	2.0	5.08	2.14	2.50	92	2.72	0.45	41
Angular	4.0	10.16	2.30	2.72	92	2.65	0.44	42
Round	2.0	5.03	2.14	5.70	92	2.72	0.45	37
Round	4.0	10.16	2.12	2.24	90	2.50	0.45	38

the manometers placed in the bed. The flow depths presented are an average value derived from the six manometers along the embankment slope. After recording the data and documenting observations, the flow was increased. The procedure was repeated until stone movement and/or riprap layer failure occurred.

The failure criterion of the riprap layer was when the filter blanket, or more often, the geofabric, was exposed. In many cases, concentrated flows would scour a localized zone along the embankment. However, rock movement from up slope would subsequently fill and stabilize the scour area. When rock movement could no longer adequately replenish rock to the scour or failure zone, catastrophic failure was observed. Therefore, catastrophic failure could occur prior to geofabric exposure due to the dynamic rock movement along the bed and due to poor conditions for observing the bedding resulting from the significant turbulence, bubbles, and air entrainment of the cascading flows. The times from the initiation of flow to the rock layer failure ranged from 2 to 4 hours depending upon riprap size.

RESULTS

Twenty-six flume tests were conducted with riprap placed on embankment slopes of 0.01 to 0.20 and subjected to overtopping flows until riprap failure, or collapse, occurred. Twenty-one tests were performed using angular shaped stones and five tests evaluated rounded shaped stones. In 15 tests, the unit discharge at stone movement, or threshold flow, and riprap channelization was recorded. A summary of the test parameters measured for each test is presented in Table 2.

It was observed in the early stages of each test that the smaller stones on the riprap surface were often washed out, leaving the upper layer of larger stones to armor the remainder of the embankment. On slopes greater than 0.02, cascading flows resulted. The plunging and impacting flow conditions often caused the larger stones to move and/or adjust until interlocking, wedging, and/or packing occurred between adjacent stones, particularly during discharges approaching the failure discharge on the steeper embankment slopes. During the adjustment process, stones often penetrated the water surface, thereby increasing the white water appearance. When the riprap layer failed, a catastrophic failure was observed on all slopes greater than 0.02.

ANGULAR-STONE FAILURE

Riprap specifications have traditionally stipulated that a high-quality, angular-shaped stone (preferably crushed) be used for placement in the field. Angular stone tends to interlock or wedge and subsequently resist sliding and rolling. In addition, fewer fines are required to fill the voids of crushed material compared with a similarly graded rounded stone.

In an attempt to determine the riprap layer stability for angular shaped stones when subjected to overtopping flow, the riprap layer median stone size, D_{50} , was correlated to the overtopping unit discharge at failure, q_f , for the angular shaped stones, as presented in Fig. 2. It is observed in Fig. 2 that the data represent a family of parallel relationships that correlates the unit discharge at failure to the embankment slope, S , and median stone size. A composite relationship was formulated collapsing the data presented in

TABLE 2. Data Summary

Run (1)	Flume (2)	Stone shape (3)	Riprap D_{50} (in.) (4)	Riprap D_{50} (cm) (5)	Riprap thickness (in.) (6)	Layer (in.) (7)	Slope (8)	q failure (cfs/ft) (9)	q failure ($m^3/s\text{-}m$) (10)	t/D_{50} (11)	q failure / q failure (12)	q channel / q failure (13)
7	Outdoor	Angular	4.1	10.4	12	30.5	0.20	1.81	0.17	2.9	0.77	0.90
10A	Outdoor	Angular	5.1	13.0	12	30.5	0.20	3.56	0.33	2.4	0.79	0.88
15	Outdoor	Angular	6.2	15.7	12	30.5	0.20	4.43	0.41	1.9	0.75	0.85
18	Outdoor	Angular	2.2	5.6	6	15.2	0.20	0.50	0.05	2.7	0.73	0.93
21	Outdoor	Rounded	4.0	10.2	12	30.5	0.20	0.95	0.09	3.0	0.79	0.88
22	Outdoor	Rounded	4.0	10.2	12	30.5	0.20	0.95	0.09	3.0	0.80	0.89
29	Outdoor	Angular	2.0	5.1	4	10.2	0.10	0.85	0.08	2.0	0.66	0.85
31	Outdoor	Angular	2.0	5.1	6	15.2	0.10	1.00	0.09	3.0	0.62	0.82
32	Outdoor	Angular	2.0	5.1	6	15.2	0.10	1.11	0.10	3.0	0.76	0.86
36	Outdoor	Rounded	4.0	10.2	6	15.2	0.10	1.99	0.18	1.5	0.76	0.84
38	Outdoor	Rounded	4.0	10.2	12	30.5	0.10	2.09	0.19	3.0	0.66	0.86
42	Outdoor	Angular	4.0	10.2	8	20.3	0.10	3.51	0.33	2.0	0.77	0.92
44	Outdoor	Angular	4.0	10.2	12	30.5	0.10	3.79	0.35	3.0	0.78	0.86
46	Outdoor	Rounded	2.0	5.1	6	15.2	0.10	0.69	0.06	3.0	0.67	0.83
51	Outdoor	Angular	4.0	10.2	12	30.5	0.10	4.12	0.38	3.0	0.75	0.89
107	Indoor	Angular	2.2	5.6	6	15.2	0.02	4.53	0.42	2.7	---	---
111	Indoor	Angular	1.02	2.6	3	7.6	0.02	1.11	0.10	2.9	---	---
120	Indoor	Angular	1.02	2.6	3	7.6	0.10	1.50	0.14	2.9	---	---
125	Indoor	Angular	1.02	2.6	3	7.6	0.10	0.36	0.03	2.9	---	---
126	Indoor	Angular	1.02	2.6	3	7.6	0.10	0.34	0.03	2.9	---	---
127	Indoor	Angular	1.02	2.6	3	7.6	0.10	0.31	0.03	2.9	---	---
128	Indoor	Angular	1.02	2.6	3	7.6	0.10	0.42	0.04	2.9	---	---
129	Indoor	Angular	2.2	5.6	6	15.2	0.10	1.12	0.10	2.7	---	---
130	Indoor	Angular	2.2	5.6	6	15.2	0.10	1.25	0.12	2.7	---	---
131	Indoor	Angular	2.2	5.6	6	15.2	0.10	1.25	0.12	2.7	---	---
132	Indoor	Angular	2.2	5.6	6	15.2	0.08	1.81	0.17	2.7	---	---

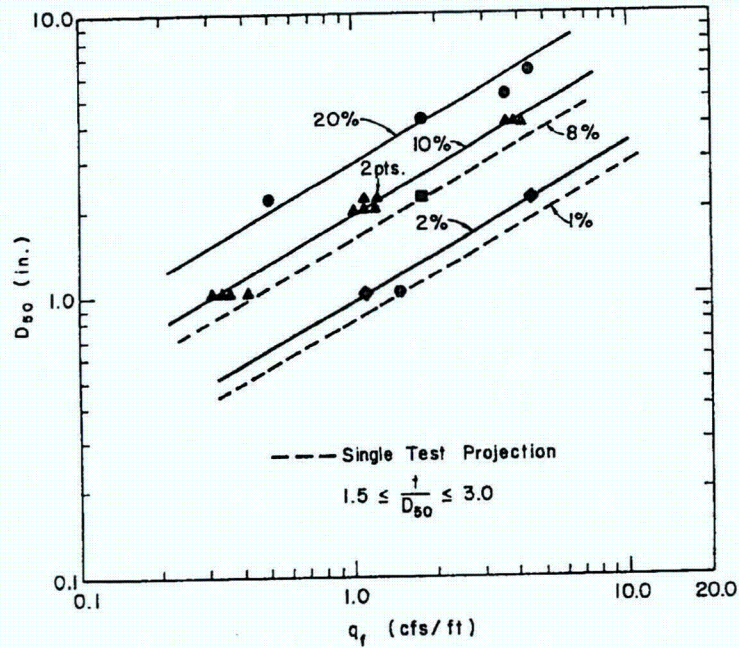


FIG. 2. Unit Discharge at Failure versus Median Stone Size

Fig. 2 into single envelope for angular stones as shown in Fig. 3. A power regression was performed on the parametric expression relating median stone size to the embankment slope and overtopping unit discharge at failure. The results are expressed as:

$$D_{50} = 5.23S^{0.43} q_f^{0.56} \dots \dots \dots (10)$$

Eq. (10) provides the user a means to estimate the minimum median stone size required to withstand a design overtopping unit discharge on an embankment with specific design slope. However, (10) indicates the riprap layer failure criteria and should be adjusted to prevent stone movement.

A safety factor may be derived for adjusting the stone size by enveloping the scattered data shown in Fig. 3. The maximum deviation about the power regression fit, (10), is approximately 20%. Therefore, a safety factor of 1.20 is recommended.

It is observed in (10), that the median stone size is determined independent of the rock specific gravity. Since (10) is an empirical relationship derived from riprap with the same specific gravity, $\gamma = 2.65$, the affect of variable specific gravity on stone sizing could not be evaluated.

The writers acknowledge that the empirical curves representative of 1, 2, and 8% embankment slopes are based on only four failure tests. However, the extensive costs associated with near prototype experimentation significantly limited the extent of the testing program. The relationship for angular-shaped stones presented in Fig. 3 provide a means for confidently estimating

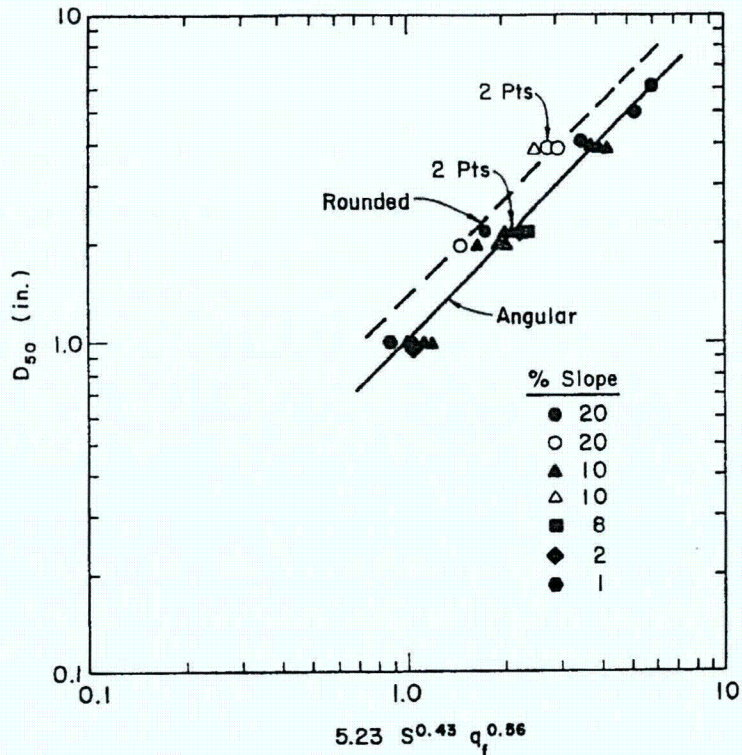


FIG. 3. Composite Riprap Layer Failure Envelope

the median stone size necessary for stabilizing an embankment of 1 to 20% subjected to overtopping flow conditions. Application of this stone sizing relationship beyond the test parameters presented are at the users' risk.

ROUNDED-STONE FAILURE

A series of five failure tests were conducted evaluating the stability of rounded-shaped stones with median diameters of 2 and 4 in., placed on 10 and 20% slopes as presented in Table 2. Test procedures were identical for both angular- and rounded-shaped riprap layers. Round rock was defined as rock with no intersecting surfaces, but rather a single, continuous, smooth-curved surface. During mining, transport, and handling, a portion of the rock fractured and became faced. The faced rock comprised approximately 5% of the rounded rock tested.

To compare the stability of rounded stone with the angular stone, the unit discharges at failure for 2- and 4-in. rounded and 2- and 4-in. angular-shaped stones were compared for a 10% slope with 3 D₅₀ layer thickness. It was determined from the results in Table 2 that the rounded stones failed at a unit discharge 32 and 45% lower than the angular stone for the 2- and 4-

in. stone sizes, respectively. Although these results represent only one set of test conditions, they are indicative of the stability relationship between angular and rounded stones.

The five rounded-stone failure points were plotted in Fig. 3 adjacent to the angular-stone failure relationship. It is observed that the rounded stones reflect a linear relationship parallel to the regression curve for the angular-shaped stone. The rounded-shape riprap fails at a unit discharge of approximately 40% less than angular-shaped stones of the same median stone size.

Usually, when angular stones moved, they traveled a short distance and wedged into other stones. When the rounded stones moved, they often rolled down the entire embankment without intermediate lodging. Stone shape appears to significantly affect riprap layer stability for overtopping conditions.

The suggested relationship between angular- and round-shaped stones is based on limited data. The rounded stone relationship presented in Fig. 3 is not recommended for design. However, the angular- and round-shaped stone relationships appear to be indicative of how shape influences embankment stability.

STONE MOVEMENT

The unit discharge at stone movement, *q_m*, was recorded in 14 of the failure tests as indicated in Table 2. Stone movement observations were verified with videotape recordings. The stone movement was normalized by dividing the unit discharge at movement by the unit discharge at failure. The unit discharge at movement to unit discharge at failure ratio ranged from 0.62 to 0.79 with a mean value of 0.74 for both angular and rounded stone.

Since it is imperative that the riprap layer be designed to prevent failure, the median stone size should be sized to resist stone movement. Therefore, the failure unit discharge, *q_f*, must be adjusted by the stone movement to stone failure ratio where

$$q_{design} = \frac{q_f}{0.74} = 1.35q_f \dots \dots \dots (11)$$

Eq. (10) is modified such that the riprap median stone size is designed to resist stone movement using the design unit discharge as:

$$D_{50} = 5.23S^{0.43} q_{design}^{0.56} \dots \dots \dots (12)$$

Eq. (12) is applicable to angular-shaped riprap.

CHANNELIZATION

In 15 of the 26 tests, channels formed in the riprap layer, as shown in Fig. 4, conveying unit discharges greater than expected under sheet flow conditions. The channels appeared to form as flows were diverted around the larger stones and directed into areas or zones of the smaller stones. The smaller stones were moved, creating a gap or notch between the larger stones. The flow concentrated into these notches, thereby increasing the localized unit discharge. The newly formed subchannel would quickly migrate downstream. Flow channelization occurred after stone movement and immediately prior to collapse of the riprap layer.



FIG. 4. Flow Channelization in 2-in. Layer of Angular Riprap on 10% Slope

During four tests, 7, 10A, 15, and 18, the subchannel depth and width were measured and localized velocities were taken when initially observed. The sheet flow unit discharge at the time of subchannel development was compared to the unit discharge estimated in the subchannel. The ratio of the subchannel flow unit discharge to the sheet flow unit discharge was 3.33, 2.24, 1.67, and 1.33 for the 2.2-, 4.1-, 5.1-, and 6.2-in. stones, respectively. The results indicate that flows can concentrate and form subchannels in the riprap layer. Therefore, flow concentrations of 3 are possible and may need to be incorporated into the design process.

The flow concentration factor may be incorporated into the stone size analysis by multiplying the failure unit discharge, q_f in (11), by the flow concentration factor, which ranges from 1 to 3. An increase of the flow concentration factor of 100% (i.e., 1 to 2) will result in a stone size increase of approximately 50%. The selection of a flow concentration factor is dependent upon the hazard level of the protected surface.

Incipient channelization was documented during 15 of the tests and verified with videotape recordings. The incipient channelization unit discharge, q_c , was normalized to the unit discharge at failure, q_f , for each test. The q_c/q_f ratios are presented in Table 2. The average point of incipient subchannel formation occurs at approximately 88% of the unit discharge at failure. Therefore, it is possible to predict the unit discharge at which channelization will occur on a riprap layer subjected to overtopping.

COMPARISON OF DESIGN ALTERNATIVES

The stone sizing procedures presented in (12) Olivier (1967), and Stephenson (1979) were compared by applying the appropriate stone sizing equations to the same design conditions. Stone sizing computations were conducted for unit discharges of 1.25 cfs (0.035 m³/s) and 4.0 cfs (0.113 m³/s) on embankment slopes of 0.10 and 0.20. The stones were assumed

TABLE 3. Design Comparison

Procedure (1)	Unit (cfs) (2)	Discharge, q (m ³ /s) (3)	Embankment slope (4)	Median rock (in.) (5)	Size (cm) (6)
Eq. (12)*	1.25	0.035	0.10	2.6	6.6
	1.25	0.035	0.20	3.5	8.9
	4.0	0.113	0.10	5.0	12.7
Olivier	4.0	0.113	0.20	6.7	17.0
	1.25	0.035	0.10	2.4	6.1
	1.25	0.035	0.20	4.0	10.2
Stephenson ^b	4.0	0.113	0.10	5.1	13.0
	4.0	0.113	0.20	8.8	22.4
	1.25	0.035	0.10	2.9	7.4
	1.25	0.035	0.20	5.5	14.0
	4.0	0.113	0.10	6.3	16.0
	4.0	0.113	0.20	11.9	30.2

*Safety factor not incorporated in rock sizing.

^bAssumes $n_p = 0.40$, $\phi = 40^\circ$, $C = 0.27$.

to be angular in shape, with a porosity of 0.40, friction angle of 40°, and stone specific weight of 2.65. The resulting stone sizes for each procedure is presented in Table 3.

It is observed that for the flatter embankment slope (0.10) and low unit discharge (1.25 cfs), the three procedures determine similar median stone sizes ranging from 2.4 to 2.9 in. However, as the slope steepens and the unit discharge increases, the Stephenson procedure yields conservative results compared to both the proposed procedure and the Olivier procedure. The Stephenson procedure was extremely sensitive to the porosity of the stone layer.

SUMMARY AND CONCLUSIONS

A series of 26 laboratory flume tests was conducted in which riprap protected embankments were subjected to overtopping flows until the riprap layer failed. Embankment slopes of 1, 2, 8, 10, and 20% were covered with riprap layers of median stone sizes of 1, 2, 4, 5, and/or 6 in. The results of these test provided the following findings:

1. A unique riprap design relationship was developed to determine median stone size on the basis of a design unit discharge and embankment slope for overtopping flows.
2. A criterion was developed to compare the stability of round-shape riprap with angular-shape riprap. The rounded riprap appears to require oversizing of about 40% to provide a similar level of protection as angular riprap. Additional testing is required to substantiate these initial findings.
3. The median stone size should be increased by increasing the design unit discharge by 35% to prevent stone movement.
4. Flow channelization occurred along the riprap-protected embankment when the unit discharge approached 88% of the unit discharge at failure.

5. Flow concentration can occur on riprap-protected embankments. Flow concentrations of 1.33 to 3.33 were observed.

6. Riprap design criteria for sizing riprap subjected to overtopping flow conditions is presented based on near-prototype test data.

ACKNOWLEDGMENTS

The research reported was sponsored by the office of Nuclear Material Safety and Safeguards, U.S. Nuclear Regulatory Commission.

APPENDIX. REFERENCES

Abt, S. R., Khattak, M. S., Nelson, J. D., Ruff, J. F., Shaikh, A., Wittler, R. J., Lee, D. W., and Hinkle, N. E. (1987). "Development of riprap design criteria by riprap testing in flumes: Phase I." *NUREG/CR-4651*, U.S. Nuclear Regulatory Commission, Washington, D.C., May, 111.

Abt, S. R., Wittler, R. J., Ruff, J. F., LaGrone, D. L., Khattak, M. S., Nelson, J. D., Hinkle, N. E., and Lee, D. W. (1988). "Development of riprap design criteria by riprap testing in flumes: Phase II." *NUREG/CR-4651*, U.S. Nuclear Regulatory Commission, Washington, D.C., May, 113.

Hartung, F., and Scheuerlein, H. (1970). "Design of overflow rockfill dams." *Proc. Tenth Int. Congress of Large Dams*, 1, 587-598.

Isbash, S. (1935). *Construction of dams by dumping stones into flowing water*. U.S. Army Engr. District, Eastport, Me.

Knauss, J. (1979). "Computation of maximum discharge at overflow rockfill dams." *Proc. 13th Congress of Int. Commission of Large Dams*, 143-159.

Olivier, H. (1967). "Through and overflow rockfill dams—new design techniques." *Proc., Institution of Civil Engineers*, Mar., 36, 433-471.

Powledge, G. R., and Dodge, R. A. (1985). "Overtopping of small dams—an alternative for dam safety." *Proc. Hydr. and Hydro. in Small Computer Age*, ASCE, 2, Aug., 1071-1076.

Powledge, G. R., Ralston, D. C., Miller, P., Chen, Y. H., Clopper, P. E., and Temple, D. M. (1989a). "Mechanics of overflow erosion and embankments I: Research activities." *J. Hydr. Engrg.*, ASCE, 115(8), 1040-1055.

Powledge, G. R., Ralston, D. C., Miller, P., Chen, Y. H., Clopper, P. E., and Temple, D. M. (1989b). "Mechanics of overflow erosion and embankments II: Hydraulics and design considerations." *J. Hydr. Engrg.*, 115(8), 1056-1075.

Sherard, J. C., Dunnigan, L. P., and Talbot, J. R. (1984). "Basic properties of sand and gravel filters." *J. Geotech. Engrg.*, 110(6), 684-700.

Stephenson, D. (1979). *Rockfill in hydraulic engineering*. Elsevier Scientific Publishing Co., New York, N.Y., 215.

COMPARISONS OF SELECTED BED-MATERIAL LOAD FORMULAS

By Chih Ted Yang,¹ Fellow, ASCE, and Schenggan Wan²

ABSTRACT: Comparisons are made of the overall accuracy as well as the accuracy within different ranges of sediment concentration, Froude number, and slope for seven bed-material load formulas. Four formulas that can compute bed-material load transport by size fraction are used to determine the particle size distribution of the bed materials in transportation. One-thousand, one-hundred-nineteen sets of laboratory data and 319 sets of river data in the sand size range are used to evaluate and compare the accuracy of these formulas. The overall accuracy of formulas in descending order are those of Yang, Engelund and Hansen, Ackers and White (d_{50}), Laursen, Ackers and White (d_{35}), Colby, Einstein, and Toffaleti formulas when applied to laboratory flumes. The accuracy in descending order when applied to natural rivers are the formulas by Yang, Toffaleti, Einstein, Ackers and White (d_{50}), Colby, Laursen, Engelund and Hansen, and Ackers and White (d_{35}). However, these ratings may vary depending on the values of sediment concentration, Froude number, and slope of the data used in the comparison. The study also indicates that Yang's formula by size fraction can accurately predict the size distribution of bed material in transportation, while Einstein's hiding and lifting correction factors overcorrected the effect of nonuniform size distribution of bed material on total bed-material transport.

INTRODUCTION

There are numerous sediment transport formulas developed by different investigators for the prediction of bed load, suspended load, and total bed-material load in alluvial channels. Comparisons of the accuracy of these formulas were made by Yang and Stall (1973), White et al. (1975), Yang (1976), Alonso (1980), Brownlie (1981), Yang and Molinas (1982), the ASCE Task Committee ("Relationships between Morphology" 1982), Yang (1988), Vetter (1989), and the German Association for Water Resources and Land Improvement (1990), among others. These comparisons emphasize the overall accuracy of formulas without given detailed information of the hydraulic and sediment conditions under which measurements were made. Depending on the conditions under which data were collected for comparisons, the same formula could have different ratings of accuracy. This often causes confusion in the profession in the selection of formulas for solving engineering problems.

Measured sediment concentration, Froude number, and slope are used as parameters to define the hydraulic and sediment conditions. The analyses in this paper are limited to total bed-material load formulas due to the lack of general criteria to separate bed load from suspended load. Comparisons between computed bed-material size distribution and size distribution of bed materials in bed and in transportation are also made in this paper. The computer programs published by Stevens and Yang (1989) are used herein for

¹Int. and Special Proj. Coordinator, U.S. Bureau of Reclamation, Denver, CO 80225.

²Sr. Engr., Nanjing Hydr. Res. Inst., Nanjing, China.

Note. Discussion open until January 1, 1992. To extend the closing date one month, a written request must be filed with the ASCE Manager of Journals. The manuscript for this paper was submitted for review and possible publication on June 14, 1990. This paper is part of the *Journal of Hydraulic Engineering*, Vol. 117, No. 8, August, 1991. ©ASCE, ISSN 0733-9429/91/0008-0973/\$1.00 + \$.15 per page. Paper No. 26039.

RIPRAP SIZING AT TOE OF EMBANKMENT SLOPES

Calculation C-02 Project 35DJ2600 Appendix B Page B-20 of 37

By Steven R. Abt,¹ Fellow, ASCE, T. L. Johnson,² Member, ASCE,
Christopher I. Thornton,³ and Stuart C. Trabant⁴

ABSTRACT: A pilot study was conducted to evaluate existing rock-sizing techniques for stabilizing transition toes of embankments. The U.S. Bureau of Reclamation and the U.S. Army Corps of Engineers (Campbell) procedures were applied and determined to be conservative in sizing riprap. Embankment-overtopping tests were conducted placing 8.9, 13.0, and 19.8-cm-diameter stones at the slope transition. An alternative method was developed for sizing toe rock based upon the unit discharge, embankment slope, and flow concentration. The results indicate that an embankment toe can be stabilized with a smaller median stone size than previously anticipated. These results were verified for unit discharges of 0.54 m³/s/m or less.

INTRODUCTION

Rock toes, or toe basins, are often placed at the base of slope to stabilize and/or prevent rock placed on the side slope; serve as a toe drainage channel; serve as an impact basin and provide for energy dissipation from tributary flow; and provide erosion protection at the toe, transition flow from the side slope to adjacent properties, and/or provide gully intrusion protection to the embankment. Therefore, proper rock sizing is an imperative element of the design process to meet the project requirements while minimizing project costs.

Rock-sizing procedures have been developed by Isbash (1935), Olivier (1967), Hartung and Scheuerlein (1970), Stephenson (1979), and Abt and Johnson (1991) that can be applied for protecting embankment top slopes and side slopes for parallel flow conditions. However, these procedures were derived from through-flow and overtopping-flow conditions and are not considered applicable to flow transitioning from a side slope onto a horizontal or near-horizontal toe. In most cases, riprap placed at the toe of an embankment slope must be sized to ensure stability as runoff transitions from the embankment slope to the toe.

The U.S. Bureau of Reclamation (USBR) developed a riprap design procedure for applications in stilling basins (US-DOI 1978) founded on the work of Berry (1948). The USBR procedure is empirically based from extensive laboratory testing and field observations. The procedure estimates the median stone size as a function of the localized bottom velocity (in feet per second) of the flow, V_b , at the location where the flow transitions onto a stone-filled basin. If the bottom velocity cannot be determined, the local average velocity may be substituted to size the rock. The local average velocity can be determined using the U.S. Army Corps of Engineers procedures (USACE 1991). The stone size and/or stone weight can be determined from Fig. 1 (developed in English units).

Campbell (1966) presented a velocity-based riprap design procedure for stone placed in channels for bank stability and in stilling basin applications. Using the Isbash approach to rock sizing and applying the logarithmic law velocity distribution, Campbell developed a series of relationships between velocity

and stone size as presented in Fig. 2. Campbell presented velocity in feet per second, stone diameters in feet, and stone weights in pounds.

The USBR and Campbell rock-sizing procedures were developed to dissipate energy and provide a stable toe as flow transitions into a stilling basin or similar structure. The rock was sized to resist movement on a flat toe in the hydraulic jump development region of flow. These procedures are difficult to apply for relatively small rock requirements (<0.3 m). Both procedures have been routinely applied in engineering practice for sizing rock placed at the transitions of compound slopes (i.e., toe rock at the base of a slope) because alternative procedures have not yet been formulated. Interestingly, both procedures are perceived to yield conservative rock sizes.

A pilot program was performed to test and evaluate the USBR and Campbell rock-sizing procedures when applied to flow transitioning from an embankment side slope onto a rock toe. The experimental program was designed to observe and document rock movement and/or failure of riprap placed at the toe of an embankment and subjected to flow parallel to the embankment, thereby, transitioning into a rock toe.

TEST PROGRAM

Facility

An outdoor, concrete facility was used to accommodate a pilot, near-prototype experimental program. The model consisted of a supply pipeline with a control valve, a headbox with a manifold, an embankment, a rock toe, and an outlet sluice. A schematic profile of the test section is presented in Fig. 3.

The embankment was constructed in the test section with dimensions of 29.3 m (96.2 ft) long and 2.4 m (7.8 ft) wide. The embankment consisted of a moistened sand-fill material placed to a height of 1.83 m (6 ft). The top slope was 4.6 m (15 ft) long with a slope of 0.5%. The side slope was approximately 4.6 m (15 ft) long with a slope of 20%. The toe-of-the-slope (rock toe) basin was approximately 4.9 m (16 ft) in length with a rock depth transitioning from 0.91 m (3 ft) to 0.61 m (2 ft) as indicated in Fig. 3. A sand/clay soil was placed adjacent to the toe rock outlet extending downstream approximately 12.2 m (40 ft) at a slope of approximately 3% to simulate adjacent field conditions.

The embankment top slope and side slope were covered with a stabilized riprap layer of 8.9 cm (3.5 in.) diameter rock with a minimum depth of 1.5 times the median rock D_{50} . Rock was placed at the toe and smoothly transitioned the embankment side slope to the toe as indicated in Fig. 3.

Riprap

The riprap placed at the toe for each of three tests had median stone sizes of 8.9 cm (3.5 in.), 13.0 cm (5.1 in.), and

¹Prof., Dept. of Civ. Engrg., Colorado State Univ., Ft. Collins, CO 80523.

²Sr. Hydr. Engr., Ofc. of Nuclear Mat. Safety and Safeguards, U.S. Nuclear Regulatory Commission, Washington, DC 20555.

³Res. Assoc., Dept. of Civ. Engrg., Colorado State Univ., Ft. Collins, CO.

⁴Hydr. Engr., Mussetter Engineering Inc., Ft. Collins, CO 80524.
Note. Discussion open until December 1, 1998. To extend the closing date one month, a written request must be filed with the ASCE Manager of Journals. The manuscript for this paper was submitted for review and possible publication on December 3, 1996. This paper is part of the *Journal of Hydraulic Engineering*, Vol. 124, No. 7, July, 1998. ©ASCE, ISSN 0733-9429/98/0007-0672-0677/\$8.00 + \$.50 per page. Paper No. 14718.

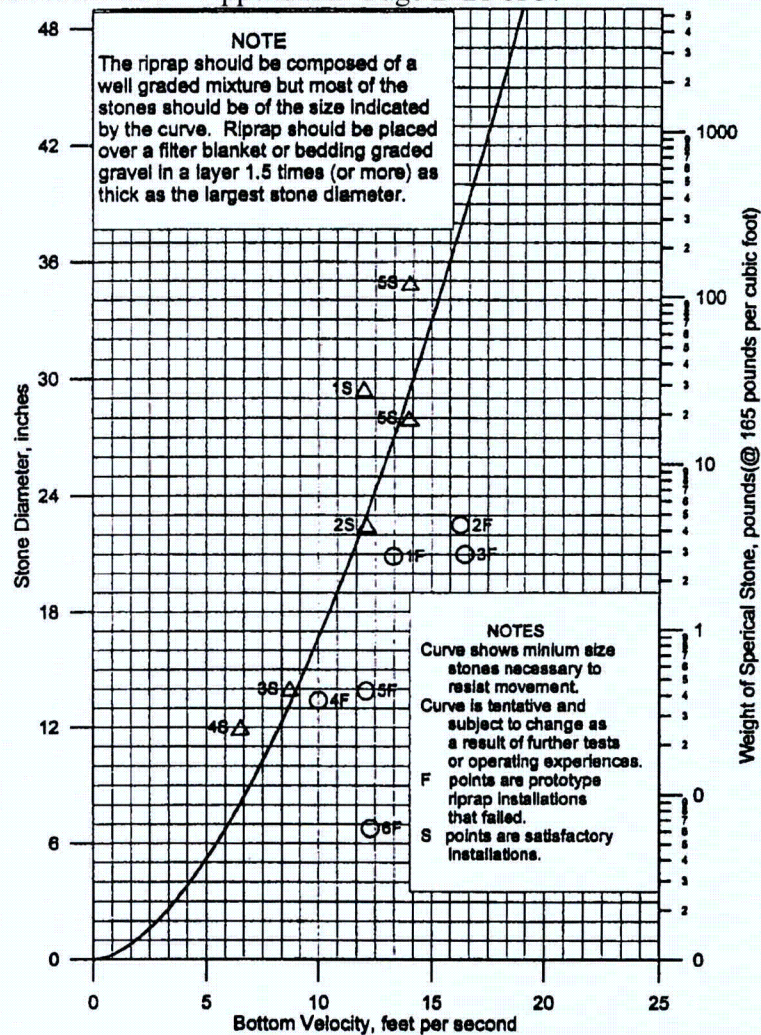


FIG. 1. Parametric Curve Used To Determine Maximum Stone Size in Riprap Mixture as Function of Channel Flow (USDOI 1978)

19.8 cm (7.8 in.), respectively. The stones were angular in shape with a specific gravity of 2.63. The coefficients of uniformity of the riprap ranged from 1.13 to 1.25 and are considered uniform.

Instrumentation

Instrumentation used to document the rock performance included a point gauge for monitoring the water surface on the top slope and slide slope of the embankment and a total station survey instrument with prism for monitoring the bed elevations at and near the toe. Velocities were measured using a Marsh-McBirney magnetic flowmeter, which was calibrated immediately prior to its use. Videotape and still photographs were used to visually document each test.

Test Procedure and Program

Once the embankment was constructed, a detailed survey was performed to document the pretest stone surface elevations. A 0.3-m grid was established throughout the toe basin area. The grid elevations served as the base elevations for monitoring riprap movement during and after each flow increment.

Each rock toe was tested in the same manner. The flow to the facility was initiated, and the headbox was slowly filled. Care was taken to prevent surging or pulsation of the flow as it first overtopped the embankment and entered the test sec-

tion. The discharge was increased to a flow of approximately 0.028 m³/s/m (1 cfs/ft). Flow was allowed to stabilize; then data were collected at four locations throughout the test section. Flow velocities were recorded at the embankment crest (Section 1), midslope (Section 2), toe of the slope immediately upstream of the hydraulic jump (Section 3), and 1.5-m downstream of the toe in the basin as indicated in Fig. 3. Point velocity measurements were taken at 0.6 times the flow depth from the surface at quarter intervals across the flume. Bed elevations were determined at the toe of the slope each time velocity measurements were obtained. After the velocity and bed elevations were recorded, the flow was increased and the data collection repeated. The process continued until the rock toe failed. The test was then terminated, the toe basin documented, and the embankment and/or toe basin reconstructed.

The testing program consisted of three tests; each test using one of the rock sizes (8.9, 13.0, and 19.8 cm) in the toe. The program test focused on the rock placed at and immediately downstream of the location where the flow transitioned from the side slope to the rock toe. It is acknowledged that the flow turbulence at the impact zone made direct observation difficult. Therefore, observations of the rock included monitoring audible vibrations of the stone. In addition to the vibrations, the point gauge and survey rod with base plate were used to monitor vertical displacement prior to stone entrainment or horizontal dislodgment. Rock movement was defined to be when stone was horizontally dislodged at the toe. Toe failure oc-

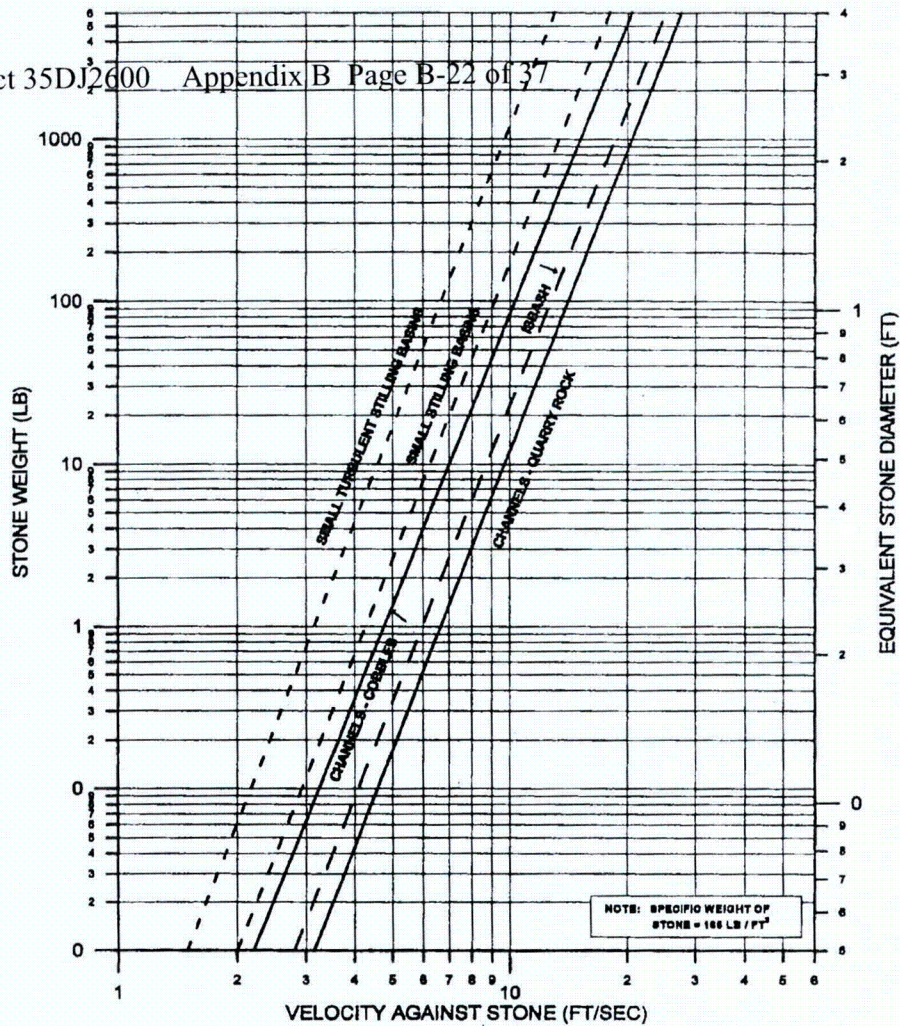


FIG. 2. Campbell Velocity-Stone-Sizing Relationships (Campbell 1966)

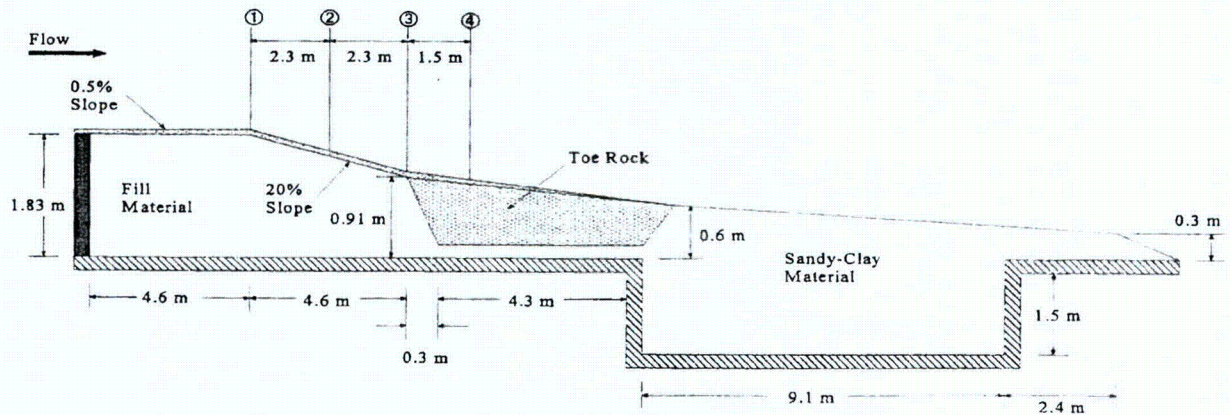


FIG. 3. Schematic Profile Section of Test Embankment

curred when the elevation of the toe degraded the equivalent of one median stone size. Although this is not a conservative definition of failure, it provides measurable criteria during testing.

RESULTS

When overtopping began, flow was conveyed down the embankment slope and transitioned onto the toe. Rock usually settled and/or adjusted to resist the impinging forces. Rock adjustment to incremental flow increases was not considered

a state of rock movement. As the flow increased, a point was attained where individual stones began to vibrate and/or vertically displace. Rock vibrations would eventually transition to rock displacement and/or displacement. In some instances, the rock displaced a short distance across the toe basin and then settled and/or lodged into other rocks in the basin. The flow eventually entrained the rock and completely transported the rock out of the basin. Identifying the exact point of rock movement was difficult (horizontal displacement) due to the turbulent conditions.

TABLE 1. Summary of Velocities

Test (1)	D_{50} (cm) (2)	q ($m^3/s/m$) (3)	Average Velocity (m/s)				Comment (8)
			Section 1 (4)	Section 2 (5)	Section 3 (6)	Section 4 (7)	
1	19.8	0.08	1.22	1.58	1.25	0.52	
	19.8	0.18	1.54	2.61	2.38	1.04	
	19.8	0.26	1.73	2.73	3.00*	0.81	
	19.8	0.36	1.87	3.01	3.26	0.96	
	19.8	0.44	2.02	3.15	3.50	0.94	
2	19.8	0.54	2.15	3.43	3.65	—	Failure
	13.0	0.09	1.09	1.65	1.98*	0.92	
	13.0	0.18	1.50	3.15	3.05	0.83	
	13.0	0.26	1.72	3.36	2.36	1.11	
	13.0	0.36	1.83	2.99	3.20	1.32	
3	8.9	0.08	—	—	1.05*	—	Failure
	8.9	0.08	1.49	1.75	—	—	
	8.9	0.18	1.56	2.04	1.78	1.78	
	8.9	0.26	1.69	2.18	2.85	1.81	

*Rock begins to vibrate/vertically translate based on visual and auditory observations.

A summary of the test measurements indicating the unit discharge and average velocities at each of the four monitoring sections is presented in Table 1. Incipient rock vibration and/or vertical displacement was detected based upon visual observations, videotapes, and auditory assessments as annotated in Table 1. Rock movement was monitored in Sections 3 and 4 based upon periodic bed elevation contouring. It is observed that the maximum flow velocities were measured at the toe of the slope adjacent to Section 3; velocities ranged from 2.85 m/s (9.34 ft/s) to 3.65 m/s (11.97 ft/s).

The flow impinged on the rock toe and transitioned into a hydraulic jump to dissipate the energy of the flow. The data demonstrate that the velocity was significantly slowed at the jump downstream of the toe by 50–70%.

ANALYSIS

During the low-flow segments of each test, flow conditions permitted the observation (visual and auditory) of rock vibra-

tion and/or vertical displacement (incipient movement). The 8.9 cm (3.5 in.), 13 cm (5.1 in.), and 19.8 cm (7.8 in.) stones were observed to vibrate/vertically displace at velocities of approximately 1.05 m/s (3.43 ft/s), 1.98 m/s (6.48 ft/s), and 3.0 m/s (9.84 ft/s), respectively. The incipient values were plotted on the USBR (USDOI 1978) rock-sizing design curve as presented in Fig. 4. The incipient movement measurements appear to agree closely with the data used to establish the USBR criteria. These results imply that the USBR used a conservative definition of rock movement.

Traditional procedures such as the USBR (USDOI 1978) and Campbell (1966) utilize the flow velocity estimated at the transition to determine the median rock size of the riprap in the stilling area (toe basin). These procedures are empirically based and determine rock sizes based upon flow impingement at the toe. The point velocities measured at stone failure are plotted with the USBR relation as presented in Fig. 5. A relation is projected through the test results to allow a comparison of these test results with the USBR procedure. When a flow velocity of 3.65 m/s (12.0 ft/s) transitions onto the rock toe, the USBR yields a median rock size of approximately 53.3 cm (21 in.). The initial results of these flume tests indicate that a 20.3 cm (8 in.) rock would fail at the same 3.65 m/s velocity (Section 3). The USBR rock size is larger than 260% of those indicated in Fig. 5. The Campbell procedure prescribes a stable rock size of 55.9 cm (22.0 in.) at a transition velocity of 3.65 m/s. It is important to note that flow velocities depicted in the USBR and Campbell procedures is measured immediately downstream of the jump transition, whereas the velocity presented herein is measured immediately upstream of the jump transition.

The USBR and Campbell procedures apparently provide a conservative approach to stone sizing in stilling basins and for rock placed at the toe of a slope. Although the rock size derived from the flume tests requires adjustment (increased) from the failure condition to reflect a nonmovement condition, considerable differences exist between these procedures.

An analysis was performed to evaluate how the unit dis-

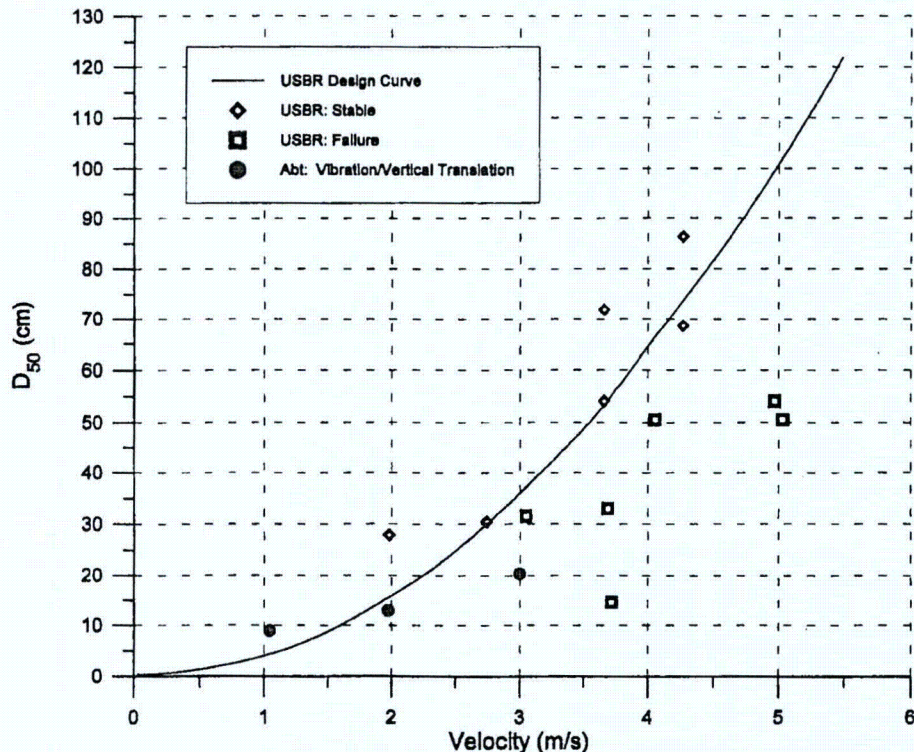


FIG. 4. Comparison of USBR Design Relation with Rock Movement Results

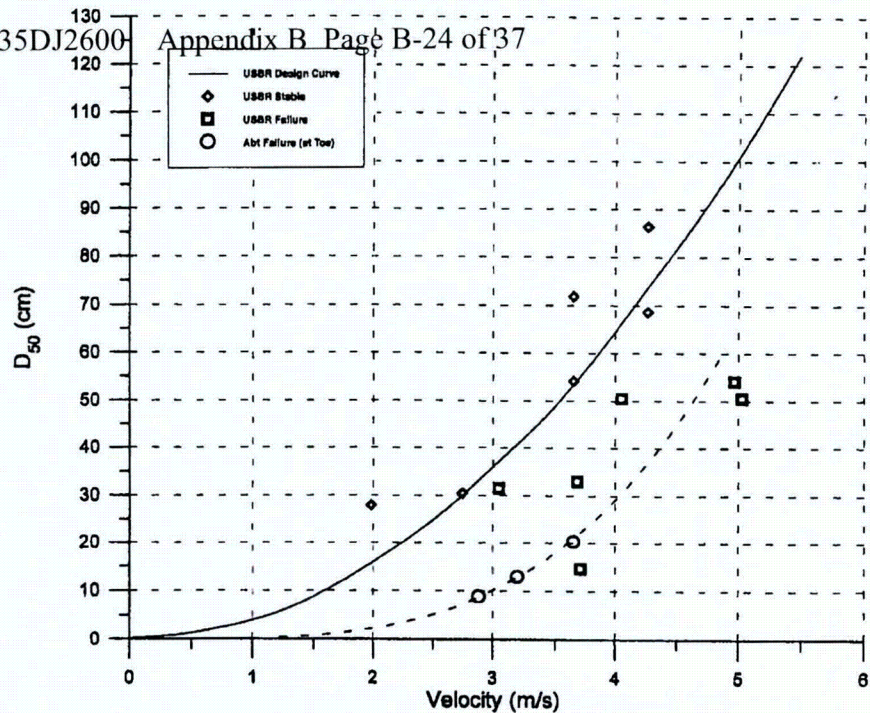


FIG. 5. Comparison of USBR Design Relation with Rock Failure Results

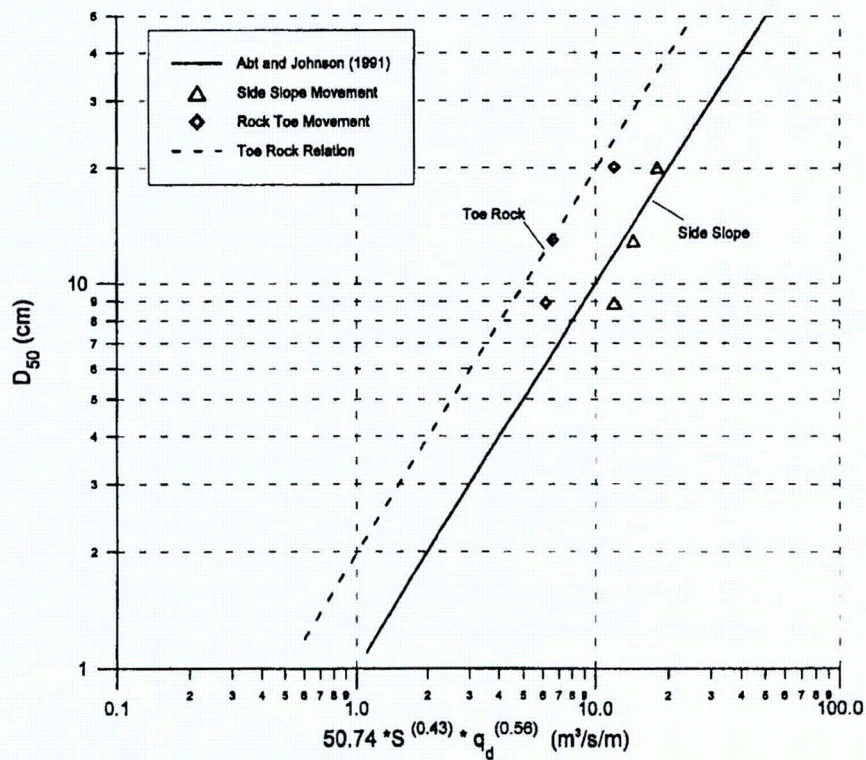


FIG. 6. Toe Rock Relations

charge affects the median rock size at the toe. Abt and Johnson (1991) formulated an expression for sizing the median rock, D_{50} , for top and side slopes of embankments as a function of the estimated design unit discharge, q_d , and the slope, S . Utilizing the unit discharge instead of the flow velocity relieves the designer from estimating the resistance to flow parameter as well as rectifying the differences between average, bottom,

and point velocities. The median stone size (Abt and Johnson 1991) designed to resist stone movement on embankment slopes is expressed as

$$D_{50} = 5.23 \times S^{0.43} q_d^{0.56} \quad (1)$$

where q_d is in cubic feet per second per foot; and D_{50} is in inches. Eq. (1), expressed in SI units is

$$D_{50} = 50.74 \times S^{0.43} \times q_d^{0.56} \quad (2)$$

where D_{50} is in centimeters; and q_d is in cubic meters per second per meter.

Stone movement, upstream of Section 3, was documented and plotted in Fig. 6. The stone movement of the embankment slope reasonably agrees with the Abt and Johnson relation. The data indicate that the Abt and Johnson relation, plus 100%, envelops the rock toe size for unit discharges $\leq 0.54 \text{ m}^3/\text{s/m}$ (5.77 cfs/ft).

An expression can be derived to size the median rock size based upon the toe rock relation presented in Fig. 6. The modified expression should incorporate (1) the rock size differential between the two relations portrayed in Fig. 6; and (2) the flow concentration, C_f , aspect of flow discussed by Abt and Johnson. Abt et al. (1988) and Abt and Johnson (1991) reported that flow channelization develops on uniformly graded slopes. Flow concentrations, or areas where flow was diverted around larger stones and directed into zones of smaller stones, created subchannels. The unit discharge in the subchannels was documented to be at least three times ($1 < C_f < 3$) the uniform unit discharge before channelization. The magnitude of C_f should depend upon the hazard level of the protected surface. For example, a C_f of 1.0 should be used for low-hazard applications, whereas a C_f of 2-3 should be used for high-hazard conditions. Therefore, the inclusion of a flow concentration factor for rock toe sizing is warranted.

Eq. (1) may be shifted such that the median stone size is designed to resist stone movement rather than failure at the transition of the toe as

$$D_{50} = 10.46 \times S^{0.43} \times (C_f \times q_d)^{0.56} \quad (3)$$

where q_d = design unit discharge in cubic feet per second; D_{50} is in inches, and C_f = flow concentration factor. Eq. (3) expressed in SI units is

$$D_{50} = 100.5 \times S^{0.43} \times (C_f \times q_d)^{0.56} \quad (4)$$

where q_d is in cubic meters per second per meter; and D_{50} is in centimeters. Extrapolation of Eqs. (3) and (4) beyond unit discharges of $0.54 \text{ m}^3/\text{s/m}$ are not recommended without further testing.

These flow tests indicate that the rock toe may be sized based upon the unit discharge and the embankment slope transitioning into the rock basin. The rock toe should minimally extend 10-stone-diameters downstream of the toe and the stone layer should be a minimum of 3-stone-diameters thick. It is recognized that these few data points do not necessarily define a definitive relation. Further, it is noted that (3) and (4) are applicable to a small range of flows ($< 0.54 \text{ m}^3/\text{s/m}$) and do not incorporate a factor of safety. However, (3) and (4) provide the user a unit discharge rather than velocity-based approach,

accounts for concentrated flows, and reduces the conservatism of design.

CONCLUSIONS

A few methods or procedures exist that size riprap placed at the toe of a slope. Existing rock-sizing methods are velocity based, focus on energy dissipation, and are extremely conservative. A near-prototype, pilot flume study was performed where flow overtopped an embankment and transitioned into a rock toe comprised of 8.9, 13.0, and 19.8 cm (median stone diameter). The test results indicate that the stone size required to stabilize the riprap layer at the toe is approximately 100% larger than the rock size required to stabilize embankment side slopes. A method was developed for sizing rock placed at an embankment toe based upon the embankment slope and unit discharge at the compound slope transition. Although the unit discharge approach to rock sizing is based upon a limited database, the results indicate that a less conservative rock size may be sufficient to stabilize the embankment toe. It is acknowledged that the database must be expanded.

ACKNOWLEDGMENT

This project was sponsored by the Office of Nuclear Material Safety and Safeguards, U.S. Nuclear Regulatory Commission. The findings and opinions expressed are those of the writers and do not necessarily represent the U.S. Nuclear Regulatory Commission or Colorado State University.

APPENDIX. REFERENCES

- Abt, S. R., et al. (1988). "Development of riprap design criteria by riprap testing in flumes: Phase II—Follow-Up Investigations." *NUREG/CR-4651, ORNL/TM-10100/V2*, U.S. Nuclear Regulatory Commission, Washington, D.C., 2, 85.
- Abt, S. R., and Johnson, T. L. (1991). "Riprap design for overtopping flow." *J. Hydr. Engrg.*, ASCE, 117(8), 959-972.
- Berry, N. K. (1948). "The start of bed load movement," MS thesis, Univ. of Colorado, Boulder, Colo.
- Campbell, F. B. (1966). "Hydraulic design of rock riprap." *Misc. Paper No. 2-777, Ofc. of the Chf. of Engrs.*, U.S. Army Wtrwy. Experiment Station, Vicksburg, Miss.
- Hartung, F., and Scheuerlein, H. (1970). "Design of overflow rockfill dams." *Proc., 10th Int. Congr. of Large Dams*, 1, 587-598.
- Isbush, S. (1935). "Construction of dams by dumping stones into flowing water." *Rep.*, U.S. Army Engrg. Dist., U.S. Army Corps of Engrs., Eastport, Maine.
- Olivier, H. (1967). "Through and overflow rockfill dams—New design techniques." *Proc., Instn. of Civ. Engrs.*, 36, 433-471.
- Stephenson, D. (1979). *Rockfill in hydraulic engineering*. Elsevier Scientific Publishing Co., New York, N.Y., 215.
- USACE. (1991). "Hydraulic design of flood control channels." *EM1110-2-1601*, Dept. of the Army, U.S. Army Corps of Engineers, Washington, D.C.
- USDOI. (1978). "Hydraulic design of stilling basins and energy dissipators." *Engrg. Monograph No. 25*, U.S. Bureau of Reclamation, U.S. Department of the Interior, Washington, D.C.

t is the time in minutes.

t_0 is a base time used in the experiments to derive coefficients (316 minutes unless specified otherwise).

For noncircular or part full culverts, the diameter D can be replaced by an equivalent depth y_e , where y_e is defined as

$$y_e = (A/2)^{1/2}$$

and A is the cross sectional area of flow. Modifying Equation (V-1) to include the equivalent depth results in the general expression.

$$\text{Dimensionless Scour Geometry} = \alpha_e \left(\frac{Q}{\sqrt{g} y_e^{5/2}} \right)^\beta \left(\frac{t}{t_0} \right)^\theta \quad (V-2)$$

where:

$$\alpha_e = \alpha 0.632 \cdot 5^{\beta-1} \text{ for } h_s, w_s, \text{ and } L_s$$

$$\alpha_e = \alpha 0.632 \cdot 5^{\beta-3} \text{ for } V_s$$

The values of the coefficients α_e , β , and θ in Equations V-1 and V-2 are given in Table V-1.

Gradation

The cohesionless bed materials presented in Table V-1 are categorized as either uniform (U) or graded (G). The grain size distribution is determined by performing a sieve analysis (ASTM DA22-63). The standard deviation (σ) is computed as:

$$\sigma = \left(\frac{d_{84}}{d_{16}} \right)^{1/2}$$

where the values of d_{84} and d_{16} are extracted from the grain size distribution. If $\sigma < 1.5$, the material is considered to be uniform; if $\sigma \geq 1.5$, the material is classified as graded.

Cohesive Soils

If the cohesive soil is a sandy clay similar to the one tested at Colorado State University by Abt et al (8), Equation (V-1) or (V-2) and the appropriate coefficients in Table V-1 can be used to estimate the scour hole dimensions. The sandy clay tested had 58 percent sand, 27 percent clay, 15 percent silt and 1 percent organic matter; had a mean grain size of 0.15 mm and had a plasticity index, PI, of 15.

Since Equations V-1 and V-2 do not include soil characteristics, they can only be used for soils similar to the ones tested. Shear number expressions, that related scour to the critical shear stress of the soil, were derived to have a wider range of applicability for cohesive soils besides the one specific sandy clay that was tested. The shear number expressions for circular culverts are:

$$\left[\frac{h_s}{D}, \frac{W_s}{D}, \frac{L_s}{D}, \text{ or } \frac{V_s}{D} \right] = \alpha \left(\frac{\rho V^2}{\tau_c} \right)^\beta \left(\frac{t}{t_o} \right)^\theta \quad (V-3)$$

and for other shaped culverts:

$$\left[\frac{h_s}{y_e}, \frac{W_s}{y_e}, \frac{L_s}{y_e}, \text{ or } \frac{V_s}{y_e} \right] = \alpha_e \left(\frac{\rho V^2}{\tau_c} \right)^\beta \left(\frac{t}{t_o} \right)^\theta \quad (V-4)$$

where: $\frac{\rho V^2}{\tau_c}$ is the modified shear number

V = outlet mean velocity

τ_c = critical tractive shear stress

ρ = fluid density

$\alpha_e = \frac{\alpha}{.63}$ for h_s , W_s , and L_s

$\alpha_e = \frac{\alpha}{(.63)^3}$ for V_s

The values of the coefficients α , β , θ , and α_e in Equations V-4 and V-5 are presented in Table V-1. The critical tractive shear stress (2) is defined as

$$\tau_c = 0.0001 (S_v + 180) \tan (30 + 1.73 \text{ PI}) \quad (V-5)$$

where S_v is the saturated shear strength in pounds per square inch and PI is the Plasticity Index from the Atterberg Limits.

It is recommended that Equations V-3 and V-4 be limited to sandy clay soils with a plasticity index of 5-16.

Time of Scour

The time of scour is estimated based upon a knowledge of peak flow duration. Lacking this knowledge, it is recommended that a time of 30 minutes be used in Equations V-1, V-2, V-3, and V-4. The tests indicate that approximately 2/3 to 3/4 of the maximum scour occurs in the first 30 minutes of the flow duration.

It should be noted that the exponents for the time parameter in Table V-1 reflect the relatively flat part of the scour-time relationship and are not applicable for the first 30 minutes of the scour process.

Headwalls

Installation of headwalls (6) flush with the culvert outlet moves the scour hole downstream. However, the magnitude of the scour geometries remain essentially the same as for the case without the headwall. If the culvert is installed with a headwall, the headwall should extend to a depth equal to the maximum depth of scour.

SUMMARY

The prediction equations presented in this chapter are intended to serve along with field reconnaissance as guidance for determining the need for energy dissipators at culvert outlets. It should be remembered that the equations do not include long-term channel degradation of the downstream channel. The equations are based on tests which were conducted to determine maximum scour for the given condition and therefore represent what might be termed worst case scour geometries. The equations were derived from tests conducted by the Corps of Engineers (1), and Colorado State University (5), (6), (7), (8) and (9).

Design Procedure

1. Perform a hydrologic analysis of the drainage in which the culvert is located or to be placed. Estimate the magnitude and duration of the peak discharge. Express the discharge in cfs and the duration in minutes.

The discharge intensity is

$$D.I. = \frac{Q}{\sqrt{g} D^{5/2}} \text{ for circular culverts flowing full}$$

$$D.I. = \frac{Q}{\sqrt{g} y_e^{5/2}} \text{ for other shapes}$$

where $y_e = \left(\frac{A}{2}\right)^{1/2}$

FOR COHESIONLESS MATERIALS, OR THE 0.15mm SANDY CLAY

2. Compute the discharge intensity when the culvert is flowing at the peak discharge.
3. Determine scour coefficients from Table V-1.
4. Compute the scour hole dimensions from

$$\left[\frac{h_s}{D}, \frac{W_s}{D}, \frac{L_s}{D}, \text{ or } \frac{V_s}{D^3}\right] = \alpha \left(\frac{Q}{\sqrt{g} D^{5/2}}\right)^\beta \left(\frac{t}{316}\right)^\theta \quad (V-1)$$

or

$$\left[\frac{h_s}{y_e}, \frac{W_s}{y_e}, \frac{L_s}{y_e}, \text{ or } \frac{V_s}{y_e}\right] = \alpha_e \left(\frac{Q}{\sqrt{g} y_e^{5/2}}\right)^\beta \left(\frac{t}{316}\right)^\theta \quad (V-2)$$

FOR OTHER COHESIVE MATERIALS WITH PI FROM 5 TO 16

- a. Compute the culvert outlet velocity in feet/sec.
- b. Obtain a soil sample at the proposed culvert location.
- c. Perform Atterberg limits tests and determine the plasticity index, PI (ASTM D423-36).

- d. Saturate a sample and perform an unconfined compressive test (ASTM D211-66-76) to determine the saturated shear stress, S_v , in pounds per square inch.
 - e. Compute the critical tractive shear strength, τ_c , from equation V-5.
 - f. Compute the modified shear number $\frac{\rho v^2}{\tau_c}$
3. Determine scour coefficients from Table V-1.
 4. Compute the desired scour hole dimensions from

$$\left[\frac{h_s}{D}, \frac{W_s}{D}, \frac{L_s}{D}, \text{ or } \frac{V_s}{D} \right] = \alpha \left(\frac{V^2}{\tau_c} \right)^\beta \left(\frac{t}{316} \right)^\theta$$

for circular culvert

or

$$\left[\frac{h_s}{y_e}, \frac{W_s}{y_e}, \frac{L_s}{y_e}, \frac{V_s}{y_e^3} \right] = \alpha_e \left(\frac{V^2}{\tau_c} \right)^\beta \left(\frac{t}{316} \right)^\theta$$

for noncircular culverts.

Example Problem Cohesionless Material

Determine the scour geometry--maximum depth, width, length and volume of scour--for a proposed circular 30-inch C.M.P. discharging an estimated 50 cfs when flowing full. The downstream channel is composed of a graded gravel material.

1. The duration of the peak discharge of 50 cfs is not known. Therefore, a peak flow duration of 30 minutes will be estimated.
2. The circular, 30-inch C.M.P. at 50 cfs will have a discharge intensity of

$$D.I. = \frac{50}{\frac{\sqrt{g} (30)^{5/2}}{12}} = \frac{50}{(5.67)(2.5)^{5/2}} = 0.89$$

3. The coefficients of scour obtained from Table V-1 are:

	α	β	θ
Depth of Scour	1.49	.50	.03
Width of Scour	8.76	0.89	.10
Length of Scour	13.09	0.62	.07
Volume of Scour	42.31	2.28	.17

4. Scour hole dimensions:

$$\text{depth: } \frac{h_s}{D} = \alpha \left(\frac{Q}{\sqrt{g} D^{2.5}} \right)^\beta \left(\frac{t}{316} \right)^\theta$$

$$= 1.49 (0.89)^{0.50} (0.09)^{.03}; h_s = 3.27 \text{ ft}$$

$$\text{width: } \frac{W_s}{D} = 8.76(0.89)^{0.89} (.09)^{.10}; W_s = 15.5 \text{ ft}$$

$$\text{Length: } L_s = 13.09(0.89)^{0.62} (.09)^{.07}; L_s = 25.72 \text{ ft}$$

$$\text{Volume: } V_s = 42.31(0.89)^{2.28} (.09)^{.17}; V_s = 335.79 \text{ ft}^3$$

5. The location of the maximum scour (Figure V-2)

$$0.4 (L_s) = .4 (25.72) = 10.3 \text{ ft downstream of the culvert outlet}$$

Example Problem Cohesive Material

Determine the scour geometry—maximum depth, width, length and volume of scour for an existing circular 24-inch C.M.P. discharging an estimated 40 cfs when flowing full. The downstream channel is composed of a sandy-clay material.

1. The duration of the peak discharge of 40 cfs is not known. Therefore, a peak flow duration of 30 minutes will be estimated.
2. a. The average velocity at the culvert outlet is:

$$V = \frac{Q}{A} = \frac{40.0}{3.14} = 12.74 \text{ fps}$$

- b-e. The sandy-clay material was tested and found to have a Plasticity Index (PI) of 12 and a saturated shear strength (Sv) of 240 psi.

The critical tractive shear can be estimated by substituting into Equation V-5

$$\tau_c = 0.001 (240 + 180) \tan (30 + 1.73(12))$$

$$0.001(420) \tan (50.76) = 0.51 \text{ lb/ft}^2$$

- f. The modified shear number $S_{n_{mod}} = \frac{(\rho V^2)}{\tau_c}$ is:

$$S_{n_{mod}} = \frac{1.94 (12.74)^2}{0.51} = 617.4$$

3. The experimental coefficients α , β and θ from Table V-1 are

	α	β	θ
Depth	.86	.18	.10
Width	3.55	.17	.07
Length	2.82	.33	.09
Volume	.62	.93	.23

4. The scour hole dimensions are:

$$\frac{h_s}{D} = \alpha \left(\frac{\rho V^2}{\tau_c} \right)^\beta \left(\frac{t}{316} \right)^\theta$$

$$= .86(617.4)^{.18} (.09)^{.10}; \quad h_s = 2.14 \times 2 = 4.30 \text{ ft}$$

$$\frac{W_s}{D} = 3.55(617.4)^{.17} (.09)^{.07}; \quad W_s = 8.94 \times 2 = 27.9 \text{ ft}$$

$$\frac{L_s}{D} = 2.82(617.4)^{.33} (.09)^{.09}; \quad L_s = 18.92 \times 2 = 37.8 \text{ ft}$$

$$\frac{V_s}{D^3} = .62(617.4)^{.93} (.09)^{.23}; \quad V_s = 140.3 \times 2^3 = 1122.5 \text{ ft}^3$$

5. Location of maximum depth of scour (Figure V-2)

$$0.4 L_s = 0.4(37.8) = 15.1 \text{ ft downstream of culvert outlet}$$

By Steven R. Abt,¹ James F. Ruff,² Members, ASCE,
and Rodney J. Wittler,³ Associate Member, ASCE

INTRODUCTION

Estimating flow through rockfill and protective rock covers can be a useful procedure for designing or evaluating flood control, waste repository, and waterways structures. Often, a knowledge of rockfill and rock cover transmissibility and the effect of through-flow forces on the stone are needed for structural stability analyses. Through-flow velocity is defined as the average velocity of water flow through rock voids. An understanding of turbulent flow in a rock medium is needed for through-flow analyses.

Numerous investigators have analyzed turbulent through flow, including Weiss (1951), Escande (1953), Olivier (1967), and Stephenson (1979). Wilkins (1956, 1963) performed laboratory transmissivity tests on cylindrical specimens, resulting in the relation

$$V_v = 32.9m^{0.5}i^{0.54} \quad (1)$$

where V_v = the average velocity of water through rock voids in inches per second; i = the hydraulic gradient; and m = the hydraulic mean radius of rock voids in inches (volume of voids divided by total surface area of the particles).

Parkin (1963; Parkin et al. 1966) performed tests on clean, angular gravel (3/8–3/4 in.). Parkin derived the expression

$$i = 1.86V_v^{1.86} \quad (2)$$

where i = the hydraulic gradient and V_v = the average velocity of flow through the rock voids in feet per second.

Leps (1973) consolidated the concepts of Escande, Wilkins, and Parkin and presented an expression for the average flow through rockfill for turbulent conditions as

$$V_v = Wm^{0.5}i^{0.54} \quad (3)$$

where V_v = the average velocity of water in rockfill voids in inches per second; W = an empirical constant; m = the hydraulic mean radius in inches; and i = the hydraulic gradient. The average through-flow velocity is estimated by obtaining the appropriate value from Table 1 and inserting it into Eq. 3. Leps' relation is applicable to uniformly sized rock with a specific gravity of 2.87.

Wilkins (1956, 1963), Olivier (1967), and Stephenson (1979) reported that

¹Prof., Dept. of Civ. Engr., Colorado State Univ., Fort Collins, CO 80523.

²Prof., Dept. of Civ. Engr., Colorado State Univ., Fort Collins, CO.

³Res. Hydr. Engr., U.S. Bureau of Reclamation, Denver, CO 80225.

Note. Discussion open until October 1, 1991. To extend the closing date one month, a written request must be filed with the ASCE Manager of Journals. The manuscript for this paper was submitted for review and possible publication on January 23, 1990. This paper is part of the *Journal of Hydraulic Engineering*, Vol. 117, No. 5, May, 1991. ©ASCE, ISSN 0733-9429/91/0005-0670/\$1.00 + \$.15 per page. Paper No. 25842.

TABLE 1. Coefficients for Estimating Through Flow (for Eq. 3)

Rock Size		$Wm^{0.5}$ (3)
in. (1)	cm (2)	
0.75	1.9	10
2	5.1	16
6	15.2	28
8	20.3	32
24	61.0	58
48	121.9	84

Note: Adapted from Leps (1971).

the average interstitial, or through-flow, velocity was a function of the riprap properties and the gradient. However, in the preliminary design process, the engineer must assume a representative stone size and gradation before extensive material testing or analysis of a rock source is done. Therefore, a procedure that predicts the average through-flow velocity for riprap and rockfill would be helpful. This note presents a method.

EXPERIMENTAL PROGRAM

An experimental program was conducted by Abt et al. (1987, 1988) at Colorado State University in which embankments with slopes ranging from 1–20% were constructed in recirculating flumes. These model embankments were similar to those designed for waste repositories. The embankments consisted of a compacted sand material covered with a geotextile. A 6-in. (0.15-m) sand-gravel bed was placed atop the geotextile. Riprap was placed on top of the bedding material in uniform layer thicknesses ranging from 3 in. (7.6 cm) to 12 in. (30.5 cm). The embankments were constructed horizontally upstream of the crest and transitioned to the desired downstream slope. Water overtopped the embankment crest and flowed through the riprap.

The riprap was obtained from a limestone quarry. Median stone sizes D_{50} , ranged from 1.02 in. (2.6 cm) to 6.2 in. (15.8 cm), as presented in Table 2. The rock specific gravity was 2.65, the gradation d_{84}/d_{16} , ranged from 1.80 to 2.72, and the stones were angular.

A tracer injection and recording system was developed to document the flow velocities through the riprap layer. The system consisted of a pressure-operated tracer injector, tracer-sensitive probes, a multichannel selector, and a multichannel strip chart recorder. Each tracer-sensitive probe was fabricated with three tracer-sensitive elements placed in the lower 8 in. (20.3 cm) of the probe. The tracer injector was fabricated with three injection ports. The injector port spacing was similar to the spacing of the tracer-sensitive elements in the probe; the spacing was 3 in. Fig. 1 shows a schematic of the injector and sensor in the rock layer. A salt solution was used as the tracer.

The injector ports were approximately aligned in the riprap layer with the elements in the tracer-sensitive probe. The lowest injector was approximately 1 in. (2.54 cm) above the riprap-bedding interface. The injector was placed 10–12 in. (25.4–30.5 cm) upstream from the first tracer-sensitive probe.

TABLE 2. Interstitial Velocity Summary

Test number (1)	Median Stone Size, D_{50}		D_{10}		Riprap Layer Thickness		Embankment slope (8)	Average Interstitial Velocity V_i	
	in. (2)	cm (3)	in. (4)	cm (5)	in. (6)	cm (7)		fps (9)	cm/s (10)
	61	1.02	2.6	0.6	1.5	3		7.6	0.01
71	1.02	2.6	0.6	1.5	3	7.6	0.02	0.13	4.0
91	1.02	2.6	0.6	1.5	3	7.6	0.10	0.24	7.3
41	2.2	5.6	1.1	2.8	6	15.2	0.01	0.15	4.6
31	2.2	5.6	1.1	2.8	6	15.2	0.02	0.23	7.0
101	2.2	5.6	1.1	2.8	6	15.2	0.10	0.36	11.0
111	2.2	5.6	1.1	2.8	6	15.2	0.10	0.37	11.3
3	4.1	10.4	2.0	5.1	12	30.5	0.20	0.72	21.9
4	4.1	10.4	2.0	5.1	12	30.5	0.20	0.97	29.6
8	5.1	13.0	3.45	8.8	12	30.5	0.20	1.04	31.7
9	5.1	13.0	3.45	8.8	12	30.5	0.20	0.86	26.2
14	6.2	15.7	3.8	9.7	12	30.5	0.20	1.47	44.8
26	2.0	5.1	1.03	2.6	3	7.6	0.10	0.46	14.0
28	2.0	5.1	1.03	2.6	4	10.2	0.10	0.50	15.2
30	2.0	5.1	1.03	2.6	6	15.2	0.10	0.54	16.5
39	4.0	10.2	2.0	5.1	6	15.2	0.10	0.62	18.9
41	4.0	10.2	2.0	5.1	8	20.3	0.10	0.66	20.1
47	4.0	10.2	1.2	3.0	12	30.5	0.10	0.48	14.6
50	4.0	10.2	2.38	6.0	12	30.5	0.10	0.66	20.1

The second probe was 20–24 in. (50.3–61.0 cm) downstream from the injector. Velocity measurements were taken in the upper third and lower third segments of the embankment slope.

In each of the 19 tests, flow was established in the flume with the water surface stabilized at a point just above the riprap surface. The tracer was then injected into the rock layer. An event marker on the strip chart recorder indicated when the injector was triggered. Output from the tracer-sensitive probe elements also was recorded on the strip chart so that tracer concentration versus time could be observed and documented. A tracer concentra-

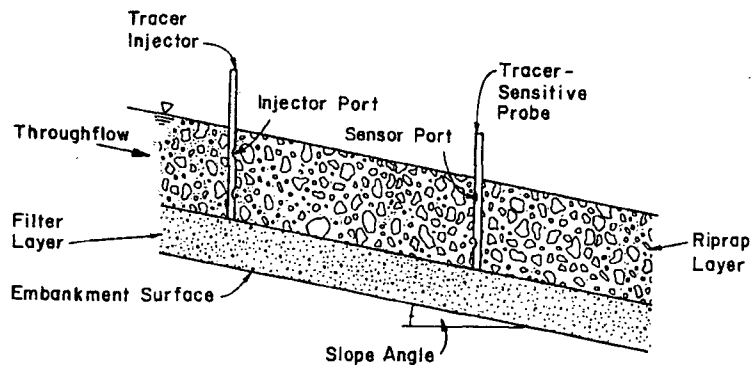


FIG. 1. Schematic of Tracer, Injector, and Sensor in Rock Layer

tion curve was recorded for each injector port. The peak of the concentration curve was used to estimate the interstitial velocity. Knowing the time of injection, travel time between injector and tracer ports, and the distance between ports, one could compute the average interstitial velocity for each test condition in the rock layer. Each velocity reported in Table 2 represents the average value of one-to-five velocity measurement locations in each profile. The number of velocity measurements taken was a function of the layer thickness; a 3-in. (7.62 cm) layer allowed space for a single velocity measurement.

RESULTS

The average interstitial velocities V_i that resulted from the 19 flume tests are presented in Table 2. Velocities through the rock layers ranged from 3–44.8 cm/s for embankment slopes of 1–20%, respectively. At a constant slope of 10%, average interstitial velocities ranged from 7.3–20.1 cm/s for median stone sizes of 2.6–10.2 cm, respectively.

A sensitivity analysis was performed, relating the rock size and embankment gradient to the average interstitial velocity. Representative stone sizes of D_{50} , D_{40} , D_{30} , D_{20} , D_{15} , and D_{10} , in conjunction with the slope, were correlated with the measured interstitial velocity. The analysis indicated that

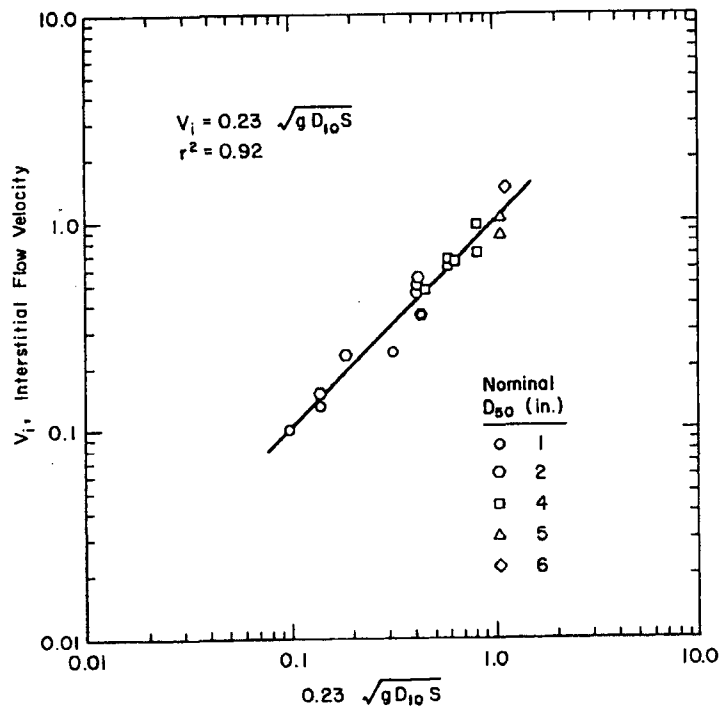


FIG. 2. Average Interstitial Velocity through Riprap as Function of D_{10} and Gradient

The D_{10} stone diameter (at which 10% of the weight is finer) provided the highest coefficient of correlation of the stone sizes tested. The interstitial velocities are shown in Fig. 2, as a function of the rock size D_{10} and the slope. A linear regression analysis yielded the expression

$$V_i = 0.23(gD_{10}S)^{1/2} \dots \dots \dots (4)$$

where V_i = the average interstitial velocity in feet per second; g = the acceleration of gravity in ft/sec^2 , D_{10} is in inches, and S = the gradient expressed in decimal form. The correlation coefficient for Eq. 4 is $r^2 = 0.92$. It appears that the D_{10} stone size controls the rate of flow through the stone layer void space. Eq. 4 can be expressed in SI units as

$$V_i = 0.79(gD_{10}S)^{1/2} \dots \dots \dots (5)$$

The flow distance between the injector port and the sensor port was dependent on the probe placement in the rock layer. In some instances, the injector discharged directly into a large stone, resulting in immediate tracer dilution and the tracer taking a sinuous path toward the sensor. In other cases, the injector discharged into a void between the stones, resulting in a shortened path between injector and sensor. Because of the high variability in flow distance, the average interstitial velocities through the rock layer varied $\pm 40\%$. Velocity variability was dependent on stone size.

CONCLUSIONS

A series of 19 flume tests was conducted, in which flow was routed through a riprap layer, and the average interstitial, or through-flow, velocity was measured and recorded. Flow measurements varied $\pm 40\%$ about the average velocity. A predictive relationship was developed in which the average interstitial velocity was determined to be a function of the embankment slope and rock size D_{10} , as presented in Eq. 4. The predictive relationship provides the designer with a method for estimating through flow based upon a representative stone size, gradation, and embankment slope. The relationship was developed for stone sizes with a D_{50} ranging from 2.6 cm to 15.7 cm, and D_{10} ranging from 1.5 cm to 9.7 cm.

ACKNOWLEDGMENT

This research was sponsored by the Office of Nuclear Material Safety and Safeguards, U.S. Nuclear Regulatory Commission.

APPENDIX. REFERENCES

- Abt, S. R., Khattak, M. S., Nelson, J. D., Ruff, J. F., Shaikh, A., Wittler, R. J., Lee, D. W., and Hinkle, N. E. (1987). "Development of riprap design criteria by riprap testing in flumes: Phase I." *NUREG/CR-4651*, U.S. Nuclear Regulatory Commission, Vol. 1, 48-53.
- Abt, S. R., Wittler, R. J., Ruff, J. F., LaGrone, D. L., Khattak, M. S., Nelson, J. D., Hinkle, N. E., and Lee, D. W. (1988). "Development of riprap design criteria by riprap testing in flumes: Phase II." *NUREG/CR-4651*, U.S. Nuclear Regulatory Commission, Vol. 2, 57-65.
- Escande, L. (1953). "Experiments concerning the infiltration of water through a rock mass." *Proc., Minnesota Int. Hydrology Convention*.

- Os, T. M. (1973). "Flow through rockfill." *Embankment dam engineering*, John Wiley and Sons, 87-107.
- Olivier, H. (1967). "Through and overflow rockfill dams—New design techniques." *J. Inst. of Civ. Engrg.*, 36, 433-471.
- Parkin, A. K. (1963). "Rockfill Dams with Inbuilt spillway." *Bulletin No. 6*, Water Resources Edn. Australia, Melbourne, Australia.
- Parkin, A. K., Trollope, D. H., and Lawson, J. D. (1966). "Rockfill structures subject to water flow." *J. Soil Mech. Found. Div.*, ASCE, (6), 135.
- Stephenson, D. (1979). *Rockfill in hydraulic engineering: Developments in geotechnical engineering 27*, Elsevier Scientific Publishing Company, Amsterdam, the Netherlands, 38-60.
- Weiss, A. (1951). "Construction technique of passing floods over earth dams." *Trans. ASCE*, 116, 1158-1173.
- Wilkins, J. K. (1956). "Flow of water through rockfill and its application to the design of dams." *Proc., Second Australian—New Zealand Soil Conf.*, Mechanics and Foundation Engrg., Christchurch, New Zealand.
- Wilkins, J. K. (1963). "The stability of overtopped rockfill dams." *Proc. Fourth Australian Conf. on Soil Mech. Found. Engrg.*, Adelaide, Australia, 1-7.

JACOBS

Calculation Cover Sheet

(Ref. FOWI 116 Design Calculations)

Calculation No:
C-03

Page 1 of 20 – Plus
Appendices 53 Pgs

Rev. No.: 0

Revision Date:

Previous Revision
Date:

Current Revision
Date: 1/09/08

Issuing Department:

Federal Operations Design Engineering

Supersedes:

Client: Energy solutions
Project Title: Moab UMTRA
Project Number: 35DJ2600
System:

Engineering Discipline: Civil

Calculation Title: Wedge Longevity

Purpose:

Runoff from the area between the top of the Book cliffs and the waste cell will be diverted around the cell by a wedge constructed of approximately 3,000,000 cubic yards of excavated material placed between the Book Cliffs and the cell. The purpose of this calculation is to analyze the ability of the "wedge" to survive for the 1000 year life of the disposal cell.

Prepared by: Bob Yager

Robert E. Yager

Date: 1/09/08

Checked by: Bill Barton

Bill Barton

Date: 1/25/08

Engineering Managers Approval: Bill Barton

Bill Barton

Date: 1/25/08

C03_Wedge_Longevity_Calcs_Pgs01-20_Moab010908.doc The current applicable version of this publication resides on Jacobs' Intranet. All copies are considered to be uncontrolled. Copyright Jacobs Engineering Group Inc., 2007

Revision History:

Pages Affected By Revision	Revised/Added/Deleted	Description of Revision
All		

Description of Calculation:

- Determine the runoff from the watersheds between the book cliffs and the wedge and from the top of the wedge for design storms with return intervals from 1 year to the pmp.
- Calculate the potential sediment transport in a hypothetical channel that routes the runoff along the north side of the wedge and around the disposal cell using methods from Johnson, 2002.
- Calculate the sediment yield of the areas between the Book Cliffs and the wedge using the Modified Universal Soil Loss equation (MUSLE) (Nelson, et. al., 1986)
- Calculate the sediment yield from the top of the wedge using the MUSLE to determine the potential reduction in the height of the wedge due to direct rainfall. .
- Compute the net potential sediment addition to or subtraction from the wedge.
- Calculate the potential depth of gullies formed on the top and side slopes of the wedge using the methodology of Johnson, 2002 to determine whether the wedge may be breached by gullying.

Assumptions:

- The 1-hour PMP event is estimated to be 8.2 inches, ("Site Drainage—Hydrology Parameters" calculation, Draft RAP Attachment 1, Appendix E).
- The rainfall frequency-depth-duration data were developed in the Draft RAP. The 1 year rainfall depth was taken from the NOAA Atlas 14 (http://hdsc.nws.noaa.gov/hdsc/pfds/sa/ut_pfds.html).
- Over a period of 1000, years 12.7% of the total rainfall will become runoff (Johnson, 2002).
- The unit weight of compacted soil in the wedge is 103.5 pcf and of undisturbed soil between the Book cliffs and the wedge is 91.3 pcf.
- Since the results of this calculation indicate that most of the erosion of soil in the channel along the north side of the wedge will be uncompacted sediment from the area between the Book Cliffs and the wedge, it has been assumed that the unit weight of all soil transported in the channel is 91.3 pcf. This is a conservative assumption as erosion of compacted soil would result in less volume for a given weight of eroded soil.

Design Inputs:

See following pages

Software:

Title	Developer	Versions	Revision Level
EXCEL	Microsoft	2002	
HEC-HMS	USACE	3.1.0	

C03_Wedge_Longevity_Calcs_Pgs01-20_Moab010908.doc The current applicable version of this publication resides on Jacobs' Intranet. All copies are considered to be uncontrolled. Copyright Jacobs Engineering Group Inc., 2007

JACOBS

(Ref. FOWI 116 Design Calculations)

Calculation Sheet

Project: 35DJ2600
Calculation Number: C-03
Page 5 of 20 – Plus Appendices 53 Pgs

Calculation Section:

See following pages

C03_Wedge_Longevity_Calcs_Pgs01-20_Moab010908.doc The current applicable version of this publication resides on Jacobs' Intranet. All copies are considered to be uncontrolled. Copyright Jacobs Engineering Group Inc., 2007

Conclusions/Recommendations:

See following pages

Reference:

See following pages

DESCRIPTION OF CALCULATION:

Runoff from the area between the top of the Book cliffs and the waste cell will be diverted around the cell by a wedge constructed of approximately 3,000,000 cubic yards of excavated material placed as shown in Figure 1. The purpose of this calculation is to analyze the ability of the "wedge" to survive for the 1000 year life of the disposal cell.

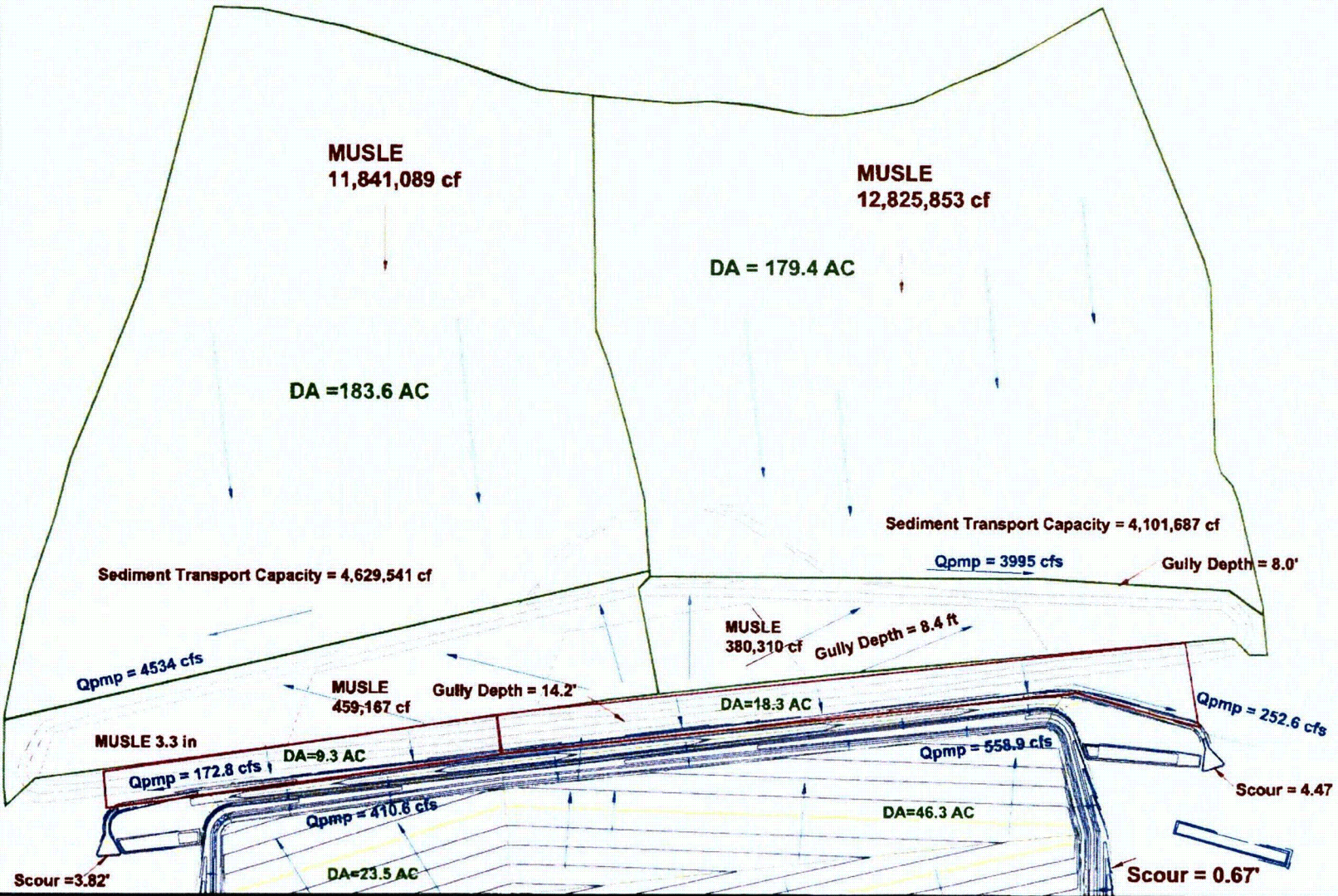
METHOD OF SOLUTION:

- Determine the runoff from the watersheds between the book cliffs and the wedge and from the top of the wedge for design storms with return intervals from 1 year to the PMP.
- Calculate the potential sediment transport in a hypothetical channel that routes the runoff along the north side of the wedge and around the disposal cell using methods from Johnson, 2002.
- Calculate the sediment yield of the areas between the Book Cliffs and the wedge using the Modified Universal Soil Loss equation (MUSLE) (Nelson, et. al, 1986)
- Calculate the sediment yield from the top of the wedge using the MUSLE to determine the potential reduction in the height of the wedge due to direct rainfall.
- Compute the net potential sediment addition to or subtraction from the wedge.
- Calculate the potential depth of gullies formed on the top and side slopes of the wedge using the methodology of Johnson, 2002 to determine whether the wedge may be breached by gulying.

ASSUMPTIONS:

- The 1-hour PMP event is estimated to be 8.2 inches, ("Site Drainage—Hydrology Parameters" calculation, Draft RAP Attachment 1, Appendix E).
- The rainfall frequency-depth-duration data were developed in the Draft RAP. The 1 year rainfall depth was taken from the NOAA Atlas 14 (http://hdsc.nws.noaa.gov/hdsc/pfds/sa/ut_pfds.html).
- Over a period of 1000 years, 12.7% of the total rainfall will become runoff (Johnson, 2002).
- The unit weight of compacted soil in the wedge is 103.5 pcf and of undisturbed soil between the Book cliffs and the wedge is 91.3 pcf.
- Since the results of this calculation indicate that most of the erosion of soil in the channel along the north side of the wedge will be uncompacted sediment from the area between the Book Cliffs and the wedge, it has been assumed that the unit weight of all soil transported in the channel is 91.3 pcf. This is a conservative assumption as erosion of compacted soil would result in less volume for a given weight of eroded soil.

Figure 1. Location and Configuration of the Wedge



CALCULATION SECTION:

Unit hydrographs for the two drainage areas between the Book Cliffs and the wedge are developed in Unit Hydrographs.xls WedgeErosionEast.xls WedgeErosionWest.xls. Runoff calculations are performed using HEC-HMS using the project: WedgeDrainage.hms Drainage area properties for other watersheds are in WatershedParms.xls

Sediment Transport Capacity**Drainage Area Characteristics**

Two drainage areas were delineated between the Book Cliffs and the wedge draining to the southeast and to the southwest. Two more were delineated on top the wedge draining to the northeast and the northwest. These drainage areas are shown in Figure 1.

For the undisturbed watersheds north of the wedge composite curve numbers were developed. The western drainage is approximately 63% Toddler-Ravola-Glenton families association with an HSG of B and a constant infiltration rate of 0.2 – 0.6 inches/hr. The remainder is Hanksville family-Badland complex with an HSG of C and an infiltration rate of 0.0 – 0.06 inches/hr (WEB Soil Survey, <http://websoilsurvey.nrcs.usda.gov/app/WebSoilSurvey.aspx>, and Appendix B). The Eastern drainage is approximately 49% Toddler-Ravola-Glenton and 51% Hanksville family-Badland complex. The following curve numbers have been assigned, a runoff curve number of 75 to the type B soils for semiarid rangelands with herbaceous cover in fair to poor condition and 87 to the type C soils for the same use in poor condition (TR-55,), composite curve numbers of 79.4 for the western drainage and 81.1 for the eastern. Computing initial abstraction using the NRCS curve number approach yields 0.52 inches for the western drainage and 0.47 for the eastern. The NRCS initial abstraction is

$$I_a = 0.2 \left[\frac{1000}{CN} - 10 \right]$$

Assuming a constant infiltration of 0.3 inches/hr for the type B soils and 0.03 for type C results in constant infiltration rates of 0.20 in/hr for the western drainage and 0.16 for the eastern. For the compacted soil comprising the wedge an initial abstraction equal to 0.2 inches was assumed with a constant infiltration rate of 0.1 in/hr. These loss values were used for all storms except the PMP for which the initial abstraction was set equal to 0.0.

Pertinent properties of the four drainage areas are computed in UnitHydrographs.xls and WaterShedParms.xls and listed in Table 1. The flow lengths are used to develop a unit hydrograph using the USBR methodology and the Lag time is used in the SCS unit hydrograph method. The mean of the Kirpich and SCS time of concentration formulas is used for the time of concentration.

The Kirpich equation is $T_c = 0.0078 \frac{L^{0.77}}{S^{0.385}}$ where

T_c = time of concentration (minutes)

L = slope length (feet [ft])

S = slope (ft/ft).

and the SCS equation is $T_c = \left(\frac{11.9L^3}{H} \right)^{0.385}$ where

T_c = time of concentration (hours)
 L = slope length (miles)
 H = slope height (ft).

Table 1. Drainage Area Characteristics

Drainage Area	Area (acres)	Max Flow Length (ft)	Flow Length Opposite Centroid	Time of Conc (min)	Lag = 0.6 T_c	Initial Abstraction (inches)	Const Inf Rate (in/hr)
Northwest of Wedge	183.6	4911	3078	NA	NA	0.52	0.20
Northeast of Wedge	179.4	5126	3309	NA	NA	0.47	0.16
West Side of Wedge	37.1	3140	NA	25.5	15.3	0.30	0.10
East Side of Wedge	31.6	2942	NA	24.5	14.7	0.30	0.10

Runoff Hydrograph Calculations

For the two largely undisturbed drainage areas between the book cliffs and the wedge, unit hydrographs were developed using the methodology of the U.S. Bureau of Reclamation (USBR, 1987). These unit hydrographs are computed in UnitHydrographs.xls. For the two drainage areas on top the wedge the SCS unit hydrograph was used. The USBR method was developed for natural areas in the west and is not appropriate for the wedge constructed of compacted soil. The runoff hydrographs were computed using the Computer Program HEC-HMS (USACE 2007).

Rainfall Depths Applied

The series of storms for the runoff calculations was developed from the Hydrology data in the draft RAP and NOAA Atlas 14. The number of storms of each depth was chosen conservatively as follows.

- A storm with rainfall depth equal to or greater than the 1000 year storm occurs on the average once every 1000 years. Since the rainfall depth may be any depth between the 1000 year storm and the PMP, the PMP was used for this storm.
- A storm with rainfall depth equal to or greater than the 500 year storm occurs on the average twice every 1000 years. Since the rainfall depth may be any depth between the 500 year storm and the 1000 year storm, the 1000 year rainfall depth was used for this storm. Since the PMP accounts for one of these storms, only one 1000 year storm was used.
- A storm with rainfall depth equal to or greater than the 200 year storm occurs on the average five times every 1000 years. Since the rainfall depth may be any depth between the 200 year storm and the 500 year storm, the 500 year rainfall depth was used for this storm. Since two larger storms have already been applied, three 500 year storms were used.

Following this logic through storms of all available return periods resulted in the distribution of rainfall depths and number of storms listed in Table 2. All storms represent 24 hour precipitation depth except for the PMP which is a 6 hour depth.

Table 2 Distribution of storms used in computing sediment transport capacity.

Return Interval Represented	Return Interval	Precipitation Depth (inches)	Number of Storms Equal or Greater than	Number of Storms of Depth Employed
-----------------------------	-----------------	------------------------------	--	------------------------------------

C03_Wedge_Longevity_Calcs_Pgs01-20_Moab010908.doc The current applicable version of this publication resides on Jacobs' Intranet. All copies are considered to be uncontrolled. Copyright Jacobs Engineering Group Inc., 2007

(years)	Employed (years)		Interval Represented	
1000	PMP (6 hour)	9.0	1	1
500	1000	3.73	2	1
200	500	3.15	5	3
100	200	2.58	10	5
50	100	2.35	20	10
25	50	2.12	40	20
10	25	1.91	100	60
5	10	1.63	200	100
2	5	1.42	500	300
1	2	1.16	1000	500
< 1	1	0.93	Unknown	1000

The runoff from each area was computed using HEC-HMS with the results from the wedge and from the book cliffs area flowing to the west combined into one hydrograph and to the east into another. A five minute time step was used.

Sediment Transport Capacity

The capacity of the flow to the east and the flow to the west along the north edge of the wedge (Figure 2) was estimated using a procedure in NUREG 1623 (Johnson 2002).

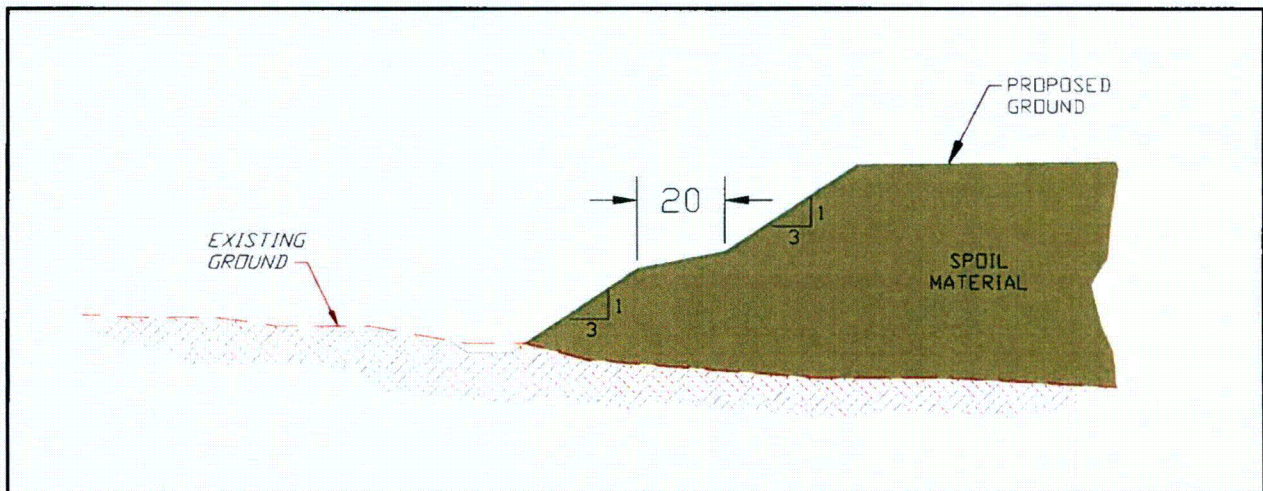


Figure 2 Cross section of the north edge of the wedge.

In this method the sediment transport capacity of a channel can be computed as

$$q_s = c_{s1} h^{c_{s2}} V^{c_{s3}}$$

where

q_s = unit sediment transport rate in ft^2/s (unbulked)

V = velocity in ft/s

h = flow depth in feet

NUREG 1623 gives the coefficient and exponents as a function of grain size distribution. Those that most closely correspond to the grain size distribution of the native soil are:

$$C_{s1} = 3.3 \times 10^{-5}$$

$$C_{s2} = 0.715$$

$$C_{s3} = 3.30$$

A hypothetical trapezoidal channel with a bottom width of 3 feet and a side slope of 1.5 horizontal to 1 vertical was assumed based on field observations of West Kendall Wash. The slope of the channel was assumed to be 0.007 to the east and 0.009 to the west as determined from the topography of the site and the location of the wedge. A table was constructed of sediment transport in cfs as a function of discharge in each channel. The flow in each 5 minute period of a runoff hydrograph was then used to interpolate to find the sediment transport during each 5 minute increment of the hydrograph. The sediment transport of each hydrograph was then computed as the sum of these 5 minute contributions.

For the channel shown below in Figure 3 with a discharge Q , a depth h , and a top width T , the volume of sediment transport capacity in a five minute period was calculated as follows. q_s was computed as above. Since this is the unbulked volume transport rate the unit weight was assumed to be 165 pcf. The value of q_s will vary across the channel as it depends on both the velocity and depth of flow. As a conservative approach, the value q_s computed for the full depth, h , was applied throughout the channel. The total rate of sediment transport in cubic feet/sec (unbulked) was computed as

$$Q_s(\text{unbulked}) = q_s T$$

and the rate in cf/5 min (bulked) as

$$Q_s(5 \text{ min}_\text{ bulked}) = Q_s(\text{unbulked}) * (300 \text{ sec}) * \frac{165 \text{ pcf}}{91.3 \text{ pcf}}$$

These 5 minute contributions were summed for each of the 5 minute flow periods of a storm hydrograph to compute the total sediment transport potential in cubic feet of the native soil from a single storm.

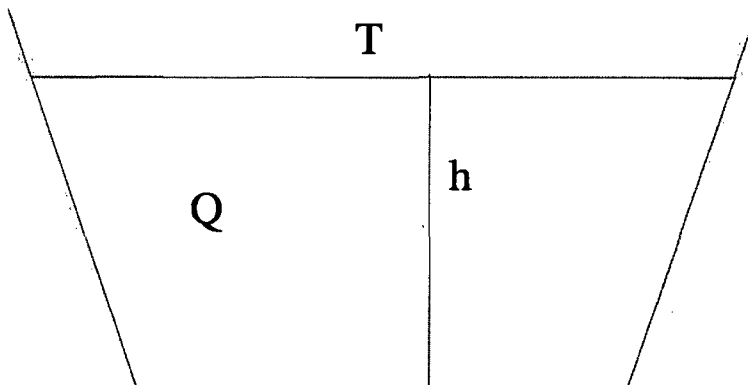


Figure 3 Cross Section of Hypothetical Channel along the North Edge of the wedge.

This calculation was repeated for all the storms listed in Table 2 and the total potential sediment transport during 1000 years was computed.

Unaccounted for Runoff

The total runoff of water in the listed storms was also computed. Since the annual rainfall at Thompson Springs during the period (1971-2000) was 9.97 inches (reference), and NUREG 1623 states that a reasonable estimate of the ratio of runoff to rainfall in the semi-arid regions of the western United States is 0.127, a volume of total expected runoff during 1000 years was computed. Comparing this volume with that computed from the listed storms indicated that over half the runoff had not been accounted for.

Assuming that the sediment concentration in this additional runoff will be equal to the average concentration in the runoff from the one year storm, an additional volume of sediment transport was added by multiplying the average concentration in the runoff from the one year storm by the volume of additional runoff.

Sediment Supply from the Book Cliffs Area

The runoff from the area between the Book cliffs and the wedge will transport sediment toward the wedge. The total sediment loss from the two watersheds delineated over a 1000 year period can be estimated with the Modified Universal Soil Loss Equation (MUSLE).

The equation is

$$A = R \times K \times LS \times VM$$

where:

- A = soil loss in tons per acre per year,
- R = rainfall factor,
- K = soil erodibility factor,
- LS = topographic factor, and
- VM = dimensionless erosion control factor relating to vegetative and mechanical factors.

The rainfall factor is 25, as given in NUREG/CR-4620 (Nelson et al. 1986) for the eastern third of Utah. The soil erodibility factor was estimated using the nomograph given in NUREG/CR-4620 (Nelson et al. 1986).

The topographic factor is calculated by the following equation:

$$LS = \frac{650 + 450 \times s + 65 \times s^2}{10,000 + s^2} \times \left(\frac{L}{72.6} \right)^m$$

where:

- s = slope steepness in percent,
- L = slope length in ft, and
- m = exponent dependent upon slope steepness.

The dimensionless erosion control factor used for the undisturbed watersheds was 0.4, from Table 5.3 of NUREG/CR-4620 (Nelson et al. 1986), representing seedings of 0 to 60 days to mimic light vegetation in the area. Over an extended period of time, a similar value can be expected to apply on the top of the wedge as some vegetation will develop. A slope of 3.5% was used. This is a representative slope for the area between

the wedge and the base of the Book Cliffs. Table 3 summarizes the results of the soil loss equation. The soil loss (sediment supply) from the Book cliffs area is most likely underestimated since the slope from the base to the top of the Book Cliffs is 40 – 50% and the erodibility factor of the soil is about the same for the two soil types in the watershed (Web Soil Survey and Appendix B). More sediment than calculated should be eroded from this area, but much of the additional sediment will be deposited as the slope flattens near the wedge.

Table 3. Results of Soil Loss Equation

Soil Cover	Book Cliffs Area (West)	Top of Wedge (West)	Book Cliffs Area (East)	Top of Wedge (East)
Rainfall factor, R	25	25	25	25
Silt and very fine sand (%)	60	60	60	60
Sand (%)	25	25	25	25
Organic matter (%)	2	2	2	2
Soil structure	Very fine granular	Very fine granular	Very fine granular	Very fine granular
Relative permeability	Moderate	Moderate	Moderate	Moderate
Erodibility factor	0.35	0.35	0.35	0.35
Topographic factor, LS	0.911	0.183	0.861	0.178
VM (low density seedings)	0.4	0.4	0.4	0.4
Soil loss (tons/acre/year)	3.19	0.64	3.01	0.62
Soil loss (inches/1,000 years)	19.2	3.4	18.2	3.3
Total sediment loss in 1000 years (cf)	12,825,853	459,167	11,841,089	380,310

The relative sediment yield of a more realistic watershed shape has been assessed with the Revised Universal Soil loss Equation (RUSLE) using the computer program RUSLE2 (USDA 2001). In this simulation three slopes were used, 1000 feet at 40% to represent the book cliffs, 800 feet at 3.5% and 800 feet at 2.5% to represent the area between the base of the Book Cliffs and the wedge. A RUSLE2 simulation was also performed with a the same three segments, but with each having a slope of 3.5%. The rainfall was the long term average at Thompson, about 6 miles east of the site of the waste cell and the other climate factors were those for Grand Junction, Colorado. These input parameters and the results are presented in Table 4 and Appendix C.

Table 4 Input Data and Results of RUSLE2 Estimate of Sediment Yields from t Yield from Book Cliffs Area

RUSLE2 Sediment Yield				
Segment	Length(ft)	Slope(%)	Avg Erosion(T/ac/yr)	Sed Delivery(T/ac/yr)
1	100	3.5		
2	800	3.5		
3	800	3.5		
	Net Erosion		2.6	2.6
1	100	40		
2	800	3.5		
3	800	2.5		
	Net Erosion		28	9.1

These results indicate that the assumption of a single 3.5% slope in the MUSLE calculation was conservative.

Sediment Budget

The volumes of sediments over a 1000 year period calculated with the MUSLE and the sediment transport potential along the north side of the wedge are summarized in Table 5.

Table 5 Sediment Budget for the North Side of the Wedge

Area	Sediment Transport Capacity (cf)	Sediment Yield from MUSLE (cf)
Channel along wedge to the west	4,629,541	
Channel along wedge to the east	4,101,687	
Western area between Book Cliffs and the wedge		12,825,853
Eastern area between Book Cliffs and the wedge		11,841,089
Western portion of the top of the wedge		459,167
Eastern portion of the top of the wedge		380,310
Total sediment yield toward the west portion of the wedge		13,285,020
Total sediment yield toward the east portion of the wedge		12,221,399
Ratio of sediment supply from Book Cliffs to transport capacity (west)		2.8
Ratio of sediment supply from Book Cliffs to transport capacity (east)		2.9

These results indicate that the water flowing along the northern side of the wedge to the west and the east does not have sufficient sediment transport capacity to carry away the supply of sediment from the areas between the Book Cliffs and the wedge. The northern edge of the wedge is expected to expand northward during the 1000 year life of the disposal cell and offer increasingly more protection to the cell as time passes. Even if the sediment supply from the north is discounted, the total sediment transport potential over 100 years is only about 12% of the volume of the wedge.

Erosion from top of Wedge

Due to the flat slope the predicted erosion from the top of the wedge is only 3.3 inches over a 1000 year period. This is a relatively high estimate since the longest flow paths to the east and the west were used in these estimates. Since the height of the wedge ranges from 28 to 48 feet, this is an insignificant depth of erosion.

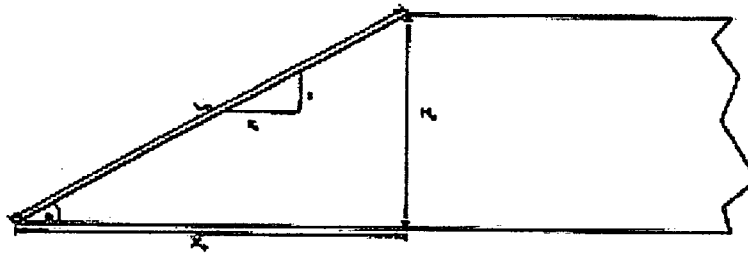
Gully Formation on Wedge

In addition to potential erosion of the wedge by runoff from the Book cliffs area and sheet and rill erosion from precipitation directly on the top of the wedge, runoff from the top of the wedge is expected to form gullies on the top and on the steep slopes as the runoff from the top of the wedge flows to the northwest and the northeast. The potential depth of these gullies can be estimated with an approach detailed in NUREG 1623. The three types of embankment geometries analyzed in this guidance document as shown in Figure 3. Gullies forming on the top of the wedge are analyzed as a Type 3 embankment and on the steep side slope as a Type 2 embankment. The effective tributary drainage area for each embankment is computed as

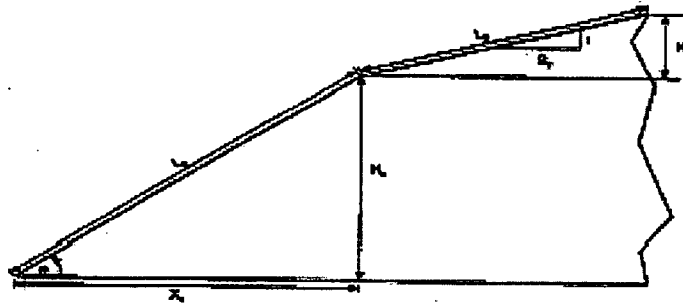
$$A = 0.276[L \cos(\theta)]^{1.636}$$

where L = total length of the flow path. A gully factor depending on the soil type, the height of the embankment and the volume of runoff to the toe of the embankment toe is

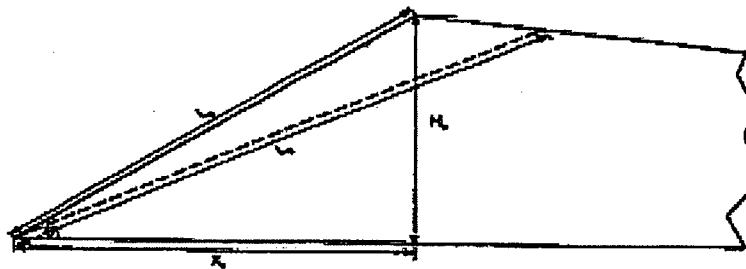
$$G_f = \frac{1}{2.80 + \left[0.197 \frac{V_r}{H_o^3} \right]^{-0.70}} \text{ for a clay content between 15 and 50\%}$$



Type 1 Embankment



Type 2 Embankment



Type 3 Embankment

Figure B-4. Three types of embankment geometry.

NUREG-1623

B-6

Figure 4 Three types of embankment geometry for gully calculations.

The estimated maximum depth of gully incision is

$$D_{\max} = G_f L_{\text{total}} S$$

where S is the original slope of the embankment. The top width of the gully at its deepest point is

$$W = \left[\frac{D_{\max}}{0.61} \right]^{1.149}$$

and the location of the deepest incision measured in units of D_{\max} downslope from the crest of the embankment is

$$D_l = 0.713 \left[\frac{V_r S}{L_o^3} \right]^{-0.415}$$

The results of these calculations are summarized in Table 6. The calculations are performed in metric units and the results converted to English units.

Table 6 Summary of Calculation of Depth of Gullies on the Wedge

Variable	Description	Top Slope West	Side Slope West	Top Slope East	Side Slope East
H_o (ft)	Height of Embankment	10	18	8	22
X_o (ft)	Horizontal Length of Embankment	1339	95	1254	92
L_o (ft)	Length of Embankment along Slope	1339	96.7	1254	94.6
θ (radians)	Embankment Slope Angle (radians)	0.0075	0.1873	0.0064	0.2347
L_2 (ft)	Distance along Top Slope (Type II)	NA	1339	NA	1254
H_2 (ft)	Height of Top Slope (Type II)	NA	10	NA	8
L_1 (ft)	Long Term Embankment Slope Length	1573	1436	1473	1349
A (sq ft)	Effective Drainage Area	72,231	60,418	64,882	53,638
V_r (cf)	Rainfall Volume	7,622,392	6,375,820	6,846,885	5,660,312
G_f	Gully Factor	0.36	0.35	0.36	0.35
D_{\max} (ft)	Maximum Gully Depth	4.2	6.5	3.4	8.0
W (ft)	Gully Width at Maximum Depth	7.7	12.7	5.9	16.0
D_l (ft)	Distance of D_{\max} from Top of Slope	248	4.1	204	4.7

Summary

As shown Figure 1 a wedge of spoil material consisting of approximately 3,000,000 cubic yards of soil excavated from the waste cell will be placed between the Book cliffs and the waste cell to divert runoff from the Book Cliffs area around the waste cell. These calculations have been performed to assess whether the wedge will continue to protect the cell during the 1000 year design life. Three possible processes by which the integrity of the wedge might be compromised have been considered.

C03_Wedge_Longevity_Calcs_Pgs01-20_Moab010908.doc The current applicable version of this publication resides on Jacobs' Intranet. All copies are considered to be uncontrolled. Copyright Jacobs Engineering Group Inc., 2007

1. Erosion of the wedge by runoff from the area between the Book Cliffs and the wedge will tend to erode the wedge as it is routed to the southwest and northwest around the wedge and the waste cell. The sediment transport capacity of this runoff during the 1000 year design life has been assessed using equations from NUREG 1623. Supply of sediment from the watersheds north of the wedge have been estimated by use of the Modified Universal Soil Loss Equation (MUSLE), as described in NUREG 4620 (Nelson et al. 1986). The assumptions made in the MUSLE have been evaluated using the RUSLE. The results of these calculations indicate that the total sediment carrying capacity of the runoff as it flows around the wedge is slightly more than 10% of the volume of the wedge. In addition, the sediment supply from the Book Cliffs area computed from the MUSLE will be approximately three times the sediment transport capacity of the flow around the wedge resulting in a net gain in the volume of the wedge over the design life of the waste cell. For each storm, the flow in the channels along the north side of the wedge will increase from near zero at the center of the wedge to the full flow calculated at the east and west ends of the channels. This will result in increasingly greater sediment transport as the flow increases along the channel. Since the sediment supply to the north edge of the wedge is expected to be comparatively uniform along the channel, the result will be that the central portion of the north edge of the wedge will migrate further northward than the east and west ends. The slope of the channels will then increase over time and a balance between sediment transport capacity and sediment supply may be achieved during the 1000 year design life of the cell.
2. Precipitation falling directly on the top of the wedge will run off toward the northeast and the northwest. This runoff will erode the wedge from the top. Application of the MUSLE to estimate the volume of sediment lost from the wedge through this mechanism indicate that the wedge will be reduced in average height by about 3 to 4 inches. With a design height ranging from approximately 20 to 48 feet, this loss of soil will not threaten the integrity of the wedge.
3. The third mechanism considered is concentration of flow as it runs off the top of the wedge and the consequent formation of gullies both on the top of the wedge and on the steep slopes to the northwest and the northeast. The depth, width, and location of the deepest portions of these gullies has been estimated with techniques described in NUREG 1623 (Johnson 2002). The results are summarized in Table 6. On top the wedge the deepest gully is estimated to be slightly over 4 feet deep, 8 feet wide, with the deepest part of the gully about 250 feet from the south edge of the wedge. The deepest gully on the steep side slope is anticipated to be about 8 feet deep, 16 feet wide, with the deepest portion about 5 feet below the slope break from the flat top to the steep side of the wedge. Neither of these gullies would pose a serious threat to the integrity of the wedge. It should be noted that because of the time period over which gullies developed that were used in developing the equations, NRC staff recommends the method be used for a design cell life of 200 years. Since the gully depth increases with time, the calculation has been extrapolated to 1000 years as the best available estimate of the extent of potential gully formation over a 1000 year design period.

Based on these calculations, we conclude that the wedge will protect the waste cell from runoff from the areas to the north and continue to function over the 1000 design life.

References:

- 10 CFR 40. U.S. Nuclear Regulatory Commission (NRC), "Domestic Licensing of Source Material," Appendix A, *Code of Federal Regulations*, February 2007.
- 40 CFR 192. U.S. Environmental Protection Agency (EPA) "Health and Environmental Protection Standards for Uranium and Thorium Mill Tailings," *Code of Federal Regulations*, February 2007.
- Abt, S.R., and T.L. Johnson, 1991. "Riprap Design for Overtopping Flow", *Journal of Hydraulic Engineering*, 117(8), pp. 959–972.
- Abt, S.R., T.L. Johnson, C.I. Thornton, and S.C. Trabant, 1998. "Riprap Sizing at Toe of Embankment Slopes", *Journal of Hydraulic Engineering*, 124(7), July.
- Abt, S.R., J.F. Ruff, and R.J. Wittler, 1991. "Estimating Flow Through Riprap", *Journal of Hydraulic Engineering*, 117(5), pp. 670–675.
- Chow, V.T., 1964. *Handbook of Applied Hydrology*, McGraw-Hill Book Company, New York, New York.
- DOE (U.S. Department of Energy), 1989. *Technical Approach Document, Revision II*, UMTRA-DOE/AL 050424.0002, December.
- DOT (U.S. Department of Transportation), 1983. *Hydraulic Design of Energy Dissipaters for Culverts and Channels*, Hydraulic Engineering Circular No. 14, September.
- Geotechnical Engineering Group, Inc. (GEG), 2005. Technical Testing; Crescent Junction, GEG Job No. 2165, December 22.
- Johnson, T.L., 2002 *Design of Erosion Protection for Long-Term Stabilization*, Final Report, NUREG-1623, U.S. Nuclear Regulatory Commission, September.
- Nelson, J.D., S.R. Abt, R.L. Volpe, D. van Zyl, N.E. Hinkle, W.P. Staub, 1986. *Methodologies for Evaluating Long-Term Stabilization Design of Uranium Mill Tailings Impoundments*, NUREG/CR-4620, U.S. Nuclear Regulatory Commission, June.
- Temple, D.M., K.M. Robinson, R.M. Ahring, and A.G. Davis, 1987. *Stability Design of Grass-Lined Open Channels*, U.S. Department of Agriculture Handbook No. 667, September.
- TR-55, Win TR-55 User Guide, US Department of Agriculture, 2003
- USDA (U.S. Department of Agriculture), 1994. "Gradation Design of Sand and Gravel Filters", *National Engineering Handbook*, Part 633, Chapter 26, October.

Appendix A
Reference Material
NUREG 4620 MUSL
NUREG 1623 Gully Formation
NUREG 1623 Channel Sediment Transport

Two basic approaches exist for the design of suitable erosion-resistant covers for a tailings impoundment surface as originally described by Nelson et al. (1983). The first approach consists of providing a cover material that will resist material transport by flowing water using the concept of critical shear stress. The second approach is based on the Universal Soil Loss Equation, an empirical method originally developed during the 1930's. The methodologies involved with both of these methods are discussed below.

5.1.1 Critical Shear Stress Approach

The critical shear stress approach consists of providing a cover material with a d_{30} grain size (i.e., 70% of the material by weight is coarser than the d_{30}) that will resist movement when subjected to the sheet flow maximum permissible velocity resulting from the application of the PMP over the entire impoundment surface. Minimum d_{30} grain sizes should be determined using the critical shear stress approach similar to the procedures discussed in Simons and Senturk (1977) applicable to overland flow. A numerical solution for selecting an appropriate d_{30} to provide armoring has been developed by Shen and Lu (1983).

The design approach described above, in which the critical grain size is selected to resist the onset of sheet erosion, should evaluate the runoff from PMP storms of different durations, such as 0.5, 1, 2, 4, and 6 hours to select the maximum d_{30} required. Rainfall depths will usually be based on 2.5 to 15 minute durations for small drainage basins as presented in Section 2.1.2. Typically, the minimum construction layer thickness is specified to be at least two times the maximum particle size. If the above approach results in a cover thickness less than about 6 inches, then other considerations - such as nonuniform placement of cover and particle breakdown due to handling, placement and weathering - would suggest that a minimum cover thickness of 10 inches should be considered. If a self-armoring cover can be provided, and there is no major concern for weathering of the cover material, the design is independent of time and the cover should remain intact indefinitely.

5.1.2 Soil Loss Equation Approach

The concept of sheet erosion was recognized by early researchers and the Universal Soil Loss Equation (USLE) was developed in the late 1930's by the Agricultural Research Service to evaluate soil conservation practices for cropland throughout the United States. After its inception, the soil loss procedure was used and modified as field experience and data were obtained incorporating the basic parameters of field slope and length, precipitation, and crop management to estimate soil losses on an annual basis. Application of the USLE to non-cropland areas and specifically for construction sites became feasible when Wischmeier et al. (1971), using basic soil loss characteristics, developed and implemented a soil erodibility factor (K) in the soil loss computation. Subsequent efforts refined the parameters used in the USLE for mining and construction activities in the interior western United States.

The Modified Universal Soil Loss Equation (MUSLE) was developed by the Utah Water Research Laboratory in 1978 for the principal objective of estimating soil losses due to highway construction activities. Alterations were made to the USLE to accommodate unique or special conditions encountered in highway construction, including steep and deep cuts and fill slopes that could cause erosion affecting adjacent or nearby roadways, streams, lakes, or inhabited areas. It is apparent that the modifications made to the USLE extend to many construction and mining sites beyond the scope of highway construction.

The Modified Universal Soil Loss Equation (MUSLE) is a mathematical model based on field determined coefficients and provides the most rational approach to evaluate the long-term erosion potential from an upland area similar to that of the area covering a reclaimed tailings pond. Recent investigations into appropriate methods of modeling major types of sheet erosion (Abt and Ruff, 1978; Nelson et al. 1983; Nyhan and Lane, 1983; and NRC, 1983), indicate that although more rigorous mathematical models are available to simulate erosion as a function of time, the use of the USLE has a strong precedent because it has a 40-year history of runoff and soil loss data.

The MUSLE is used to evaluate average soil losses for certain types of slopes as a function of time. The MUSLE does not consider the potential for gully development or intrusion as discussed in Chapter 4 because the topographic features of the tailings area are assumed to remain constant with time. Also, the MUSLE does not incorporate the concept of the PMP but rather a rainfall factor based on historical rainfall values. The MUSLE is defined by Clyde et al. (1978) as follows:

$$A = R K (LS) (VM) \quad (5.1)$$

where,

A = the computed loss per unit area in tons per acre per year with the units selected for K and R properly selected;

R = the rainfall factor which is the number for rainfall erosion index units plus a factor for snowmelt, if applicable;

K = the soil erodibility factor, which is the soil loss rate per erosion index unit for a specified soil as measured on a unit plot that is defined as a 72.6-ft length of uniform 9% slope continuously maintained as clean tilled fallow;

LS = the topographic factor, which is the ratio of soil loss from the field slope length to that from a 72.6-ft length under otherwise identical conditions;

VM = the dimensionless erosion control factor relating to vegetative and mechanical factors. This factor replaces the cover management factor (C) and the support factor (P) of the original USLE.

5.1.2.1 The Rainfall and Runoff Factor (R)

As noted by previous research at Los Alamos National Laboratory (Nyhan and Lane, 1983), the R factor as used in the MUSLE is often misinterpreted only as a rainfall factor. In reality, it must quantify both the raindrop impact and provide information on the amount and rate of runoff likely to be associated with the rain. More specifically, the R factor is described in terms of a rainfall storm energy (E) and the maximum 30-minute rainfall intensity (I₃₀). Generalized R factors applicable to the interior western United States are given in Table 5.1. For R factors in specific areas of the United States, it is recommended that erosion index distribution curves be obtained from local SCS offices.

Table 5.1. Generalized Rainfall and Runoff (R) Values.

State	Eastern Third	Central Third	Western Third
N. Dakota	50 - 75	40 - 50	40
S. Dakota	75 - 100	50	40
Montana	30 - 40	20	20 - 50
Wyoming	30 - 50	15 - 30	15 - 25
Colorado	75 - 100	40 - 50	20 - 40
Utah	20 - 30	20 - 50	15 - 40
New Mexico	75 - 100	40 - 50	20 - 40
Arizona	20 - 50	20 - 50	25 - 40

5.1.2.2 The Soil Erodibility Factor (K)

The soil erodibility factor (K) recognized the fact that the erodibility potential of a given soil is dependent on its compositional makeup, which in turn reflects the grain size distribution of the soil. To predict soil erodibility, five soil characteristics that include the percent silt and fine sand, percent sand greater than 0.1 mm, percent organic material, general soil structure and general permeability are determined. The K factor is then found by using the Wischmeier nomograph presented in Figure 5.1.

The makeup of the various soil fractions presented in Figure 5.1 is based on separating sand and silt at the 0.1 mm size. This differs from the Unified Soil Classification System which uses the No. 200 sieve size (0.075 mm) for the separation between sand and silt. The value to enter Figure 5.1 with should be the percentage of material finer than 0.1 mm in size, not the percentage passing the No. 200 sieve. Also, the determination of the Soil Erodibility Factor (K) as shown on Figure 5.1 does not specifically reference the percentage of clay (finer than 0.002 mm) contained in the material. The percentage of silt plus very fine sand to be used for Figure 5.1, therefore, is the percentage of material contained between 0.002 mm and 0.1 mm.

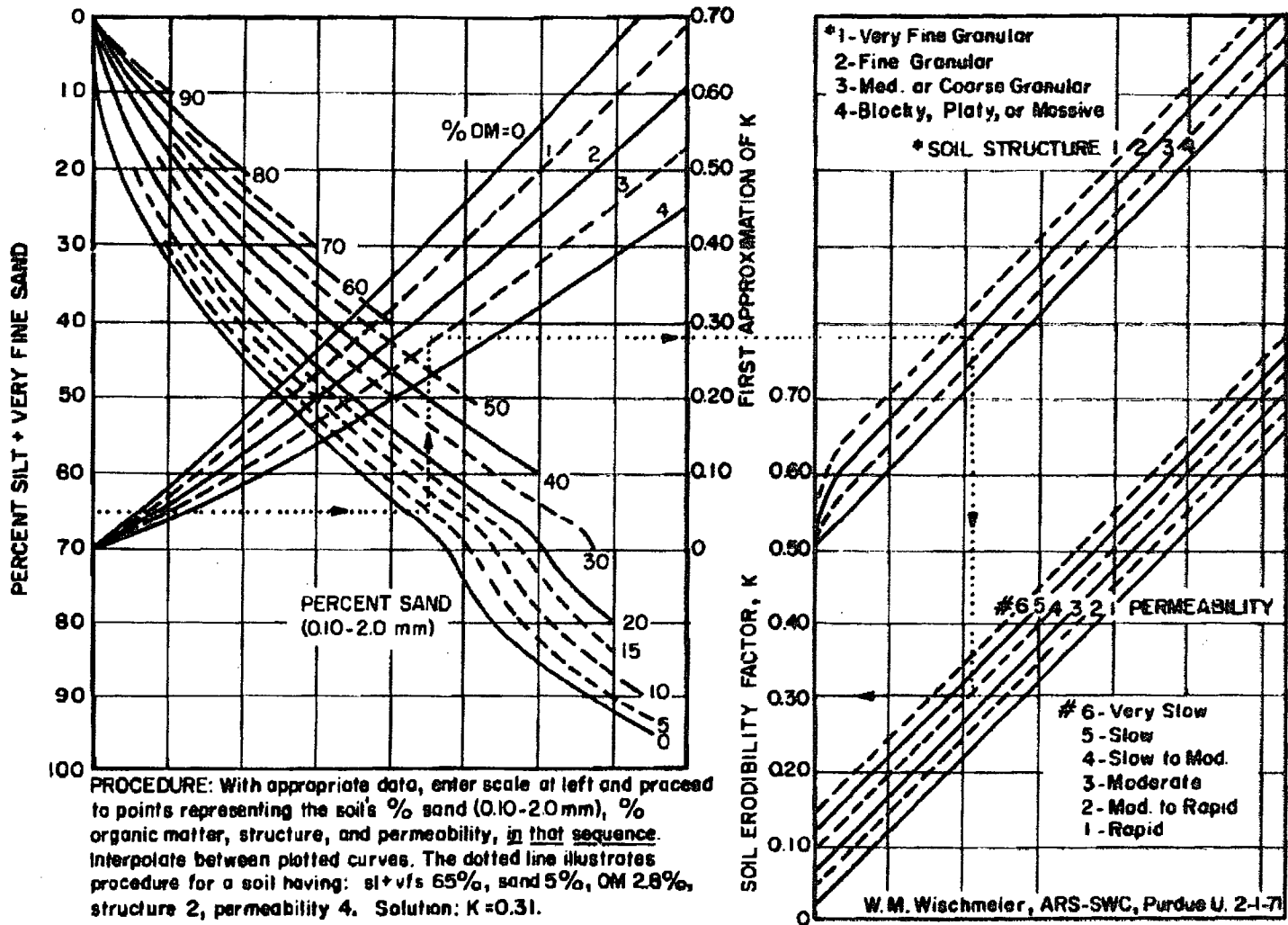


Fig. 5.1. Nomograph for determining soil erodibility factor K. Source: after Wischmeier et al., 1971.

5.1.2.3 The Topographic Factor (LS)

Although the effects of both length and steepness of slope have been investigated separately in different research efforts, it is more convenient for analytical purposes to combine the two into one topographic factor, LS. Wischmeier and Smith (1978) developed plots correlating the topographic factor for slopes up to 500 meters in length at slope inclinations from 0.5% up to 50%. Note that flat, short slopes will have less erosion than long, steep slopes and it is to the benefit of the design engineer to optimize slope length and gradients to fit the topography.

The equation to determine the LS factor is as follows:

$$LS = \frac{650 + 450s + 65s^2}{10,000 + s^2} \frac{L}{72.6} m \quad (5.2)$$

- where LS = topographic factor
- L = slope length in feet
- s = slope steepness in percent
- m = exponent dependent upon slope steepness

The slope dependent exponent m is presented in Table 5.2.

Table 5.2 Slope Dependent Exponent

Slope (percent)	m
s < 1.0	0.2
1.0 < s < 3.0	0.3
3.0 < s < 5.0	0.4
5.0 < s < 10.0	0.5
s > 10.0	0.6

5.1.2.4 The VM Factor

The VM factor is the erosion control factor applied in place of the cover and erosion control factors found in the USLE. The erosion control factor accounts for measures implemented at the construction site to include vegetation, mulching, chemical treatments and sprayed emulsions to impede or reduce erosion due to the overland flow of water. Values of the VM factor relative to site-specific conditions are presented in Table 5.3.

The VM factor is perhaps the most sensitive factor to effect the computed erosion loss for a given site. As shown by the values presented

on Table 5.3, the development of a permanent vegetative cover can have a significant impact in reducing the computed erosion loss. However, the effectiveness of a vegetative cover over long-term periods should be questioned unless other protective schemes, such as armoring of the cover with the proper size material, are also included in the design.

5.1.2.5 Example Problem

An example problem in how to use the MUSLE is provided below.

Assumptions:

Site location: Western Colorado
Site description: Uncovered tailings pond
Pond size: 160 acres
Slope: 3%
Length: 2500 ft
Material: 42% sand greater than 0.10 mm;
58% fine sand and silt less than 0.10 mm;
5% clay less than 0.002 mm;
0% organics;
(53% silt plus fine sand less than 0.1 mm);
Consistency - fine granular;
Permeability - slow to moderate.

The following factors have been determined for use in Equation 5.1.

R = 20 from Table 5.1

K = 0.50 from Figure 5.1

LS = 0.747 from Equation 5.2 and Table 5.2

VM = 1.0 (average from Table 5.3 based on an undisturbed surface)

Using Equation 5.1, the annual soil loss (A) from the tailings pond due to sheet erosion caused by flowing water is computed to be 7.47 tons/acre/year, or 1195 tons/year from the facility. Therefore, the cover is estimated to erode at a rate of 0.003 ft per year, or 0.3 ft/century.

5.2 SUMMARY AND FUTURE STUDIES

The main application of the soil loss equation approach in the evaluation of cover integrity is to determine whether it is possible for sheet erosion to penetrate the tailings cover, thereby exposing bare tailings and constituting a failure of the cover. The followup study will concentrate

Table 5.3. Typical VM Factor Values Reported in the Literature.^a

Condition	VM Factor
1. Bare soil conditions	
freshly disked to 6-8 inches	1.00
after one rain	0.89
loose to 12 inches smooth	0.90
loose to 12 inches rough	0.80
compacted bulldozer scraped up and down	1.30
same except root raked	1.20
compacted bulldozer scraped across slope	1.20
same except root raked across	0.90
rough irregular tracked all directions	0.90
seed and fertilizer, fresh	0.64
same after six months	0.54
seed, fertilizer, and 12 months chemical	0.38
not tilled algae crusted	0.01
tilled algae crusted	0.02
compacted fill	1.24 - 1.71
undisturbed except scraped	0.66 - 1.30
scarified only	0.76 - 1.31
sawdust 2 inches deep, disked in	0.61
2. Asphalt emulsion on bare soil	
1250 gallons/acre	0.02
1210 gallons/acre	0.01 - 0.019
605 gallons/acre	0.14 - 0.57
302 gallons/acre	0.29 - 0.60
151 gallons/acre	0.65 - 0.70
3. Dust binder	
605 gallons/acre	1.05
1210 gallons/acre	0.29 - 0.78
4. Other chemicals	
1000 lb. fiber Glass Roving with 60-150 gallons asphalt emulsion/acre	0.01 - 0.05
Aquatain	0.69
Aerospray 70, 10 percent cover	0.94
Curasol AE	0.30 - 0.48
Petroset SB	0.40 - 0.66
PVA	0.71 - 0.90
Terra-Tack	0.66
Wood fiber slurry, 1000 lb/acre fresh ^b	0.05
Wood fiber slurry, 1400 lb/acre fresh ^b	0.01 - 0.02
Wood fiber slurry, 3500 lb/acre fresh ^b	0.10
5. Seedings	
temporary, 0 to 60 days	0.40
temporary, after 60 days	0.05
permanent, 0 to 60 days	0.40
permanent, 2 to 12 months	0.05
permanent, after 12 months	0.01
6. Brush	
7. Excelsior blanket with plastic net	
	0.04 - 0.10

^aNote the variation in values of VM factors reported by different researchers for the same measures. References containing details of research which produced these VM values are included in NCHRP Project 16-3 report, "Erosion Control During Highway Construction, Vol. III. Bibliography of Water and Wind Erosion Control References," Transportation Research Board, 2101 Constitution Avenue, Washington, DC 20418.

^bThis material is commonly referred to as hydro mulch.

on using the MUSLE for several alternate cover designs in order to evaluate whether the proposed analytical approach can be successfully used to measure the long-term integrity of protective soil covers for uranium tailings reclamation. Alternative designs will be compared, both from a standpoint of overall integrity and construction difficulty. The covers will also be evaluated using the critical shear stress approach to determine, based on a given PMP, the minimum particle size necessary to protect the cover against long-term degradation.

APPENDIX B

METHOD FOR DETERMINING SACRIFICIAL SLOPE REQUIREMENTS

1 INTRODUCTION

In many cases where tailings extend over a large area, slope lengths may be so long that extremely gentle slopes will be needed to provide long-term stability. Such gentle slopes may necessitate the use of very large amounts of soil, such that some of these slopes (with no tailings directly under them) may extend greatly beyond the edge of the tailings pile.

In such cases, licensees may be able to demonstrate that it is impractical to provide stability for 1,000 years and may choose to show that stability for less than 1,000 years, but for at least 200 years, is a more cost-effective option. Such a design may incorporate tailings embankment "out slopes," where there are no tailings directly under the soil cover. Such slopes, designed for less than the 1,000-year stability period, may be acceptable if properly justified by the licensee.

It should be emphasized that the staff considers that a 200-year sacrificial slope design should be used only in a limited number of cases and only when a design life of 1,000 years cannot be reasonably achieved. However, it should not be assumed that the design period should immediately jump from 1,000 to 200 years. The staff concludes that the selection of a design period should proceed in a stepwise fashion, with consideration given to intermediate design periods from 200-1,000 years. In determining a minimum design, a 200-year sacrificial slope design, as presented below, may be used. However, such a design has a considerable amount of uncertainty associated with its use, due to its development by extrapolation of a relatively limited data base. Therefore, the staff considers that the procedure should be used only after other reclamation designs have been considered. The staff considers that the procedures for justifying a design period of less than 1,000 years, as discussed in Appendix C, should be carefully followed to document that a 200-year sacrificial slope design is the best design that can be reasonably provided.

2 TECHNICAL BASIS

The long-term gully erosion process has the potential to destabilize an earthen embankment or soil cover constructed to prevent waste material release to the environment. Figures B-1 and B-2 present photographs of earthen embankments damaged by gulying. It was apparent to the staff that little criteria were available that assisted the designer in predicting the potential impacts of gulying processes to long-term stability of the waste material. The NRC thereby supported a series of studies to expand the knowledge base on the potential impacts of gullies on reclaimed impoundments and provide guidance for assuring the long-term stability of the waste.

In 1985, Falk et al. conducted a pilot study in an attempt to develop a procedure to predict the maximum depth a gully may incise into a tailing slope as a function of time. Falk characterized 16 reclaimed mine and/or overburden sites in Colorado and Wyoming that demonstrated incision



Figure B-1. Damage caused by gulying.



Figure B-2. Damage caused by gullying.

on the side slope and in some cases extended into the top slope areas. Field measurements included gully length, slope length, pile height, pile age, maximum gully depth, and width, tributary drainage area, vegetative cover and soil composition. From these data, Falk et al. attempted to formulate a procedure for estimating the maximum depth of incision, width of gully, and location of the maximum incision from the crest. The estimation procedure had a limited application but indicated that an estimation procedure could potentially be developed.

Pauley (1993) performed a series of flume studies in which near prototype soil embankments were constructed simulating a reclaimed waste impoundment. Figure B-3 presents a photograph of the flume used in the study. A series of rainfall and subsequent runoff events were conducted resulting in gully incision into the embankment. The gulying processes were documented as a function of rainfall duration and volume, soil type, embankment slope and the maximum depth of incision. The results of the study indicated that the gully incision depth was a function of the clay content of the soil, volume of runoff to the gully, and the embankment height (Abt et al. 1994). The gully processes observed by Pauley and later documented by Abt et al. (1995b) in the flume study closely paralleled those observed in the field by Falk (1985) and others.

In an attempt to expand the Falk et al. (1985) data base, Abt et al. (1995a) conducted a study in which 11 field sites that demonstrated gulying on reclaimed impoundments were located, characterized, measured, and sampled in the Colorado and Wyoming region and each gully was characterized (Falk et al. 1985).

The information presented by Falk et al. (1985), Pauley (1993) and Abt et al. (1995a) was consolidated into a composite data base as reported by Abt et al. (1995b). A comprehensive procedure was presented to estimate the maximum depth of gully incision, top width of the gully, and location of the maximum incision from the crest. The procedure allows the designer to determine gully depths and to predict the location of maximum gully incision.

A review of existing waste and tailing reclamation designs in conjunction with extensive site experience indicates that three primary embankment/cover configurations are commonly proposed. The three embankment configurations or types have been proposed or constructed as presented in Figure B-4. It is important to recognize that although each embankment type is similar along the main embankment face, the top slope, and subsequent potential tributary drainage, significantly impact the maximum depth of gully incision, D_{max} , that may intrude into the main slope. Therefore, a different procedure was developed to estimate the potential tributary drainage area and volume of runoff for each embankment type.

An empirical gully incision estimation procedure is presented as a function of the embankment/cover geometry, hydrologic parameters, soil composition, and the design life. It is anticipated that the estimation procedure will provide the user the maximum depth of gully incision, the approximate location of the maximum depth of incision along the embankment slope, and the approximate top width of the gully at the point of maximum incision as schematically presented in Figure B-5. The user will need to insure that the gully incision does not expose the waste/tailings materials.

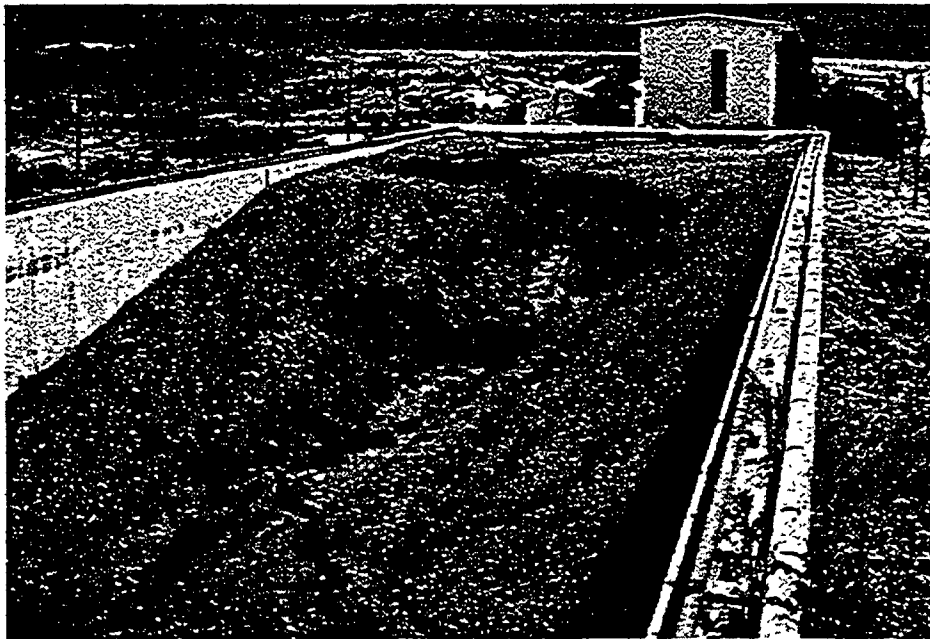
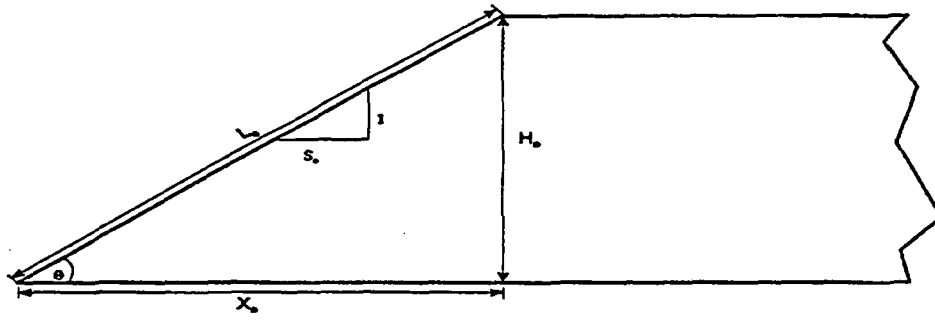
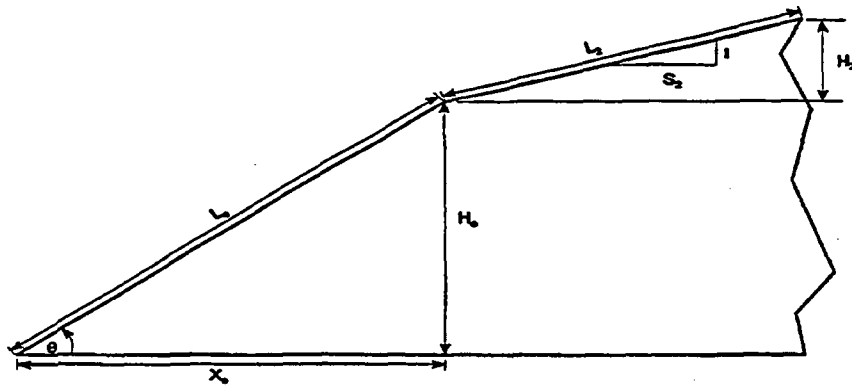


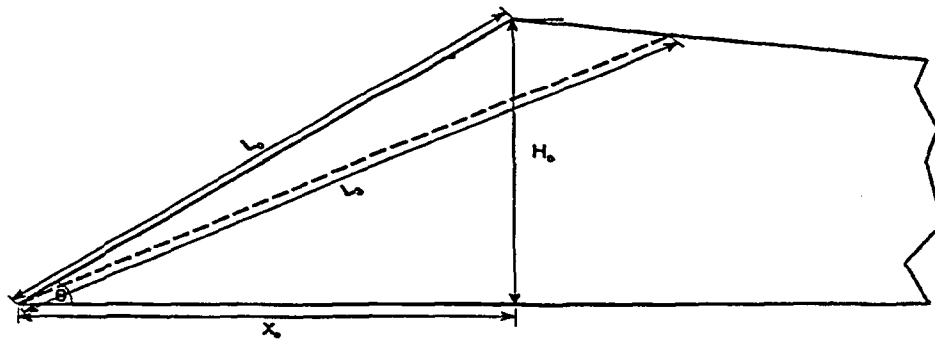
Figure B-3. Flume used by Pauley (1993).



Type 1 Embankment



Type 2 Embankment



Type 3 Embankment

Figure B-4. Three types of embankment geometry.

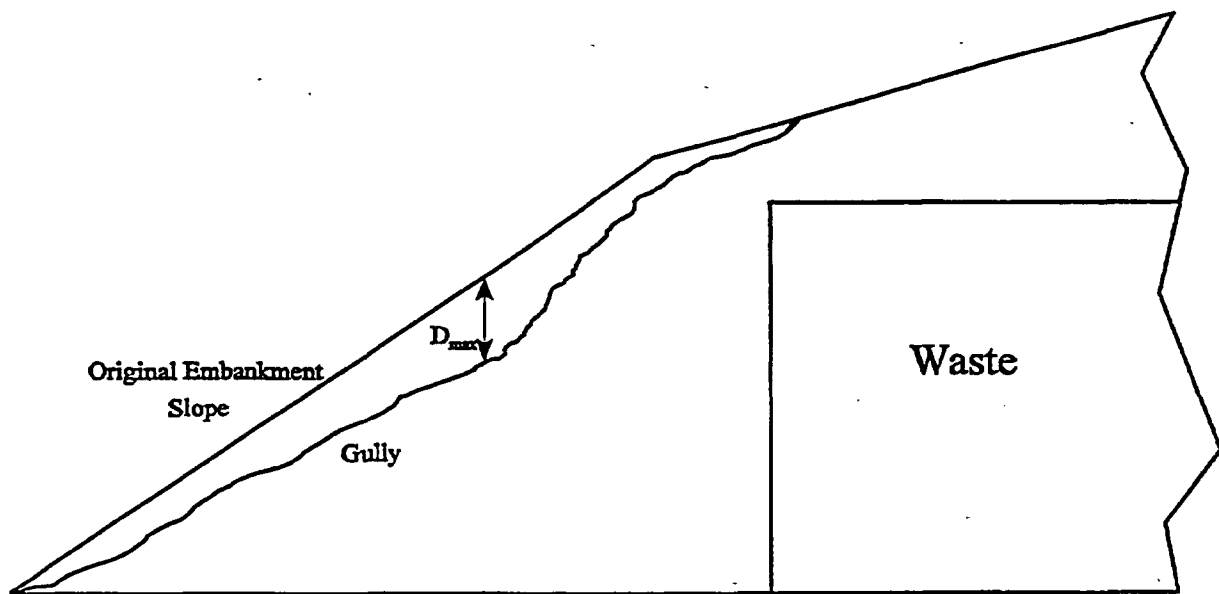


Figure B-5. Schematic of typical waste impoundment.

Staff review indicates that locating the depth of maximum gully incision is the most unpredictable part of the design procedure. The field data and flume data cannot be relied on totally to adequately describe the gully profile along the length of the slope. For example, the procedure may predict that the maximum gully depth will be 20 ft and will occur 500 ft from the embankment crest. However, not reflected in the design procedure is the possibility that the same gully could be 19 ft deep at the crest. The gully profile data available and staff experience suggest that gully depths approaching the maximum gully depth could occur near the crest. Thus, until more data are available, the staff recommends that the location of maximum gully be assumed to occur near the crest of the slope. In addition, because of the need for significant data extrapolation, the staff suggests that this procedure be used to determine sacrificial slope requirements for a 200-year period.

In situations where increasing the set back distance of waste with respect to the embankment crest is not feasible, the concept of embankment stabilization utilizing launching riprap may be examined. Abt et al. (1997) presents a preliminary approach to the stabilization technique. Figure B-6 presents a photograph of a laboratory simulation of embankment stabilization using launching riprap. Based upon the findings of the pilot test series, a set of preliminary guidelines and a design procedure is outlined by Abt et al. (1997). The procedure presented represents the pilot test series and its application has not been tested and verified under field or near prototype conditions. It is recommended that the procedures outlined by Abt et al. (1997) be applied with a high degree of engineering judgement.

3 PROCEDURES

A procedure has been developed to estimate the effects of gullying over time. The following steps outline the estimation procedure.

Step 1. Determine the embankment design life as outlined in Appendix A. Stability of the embankment must be insured for periods ranging from 200 to 1,000 years.

Step 2. Select the embankment type (Type 1, Type 2, or Type 3) and determine values of the appropriate design variables.

Embankment/cover variables applicable to all three types of embankments include the embankment height (H_o) (m), slope length (L_o) (m), slope angle (θ) (degrees), and horizontal distance from the embankment toe to the crest (X_o) (m) as presented in Figure B-4.

Step 3. Determine the embankment/cover soil composition, expressed as a percentage of the sands, silts, and clays. Discriminating thresholds for gully intrusion potential for embankments are segmented into soils with clay content less than 15 percent, clay content between 15 and 50 percent, and clay content greater than 50 percent.

Step 4. Determine the average annual precipitation (P), expressed in meters, for the embankment site. Estimates of precipitation can be obtained from U.S. Weather Bureau isohyetal maps, local climatological data, or other appropriate means.



Figure B-6. Photograph of launching riprap flume test.

- Step 5. Determine the drainage area tributary to the embankment to estimate the volume of runoff to which an embankment will be exposed in its design life. For embankments without external drainage basins, the tributary drainage area that forms on the face of the embankment will determine the total volume of runoff (Abt, Thornton, and Johnson, 1995b). The tributary drainage area that forms on the embankment face is a unique function of the type of embankment being evaluated.

Type 1 Embankment

The tributary drainage area for a Type 1 embankment may be estimated by

$$A = 0.276 * [L_o * \text{Cos}(\theta)]^{1.636} \quad (\text{B-1})$$

where: A = tributary drainage area (m²)
 L_o = original embankment length (m)
 θ = slope angle in degrees computed as Tan⁻¹(S_o)

Type 2 Embankment

The tributary drainage area for a Type 2 embankment is computed by summing the embankment face length (L_o) and the embankment top length (L_t). The resulting length (L_t) is then entered in Equation B-1 as:

$$A = 0.276 * [L_t * \text{Cos}(\theta)]^{1.636} \quad (\text{B-2})$$

where: A = tributary drainage area (m²)
 L_t = total length of embankment
 θ = slope angle in degrees computed as Tan⁻¹(S_o)

Type 3 Embankment

The tributary drainage area for a Type 3 embankment can be estimated using Equation B-1; however, an effective embankment length (L_e) must be determined. Flume and field observations indicate that a gully forming on a Type 3 embankment can extend past the crest and into the adverse slope. When this condition occurs, the effective length of the embankment is increased. To provide an estimate of the tributary drainage area at any point in time, the value of the effective embankment length is determined by estimating the final gully bottom slope. Abt et al. (1995b) reported that the gully bottom slope may be estimated as

$$S_b = [1.008 * S_o] - 0.063 \quad (\text{B-3})$$

where: S_b = gully bottom slope (rise/run)
 S_o = original embankment slope (rise/run)

The effective embankment length can then be computed as:

$$L_3 = 1.175 * L_o \quad (B-4)$$

where L_o and L_3 are expressed in meters. The tributary drainage area can then be computed using Equation B-1 where L_3 is substituted for L_o .

In situations where the embankment toe is exposed to runoff that develops on a tributary drainage area external to the embankment, the supplemental area (A_x) is added to the drainage area value computed using Equation B-1.

Step 6. The total depth of precipitation to which the site may be exposed to over the design life needs to be determined. In Step 1, the design life of the embankment was estimated. The average annual precipitation for the project site was then estimated based on Step 4. The expected depth of precipitation, in meters, is then calculated as:

$$D_t = \text{Average Precipitation Depth (m)} * \text{Design Life (years)} \quad (B-5)$$

Step 7. The runoff to rainfall ratio, R_r , is needed to convert the potential depth of precipitation for the embankment design life to potential runoff tributary to the developing gully. The U.S. Geological Survey (USGS) developed a runoff map method (Gebert et al., 1989) to determine the average annual runoff expected from any location in the United States. The USGS map provides the user the annual depth of runoff from a site specific location. The ratio of the runoff to rainfall is computed by dividing the runoff depth derived from Gebert et al. by the average annual precipitation for the appropriate locale. The average runoff-ratio using the USGS Average Annual Runoff Method is 0.127. The runoff-rainfall ratio of 0.127 provides a reasonable estimate for the arid and semi-arid regions of the western United States.

Step 8. The cumulative volume of runoff (V_r) tributary to the embankment toe, in cubic meters, is calculated as:

$$V_r = D_t * R_r * A \quad (B-6)$$

where A is the tributary drainage area, expressed in square meters, as determined in Step 5. It is acknowledged that a single storm event will significantly impact the development of the gully. Abt et al. (1995a) indicates that the total volume of runoff can serve as a predictor of the ultimate dimensions (i.e., maximum depth, width, etc.)

of the gully. The volume of runoff tributary to the gully for the embankment design life is the primary element reflecting the analysis period.

Step 9. The maximum depth of gully incision (D_{max}) can be estimated as a function of the cumulative volume of runoff, V_r , the embankment height, H_o , the embankment slope length, L_0 , L_2 , or L_3 , the embankment slope, and the clay content of the soil composition. A gully factor, G_f , was developed from the analysis described by Abt et al. (1994) for varying clay content of the proposed construction material. The gully factor is defined as:

$$G_f = \frac{D_{max}}{L_i * S_o} \tag{B-7}$$

where L_i is L_0 , L_2 , or L_3 as applicable and the embankment slope S_o , is H_o/X_o . The gully factor is computed as:

Clay content < 15%:

$$G_f = \frac{D_{max}}{L_o * S} = \frac{1}{2.25 + \left(0.789 * \frac{V_r}{H_o^3}\right)^{-0.55}} \tag{B-8}$$

Clay content > 15%, < 50%:

$$G_f = \frac{D_{max}}{L_o * S} = \frac{1}{2.80 + \left(0.197 * \frac{V_r}{H_o^3}\right)^{-0.70}} \tag{B-9}$$

Clay content > 50%:

$$G_f = \frac{D_{max}}{L_o * S} = \frac{1}{3.55 + \left(0.76 * \frac{V_r}{H_o^3}\right)^{-0.85}} \tag{B-10}$$

Step 10. The maximum depth of gully incision expected on the embankment slope may then be estimated as:

$$D_{\max} = G_f * L_i * S \quad (\text{B-11})$$

where D_{\max} is in meters.

Step 11. After the value of D_{\max} is determined, the top width of the gully at the deepest incision can be calculated as:

$$W = \left(\frac{D_{\max}}{0.61} \right)^{1.149} \quad (\text{B-12})$$

where: W = top width of gully (m)
 D_{\max} = depth of deepest gully incision (m)

Step 12. In some applications, it is important to estimate the location of the maximum gully incision to evaluate the stability of the embankment or the potential to penetrate into the waste storage area. The location of the maximum depth of incision, measured down slope from the crest, may be determined as:

$$D_i = 0.713 * \left(\frac{(V_r * S)}{L_i^3} \right)^{-0.415} \quad (\text{B-13})$$

where: D_i = location of D_{\max}
 V_r = cumulative volume of runoff (m^3)
 S_o = original embankment slope (rise/run)
 L_o = original embankment length (m)

Step 13. To provide a conservative estimate of the possible damage caused to an earthen embankment by a migrating gully, it is assumed that the maximum depth of gully intrusion occurs at the crest of the embankment. The embankment material is then assumed to erode, at the angle of repose of the embankment material, up slope of D_{\max} . The set back distance of the waste material is determined for each of the three types of embankments by assuming the embankment erodes at the angle of repose.

Step 14. If altering the set back distance is not feasible, protection may be examined utilizing launching riprap. A detailed explanation of the launching riprap application is

presented by Abt et al. (1997). The following preliminary guidelines should be followed in a launching riprap application:

- The minimum riprap size should be determined using accepted riprap sizing criteria for overtopping flow. A minimum median stone size (D_{50}) of 9 cm was found to work well in flume studies.
- The protective riprap layer should have adequate volume to provide slope coverage under maximum expected gully conditions. A layer thickness of approximately $3 D_{50}$ is recommended, depending on the volume requirements and the length of the riprap layer.

4 RECOMMENDATIONS

The stable slope should be determined using the procedures presented in Appendix A. Appropriately conservative values of input parameters should be used in the computation. Additional refinements can be made after the analysis of the sacrificial slope requirements.

In analyzing Type 2 Embankments, the top slope of the cover should be much flatter (less than or equal to 5%) than the slope of the embankment face. The gully would likely occur far upstream from the crest if the top slope were steep. The following example is presented to outline the stability assessment procedure, not to promote or compare any embankment types.

5 EXAMPLE OF PROCEDURE APPLICATION

The following example is used to outline the procedure of stability analysis of a Type 2 Embankment. Type 2 Embankments, presented in Figure B-4, are identified by an embankment slope that transitions into a flatter top slope. Embankments constructed with Type 2 geometry are evaluated by superimposing the total length of the embankment, L_1 , on the slope of the embankment face.

Step 1. Design Life

An embankment design life of 200 years will be evaluated.

Step 2. Embankment Geometry

Once the embankment type is determined, the initial design variables are required. It will be assumed that the embankment has the following physical dimensions:

H_o = embankment height	= 9 meters
L_o = embankment slope length	= 55 meters
S_o = embankment slope	= 0.15 rise/run
L_2 = top embankment length	= 100 meters
S_2 = top embankment slope	= 0.05 rise/run

Step 3. Soil Composition

It is assumed that a soil analysis has been conducted and that the embankment material is composed of 13 percent clay by volume, and has an angle of repose of 34 degrees.

Step 4. Precipitation

Local climatological data indicate an average annual precipitation of 0.20 meters for the site.

Step 5. Potential Tributary Drainage Area

The total potential tributary drainage area for a Type 2 Embankment is determined by computing the total embankment length as shown below

$$L_t = L_o + L_2 \quad (B-14)$$

where: L_t = total embankment length (m)

L_o = length of embankment face (m)

L_2 = length of embankment top slope (m)

The value determined for the total embankment length is then combined with the slope of the embankment face and entered into Equation B-2 as shown below

$$A = 0.276 * \{155 \text{ meters} * \cos(8.53)\}^{1.636} \quad (B-15)$$
$$A = 1038 \text{ meters}^2$$

Therefore, the total potential tributary drainage area for the Type 2 Embankment is 1038 square meters. It is assumed that there is no additional drainage area external to the embankment.

Step 6. Potential Depth of Precipitation

The first step in computing the total runoff volume for the site is to determine the potential depth of precipitation, D_p , that the site will be exposed to during the design life. As described in Step 6, the total depth of precipitation is the product of the average annual precipitation and the design life. Therefore,

$$D_t = 0.20 \text{ meters/year} * 200 \text{ years}$$

$$D_t = 40.0 \text{ meters of precipitation} \tag{B-16}$$

and a potential depth of precipitation of 40.0 meters is computed.

Step 7. Runoff to Rainfall Ratio

A value of 0.13 is assumed as the average runoff to rainfall ratio, R_r , for the embankment area.

Step 8. The cumulative volume of runoff, V_r , is defined as the product of the potential depth of precipitation, D_t , the runoff to rainfall ratio, R_r , and the potential tributary area, A_t . Substituting the values of D_t , R_r and A_t obtained above into Equation B-6 yields

$$V_r = 40.0 \text{ meters} * 0.13 * 1038 \text{ meters}^2$$

$$V_r = 5,400 \text{ meters}^3 \tag{B-17}$$

Therefore, the embankment slope will drain approximately 5,400 cubic meters of runoff during the 200 year design life.

Step 9. Determination of Gully Factor

The gully factor, G_f , for the embankment should be determined as outlined in Step 9. A clay content of 13 percent in the embankment material requires that Equation B-8 be used to calculate the gully factor. Substituting values for H_e and V_r into Equation B-8 gives

$$G_f = \frac{1}{2.25 + \left[0.789 * \left\{ \frac{5,399.97 \text{ meters}^3}{(9.0 \text{ meters})^3} \right\} \right]^{-0.55}}$$

$$G_f = 0.380 \tag{B-18}$$

Step 10. Maximum Depth of Gully Incision

A gully factor of 0.380 is entered into Equation B-8 to determine the maximum depth of gully incision as follows

$$D_{\max} = 0.380 * 55.0 \text{ meters} * 0.15$$

$$D_{\max} = 3.14 \text{ meters} \quad (\text{B-19})$$

Thus, after a 200 year period, a gully incision 3.14 meters deep would be expected on the face of the embankment.

Step 11. Gully Top Width

Equation B-12 presents an empirical relationship that can be used to predict gully top width, W , as a function of maximum gully incision, D_{\max} . Substituting the value of 3.14 meters computed for D_{\max} into Equation B-12 gives

$$W = \left(\frac{3.14 \text{ meters}}{0.61} \right)^{1.149}$$

$$W = 6.57 \text{ meters} \quad (\text{B-20})$$

therefore, 6.57 meters would be the estimated gully width at the point of deepest gully incision.

Step 12. Location of Maximum Depth

Equation B-13 presents an empirical relation predicting the location of D_{\max} as a function of the total volume of runoff, embankment length, and embankment slope. Substituting the values determined above into Equation B-13 gives

$$D_1 = 0.713 * \left\{ \frac{(5,399.97 \text{ meters}^3 * 0.15)}{(55 \text{ meters})^3} \right\}^{-0.415}$$

$$D_1 = 6.50 \quad (\text{B-21})$$

which represents the number of D_{\max} 's down slope from the crest the deepest incision is expected to occur. To determine the location in meters, multiply the value determined for D_1 by that determined for D_{\max} . For this example the deepest incision point will occur approximately 20.4 meters down slope from the embankment crest.

Summarizing the results obtained above yields

$$D_{\max} = 3.14 \text{ meters,}$$

$$W = 6.57 \text{ meters}$$

$$D_1 = 20.4 \text{ meters}$$

However, for long-term stability applications, the location of D_{\max} should be assumed to be at the crest of the slope.

Step 13. Set Back Distance

For conservatism, the maximum depth of incision is assumed to occur at the crest of the embankment and the material is assumed to erode at the angle of repose (34° for this example) upstream of the crest. For the conditions of this example, the set back distance would be 4.66 meters up slope from the crest of the embankment. Therefore, tailings should be located a minimum horizontal distance of 4.66 meters up slope and a vertical distance of 4.71 meters down from the embankment crest.

Step 14. Rock Launching Application

If providing adequate setback distance is not feasible, embankment stabilization with launching rock may be considered. For details and a preliminary application procedure, see Abt et al. (1997). The findings discussed by Abt et al. (1997) should be adapted to each specific site with engineering judgement. In general, a volume of rock should be provided to cover the collapsed slope with a rock layer of 1.5 times the D_{50} size, considering the depth of gully intrusion and the length. It is recommended that the required D_{50} size be specifically determined for a collapsed slope of 1V to 2H. Figure B-7 presents a schematic of the rock launching application concept.

The results of the example outlined above can then be checked with the original design of the soil cover, as described in Appendix A. Engineering judgment then determines if the design is adequate to provide the level of protection necessary throughout the design life.

6 COMPUTER APPLICATION

To aid in the analysis of the stability assessment, a computer program has been developed. The Windows™ application provides an automated method of evaluating the stability procedure described above (Thornton, 1996). The program is available from the U.S. Nuclear Regulatory

in column 6 is given from the sediment rating curve, or Equation 6. For each interval, the water yield in column 5 is calculated from multiplying columns 2 and 6. Likewise, the annual sediment yield in column 7 is calculated from Equation E-5 given Δp , Q and C_s from columns 2, 4 and 6. The interannual total sediment yield is finally obtained from the sum of column 7.

2.5 Trap Efficiency

When sediment-laden water enters reservoirs, lakes, impoundments, and settling basins, the settling of sediment will cause aggradation of the bed. The trap efficiency is used to determine how much sediment is expected to settle in backwater areas. The trap efficiency is defined as the percentage of incoming sediment for a given size fraction (i) that will settle within a given reach. The trap efficiency can be calculated as follows:

$$T_{Ei} = 1 - e^{\frac{-Xw_i}{hV}} \quad (E-7)$$

where X is the reach length; w_i is the settling velocity for sediment fraction i from Table E-4; h is the mean flow depth; and V is the mean flow velocity. The exponent is dimensionless and any consistent system of units can be used in this equation.

The sediment load that settles within the reach is given by the product of the incoming sediment load and the trap efficiency. The outgoing sediment load is calculated by subtracting the settling load from the incoming load. The trap efficiency varies with sediment size through the settling velocity. Typically, the trap efficiency is approximately one for coarse sediment, e.g., gravels, and approaches zero for fine sediment, e.g., clays.

2.6 Sediment Transport Capacity of a Channel

Simons, Li, and Fullerton (1981) developed an efficient method of evaluating sediment discharge. The method is based on easy-to-apply power relationships that estimate sediment transport based on the flow depth h and velocity V . These power relationships were developed from a computer solution of the Meyer-Peter and Müller bedload transport equation and Einstein's integration of the suspended bed sediment discharge:

$$q_s = c_{s1} h^{c_{s2}} V^{c_{s3}} \quad (E-8)$$

The results of the total bed sediment discharge are presented in Table E-2. The large values of c_{s3} ($3.3 < c_{s3} < 3.9$) show the high level of dependence of sediment transport rates on velocity. Depth has comparatively less influence ($-0.34 < c_{s2} < 0.7$).

Table E-2. Power equations for total bed sediment discharge in sand- and fine-gravel-bed streams.

$$q_s = C_{S1} h^{c_{S2}} V^{c_{S3}}$$

	D_{50} (mm)							
	0.1	0.25	0.5	1.0	2.0	3.0	4.0	5.0
Gr = 1.0								
C_{S1}	3.30×10^{-5}	1.42×10^{-5}	7.6×10^{-6}	5.62×10^{-6}	5.64×10^{-6}	6.32×10^{-6}	7.10×10^{-6}	7.78×10^{-6}
C_{S2}	0.715	0.495	0.28	0.06	-0.14	-0.24	-0.30	-0.34
C_{S3}	3.30	3.61	3.82	3.93	3.95	3.92	3.89	3/87
Gr = 2.0								
C_{S1}		1.59×10^{-5}	9.8×10^{-6}	6.94×10^{-6}	6.32×10^{-6}	6.62×10^{-6}	6.94×10^{-6}	
C_{S2}		0.51	0.33	0.12	-0.09	-0.196	-0.27	
C_{S3}		3.55	3.73	3.86	3.91	3.91	3.90	
Gr = 3.0								
C_{S1}			1.21×10^{-5}	9.14×10^{-6}	7.44×10^{-6}			
C_{S2}			0.36	0.18	-0.02			
C_{S3}			3.66	3.76	3.86			
Gr = 4.0								
C_{S1}				1.05×10^{-5}				
C_{S2}				0.21				
C_{S3}				3.71				

Definitions: q_s , unit sediment transport rate in ft²/s (unbulked); V, velocity in ft/s; h, depth in ft; $G_r = 0.5 [(D_{84}/D_{50}) + (D_{50}/D_{16})]$ gradation coefficient.

For flow conditions within the range outlined in Table E-3, the regression equations should be accurate within 10%. The equations were obtained for steep sand- and gravel-bed channels under supercritical flow. They do not apply to cohesive material.

The equations assume that all sediment sizes are transported by the flow without armoring. The sediment concentration $c_{mg/l}$ is calculated from

$$c_{mg/l} = 2.65 \times 10^6 \frac{q_s}{q} \quad (E-9)$$

where q_s is calculated from Equation E-8 and $q = V_h$ is the unit discharge in ft^2/s .

3 DESIGN AND ANALYSIS PROCEDURES

The following procedures may be used to determine: 1) sheet and rill erosion; 2) gully erosion; 3) calculated sediment yield; 4) measured sediment yield; 5) trap efficiency, and 6) sediment transport capacity of channels.

3.1 Sheet and Rill Erosion Procedure

The following sheet and rill erosion procedure based on the USLE may be used to determine soil erosion losses from upland erosion. If data are available, this approach should be supplemented with field measurements to properly calibrate and ascertain the accuracy of other procedures and/or computer models.

- Step A-1. Gather topographic, soil type and land use information. Subdivide the domain into sub-watersheds. For each sub-watershed, determine: drainage area, runoff length, average slope, soil type, percentage of canopy cover and ground cover and any particular method of soil conservation practice.
- Step A-2. Determine the mean annual rainfall erodibility factor R for the specific site location.
- Step A-3. Determine, for each sub-watershed, the soil erodibility factor K from soil samples.
- Step A-4. Determine the slope length-steepness factor LS from the runoff length and average slope.
- Step A-5. Determine the cropping-management factor C from the ground and canopy cover data.

Table E-3. Range of parameters for the Simons-Li-Fullerton method.

Parameter	Value range
Froude number	1 - 4
Velocity	6.5 - 26 ft/s
Manning coefficient n	0.015 - 0.025
Bed slope	0.005 - 0.040
Unit discharge	10 - 200 ft/s
Particle size	$D_{50} \geq 0.062 \text{ mm}$
	$D_{50} \leq 15 \text{ mm}$

Appendix B
Soil Properties from
Web Soil Survey

Report — RUSLE2 Related Attributes							
Grand County, Utah - Central Part							
Map symbol and soil name	Pct. of map unit	Hydrologic group	Kf	T factor	Representative value		
					% Sand	% Silt	% Clay
11—Chipeta complex							
Chipeta	40	D	.37	2	20.0	49.0	31.0
Chipeta	30	D	.37	2	20.0	49.0	31.0
18—Hanksville family-Badland complex							
Hanksville family	40	C	.43	3	26.5	53.5	20.0
Badland	35	—	—	—	—	—	—
31—Mesa-Chipeta-Thedalund family complex							
Chipeta	25	D	.37	2	20.0	49.0	31.0
Mesa	25	B	.28	3	66.5	20.0	13.5
Thedalund family	20	C	.37	3	42.1	37.9	20.0

Thedalund family	20	C	.37	3	42.1	37.9	20.0
52—Rizno-Rock outcrop complex							
Rizno	50	D	.28	1	63.1	26.4	10.5
Rock outcrop	25	—	—	—	—	—	—
75—Toddler-Ravola-Glenton families association							
Ravola family	25	B	.43	5	11.6	68.9	19.5
Toddler family	25	B	.43	5	24.8	52.7	22.5
Glenton family	20	B	.28	5	62.5	26.0	11.5

Description — RUSLE2 Related Attributes

RUSLE2 Related Attributes

This report summarizes those soil attributes used by the Revised Universal Soil Loss Equation Version 2 (RUSLE2) for the map units in the selected area. The report includes the map unit symbol, the component name, and the percent of the component in the map unit. Soil property data for each map unit component include the hydrologic soil group, erosion factors Kf for the surface horizon, erosion factor T, and the representative percentage of sand, silt, and clay in the surface horizon.

Ratings – 1 to 40 inches

Summary by Map Unit – Grand County, Utah - Central Part 				
Map unit symbol	Map unit name	Rating (percent)	Acres in AOI	Percent of AOI
11	Chipeta complex	31.0	9.9	0.8%
18	Hanksville family-Badland complex	41.1	224.6	19.1%
31	Mesa-Chipeta-Thedalund family complex	40.9	24.3	2.1%
52	Rizno-Rock outcrop complex	11.4	12.0	1.0%
75	Toddler-Ravola-Glenton families association	25.2	902.4	76.9%
Totals for Area of Interest (AOI)			1,173.3	100.0%

Description – Percent Clay

Clay as a soil separate consists of mineral soil particles that are less than 0.002 millimeter in diameter. The estimated clay content of each soil layer is given as a percentage, by weight, of the soil material that is less than 2 millimeters in diameter. The amount and kind of clay affect the fertility and physical condition of the soil and the ability of the soil to adsorb cations and to retain moisture. They influence shrink-swell potential, saturated hydraulic conductivity (Ksat), plasticity, the ease of soil dispersion, and other soil properties. The amount and kind of clay in a soil also affect tillage and earth-moving operations.

Most of the material is in one of three groups of clay minerals or a mixture of these clay minerals. The groups are kaolinite, smectite, and hydrous mica, the best known member of which is illite.

For each soil layer, this attribute is actually recorded as three separate values in the database. A low value and a high value indicate the range of this attribute for the soil component. A "representative" value indicates the expected value of this attribute for the component. For this soil property, only the representative value is used.

Summary by Map Unit — Grand County, Utah - Central Part 				
Map unit symbol	Map unit name	Rating (percent)	Acres in AOI	Percent of AOI
11	Chipeta complex	20.0	9.9	0.8%
18	Hanksville family-Badland complex	8.5	224.6	19.1%
31	Mesa-Chipeta-Thedalund family complex	48.3	24.3	2.1%
52	Rizno-Rock outcrop complex	62.6	12.0	1.0%
75	Toddler-Ravola-Glenton families association	47.6	902.4	76.9%
Totals for Area of Interest (AOI)			1,173.3	100.0%

Description — Percent Sand 

Sand as a soil separate consists of mineral soil particles that are 0.05 millimeter to 2 millimeters in diameter. In the database, the estimated sand content of each soil layer is given as a percentage, by weight, of the soil material that is less than 2 millimeters in diameter. The content of sand, silt, and clay affects the physical behavior of a soil. Particle size is important for engineering and agronomic interpretations, for determination of soil hydrologic qualities, and for soil classification.

For each soil layer, this attribute is actually recorded as three separate values in the database. A low value and a high value indicate the range of this attribute for the soil component. A "representative" value indicates the expected value of this attribute for the component. For this soil property, only the representative value is used.

Summary by Map Unit — Grand County, Utah - Central Part				
Map unit symbol	Map unit name	Rating (percent)	Acres in AOI	Percent of AOI
11	Chipeta complex	20.0	9.9	0.8%
18	Hanksville family-Badland complex	8.5	224.6	19.1%
31	Mesa-Chipeta-Thedalund family complex	48.3	24.3	2.1%
52	Rizno-Rock outcrop complex	62.6	12.0	1.0%
75	Toddler-Ravola-Glenton families association	47.6	902.4	76.9%
Totals for Area of Interest (AOI)			1,173.3	100.0%

Description — Percent Sand

Sand as a soil separate consists of mineral soil particles that are 0.05 millimeter to 2 millimeters in diameter. In the database, the estimated sand content of each soil layer is given as a percentage, by weight, of the soil material that is less than 2 millimeters in diameter. The content of sand, silt, and clay affects the physical behavior of a soil. Particle size is important for engineering and agronomic interpretations, for determination of soil hydrologic qualities, and for soil classification.

For each soil layer, this attribute is actually recorded as three separate values in the database. A low value and a high value indicate the range of this attribute for the soil component. A "representative" value indicates the expected value of this attribute for the component. For this soil property, only the representative value is used.

Summary by Map Unit — Grand County, Utah - Central Part				
Map unit symbol	Map unit name	Rating (percent)	Acres in AOI	Percent of AOI
11	Chipeta complex	15.0	9.9	0.8%
18	Hanksville family-Badland complex	16.8	224.6	19.1%
31	Mesa-Chipeta-Thedalund family complex	18.5	24.3	2.1%
52	Rizno-Rock outcrop complex	5.0	12.0	1.0%
75	Toddler-Ravola-Glenton families association	11.3	902.4	76.9%
Totals for Area of Interest (AOI)			1,173.3	100.0%

Description — Plasticity Index

Plasticity index (PI) is one of the standard Atterberg limits used to indicate the plasticity characteristics of a soil. It is defined as the numerical difference between the liquid limit and plastic limit of the soil. It is the range of water content in which a soil exhibits the characteristics of a plastic solid.

The plastic limit is the water content that corresponds to an arbitrary limit between the plastic and semisolid states of a soil. The liquid limit is the water content, on a percent by weight basis, of the soil (passing #40 sieve) at which the soil changes from a plastic to a liquid state.

Soils that have a high plasticity index have a wide range of moisture content in which the soil performs as a plastic material. Highly and moderately plastic clays have large PI values. Plasticity index is used in classifying soils in the Unified and AASHTO classification systems.

For each soil layer, this attribute is actually recorded as three separate values in the database. A low value and a high value indicate the range of this attribute for the soil component. A "representative" value indicates the expected value of this attribute for the component. For this soil property, only the representative value is used.

Summary by Map Unit — Grand County, Utah - Central Part 				
Map unit symbol	Map unit name	Rating (percent)	Acres in AOI	Percent of AOI
11	Chipeta complex	49.0	9.9	0.8%
18	Hanksville family-Badland complex	50.4	224.6	19.1%
31	Mesa-Chipeta-The dalund family complex	48.2	24.3	2.1%
52	Rizno-Rock outcrop complex	26.0	12.0	1.0%
75	Toddler-Ravola-Glenton families association	64.0	902.4	76.9%
Totals for Area of Interest (AOI)			1,173.3	100.0%

Description — Percent Silt 

Silt as a soil separate consists of mineral soil particles that are 0.002 to 0.05 millimeter in diameter. In the database, the estimated silt content of each soil layer is given as a percentage, by weight, of the soil material that is less than 2 millimeters in diameter.

The content of sand, silt, and clay affects the physical behavior of a soil. Particle size is important for engineering and agronomic interpretations, for determination of soil hydrologic qualities, and for soil classification

For each soil layer, this attribute is actually recorded as three separate values in the database. A low value and a high value indicate the range of this attribute for the soil component. A "representative" value indicates the expected value of this attribute for the component. For this soil property, only the representative value is used.

Summary by Map Unit — Grand County, Utah - Central Part 				
Map unit symbol	Map unit name	Rating (percent)	Acres in AOI	Percent of AOI
11	Chipeta complex	0.32	9.9	0.8%
18	Hanksville family-Badland complex	0.25	224.6	19.1%
31	Mesa-Chipeta-Thedalund family complex	0.32	24.3	2.1%
52	Rizno-Rock outcrop complex	0.75	12.0	1.0%
75	Toddler-Ravola-Glenton families association	1.20	902.4	76.9%
Totals for Area of Interest (AOI)			1,173.3	100.0%

Description — Organic Matter 

Organic matter is the plant and animal residue in the soil at various stages of decomposition. The estimated content of organic matter is expressed as a percentage, by weight, of the soil material that is less than 2 millimeters in diameter.

The content of organic matter in a soil can be maintained by returning crop residue to the soil. Organic matter has a positive effect on available water capacity, water infiltration, soil organism activity, and tilth. It is a source of nitrogen and other nutrients for crops and soil organisms. An irregular distribution of organic carbon with depth may indicate different episodes of soil deposition or soil formation. Soils that are very high in organic matter have poor engineering properties and subside upon drying.

For each soil layer, this attribute is actually recorded as three separate values in the database. A low value and a high value indicate the range of this attribute for the soil component. A "representative" value indicates the expected value of this attribute for the component. For this soil property, only the representative value is used.

Tables — Hydrologic Soil Group — Summary By Map Unit				
Summary by Map Unit — Grand County, Utah - Central Part				
Map unit symbol	Map unit name	Rating	Acres in AOI	Percent of AOI
11	Chipeta complex	D	5.5	0.6%
18	Hanksville family-Badland complex	C	142.0	14.5%
31	Mesa-Chipeta-Thedalund family complex	B	26.3	2.7%
75	Toddler-Ravola-Glenton families association	B	803.6	82.2%
Totals for Area of Interest (AOI)			977.4	100.0%

Grand County, Utah - Central Part

75—Toddler-Ravola-Glenton families association

Map Unit Setting

Elevation: 4,000 to 5,000 feet

Mean annual precipitation: 5 to 8 inches

Mean annual air temperature: 52 to 55 degrees F

Frost-free period: 150 to 180 days

Map Unit Composition

Ravola family and similar soils: 25 percent

Toddler family and similar soils: 25 percent

Glenton family and similar soils: 20 percent

Description of Toddler Family

Setting

Landform: Flood plains, drainageways

Landform position (three-dimensional): Talf

Down-slope shape: Linear

Across-slope shape: Concave

Parent material: Alluvium derived from sandstone and shale

Properties and qualities

Slope: 0 to 3 percent

Depth to restrictive feature: More than 80 inches

Drainage class: Well drained

Capacity of the most limiting layer to transmit water (Ksat): Moderately high (0.20 to 0.60 in/hr)

Depth to water table: More than 80 inches

Frequency of flooding: Rare

Frequency of ponding: None

Calcium carbonate, maximum content: 15 percent

Gypsum, maximum content: 3 percent

Maximum salinity: Nonsaline to slightly saline (2.0 to 8.0 mmhos/cm)

Sodium adsorption ratio, maximum: 10.0

Available water capacity: Moderate (about 8.5 inches)

Grand County, Utah - Central Part

75—Toddler-Ravola-Glenton families association

Map Unit Setting

Elevation: 4,000 to 5,000 feet

Mean annual precipitation: 5 to 8 inches

Mean annual air temperature: 52 to 55 degrees F

Frost-free period: 150 to 180 days

Map Unit Composition

- Ravola family and similar soils: 25 percent
- Toddler family and similar soils: 25 percent
- Glenton family and similar soils: 20 percent

Description of Toddler Family

Setting

- Landform: Flood plains, drainageways
- Landform position (three-dimensional): Talf
- Down-slope shape: Linear
- Across-slope shape: Concave
- Parent material: Alluvium derived from sandstone and shale

Properties and qualities

- Slope: 0 to 3 percent
- Depth to restrictive feature: More than 80 inches
- Drainage class: Well drained
- Capacity of the most limiting layer to transmit water (Ksat): Moderately high (0.20 to 0.60 in/hr)
- Depth to water table: More than 80 inches
- Frequency of flooding: Rare
- Frequency of ponding: None
- Calcium carbonate, maximum content: 15 percent
- Gypsum, maximum content: 3 percent
- Maximum salinity: Nonsaline to slightly saline (2.0 to 8.0 mmhos/cm)
- Sodium adsorption ratio, maximum: 10.0
- Available water capacity: Moderate (about 8.5 inches)

Interpretive groups

- Land capability (nonirrigated): 6e
- Ecological site: Alkali Fan (Castlevalley Saltbush) (R034XY003UT)

Typical profile

- 0 to 7 inches: Silt loam
- 7 to 12 inches: Silt loam
- 12 to 36 inches: Sandy clay loam
- 36 to 60 inches: Fine sandy loam

Description of Ravola Family

Setting

Landform: Flood plains

Landform position (three-dimensional): Talf

Down-slope shape: Linear

Across-slope shape: Concave

Parent material: Alluvium derived from sandstone and shale

Properties and qualities

Slope: 0 to 3 percent

Depth to restrictive feature: More than 80 inches

Drainage class: Well drained

Capacity of the most limiting layer to transmit water (Ksat): Moderately high (0.20 to 0.60 in/hr)

Depth to water table: More than 80 inches

Frequency of flooding: Occasional

Frequency of ponding: None

Calcium carbonate, maximum content: 40 percent

Gypsum, maximum content: 4 percent

Maximum salinity: Very slightly saline to moderately saline (4.0 to 16.0 mmhos/cm)

Sodium adsorption ratio, maximum: 10.0

Available water capacity: Moderate (about 8.5 inches)

Interpretive groups

Land capability (nonirrigated): 7s

Ecological site: Alkali Flat (Black Greasewood) (R034XY006UT)

Other vegetative classification: Alkali Flat (Black Greasewood) (034XY006UT_1)

Typical profile

0 to 3 inches: Silt loam

3 to 7 inches: Silt loam

7 to 10 inches: Fine sandy loam

10 to 29 inches: Silt loam

29 to 60 inches: Silt loam

Description of Glenton Family

Setting

Landform: Drainageways, flood plains

Landform position (three-dimensional): Talf

Down-slope shape: Linear

Across-slope shape: Concave

Parent material: Alluvium derived from sandstone and shale

Interpretive groups

Land capability (nonirrigated): 6e

Ecological site: Alkali Fan (Castlevalley Saltbush) (R034XY003UT)

Typical profile

0 to 7 inches: Silt loam

7 to 12 inches: Silt loam

12 to 36 inches: Sandy clay loam

36 to 60 inches: Fine sandy loam

Description of Ravola Family

Setting

Landform: Flood plains

Landform position (three-dimensional): Talf

Down-slope shape: Linear

Across-slope shape: Concave

Parent material: Alluvium derived from sandstone and shale

Properties and qualities

Slope: 0 to 3 percent

Depth to restrictive feature: More than 80 inches

Drainage class: Well drained

Capacity of the most limiting layer to transmit water (Ksat): Moderately high (0.20 to 0.60 in/hr)

Depth to water table: More than 80 inches

Frequency of flooding: Occasional

Frequency of ponding: None

Calcium carbonate, maximum content: 40 percent

Gypsum, maximum content: 4 percent

Maximum salinity: Very slightly saline to moderately saline (4.0 to 16.0 mmhos/cm)

Sodium adsorption ratio, maximum: 10.0

Available water capacity: Moderate (about 8.5 inches)

Interpretive groups

Land capability (nonirrigated): 7s

Ecological site: Alkali Flat (Black Greasewood) (R034XY006UT)

Other vegetative classification: Alkali Flat (Black Greasewood) (034XY006UT_1)

Typical profile

- 0 to 3 inches: Silt loam
- 3 to 7 inches: Silt loam
- 7 to 10 inches: Fine sandy loam
- 10 to 29 inches: Silt loam
- 29 to 60 inches: Silt loam

Description of Glenton Family

Setting

- Landform: Drainageways, flood plains
- Landform position (three-dimensional): Talf
- Down-slope shape: Linear
- Across-slope shape: Concave
- Parent material: Alluvium derived from sandstone and shale

Properties and qualities

- Slope: 0 to 3 percent
- Depth to restrictive feature: More than 80 inches
- Drainage class: Well drained
- Capacity of the most limiting layer to transmit water (Ksat): Moderately high (0.20 to 0.60 in/hr)
- Depth to water table: More than 80 inches
- Frequency of flooding: Rare
- Frequency of ponding: None
- Calcium carbonate, maximum content: 40 percent
- Gypsum, maximum content: 3 percent
- Maximum salinity: Nonsaline to slightly saline (0.0 to 8.0 mmhos/cm)
- Sodium adsorption ratio, maximum: 10.0
- Available water capacity: Moderate (about 7.2 inches)

18—Hanksville family-Badland complex

Map Unit Setting

- Elevation: 4,200 to 6,100 feet
- Mean annual precipitation: 6 to 8 inches
- Mean annual air temperature: 46 to 54 degrees F

- Frost-free period: 120 to 170 days

Map Unit Composition

- Hanksville family and similar soils: 40 percent
- Badland: 35 percent

Description of Hanksville Family

Setting

- Landform: Cuestas, mesas
- Down-slope shape: Linear
- Across-slope shape: Convex
- Parent material: Colluvium derived from shale and/or residuum weathered from shale

Properties and qualities

- Slope: 30 to 50 percent
- Surface area covered with stones and boulders: 7.0 percent
- Depth to restrictive feature: 20 to 40 inches to paralithic bedrock
- Drainage class: Well drained
- Capacity of the most limiting layer to transmit water (Ksat): Very low to moderately low (0.00 to 0.06 in/hr)
- Depth to water table: More than 80 inches
- Frequency of flooding: None
- Frequency of ponding: None
- Calcium carbonate, maximum content: 15 percent
- Gypsum, maximum content: 10 percent
- Maximum salinity: Nonsaline (0.0 to 2.0 mmhos/cm)
- Sodium adsorption ratio, maximum: 4.0
- Available water capacity: Low (about 5.8 inches)

Interpretive groups

- Land capability (nonirrigated): 7s
- Ecological site: Desert Clay (Castlevalley Saltbush) (R034XY103UT)
- Other vegetative classification: Desert Clay (Castlevalley Saltbush) (034XY103UT_1)

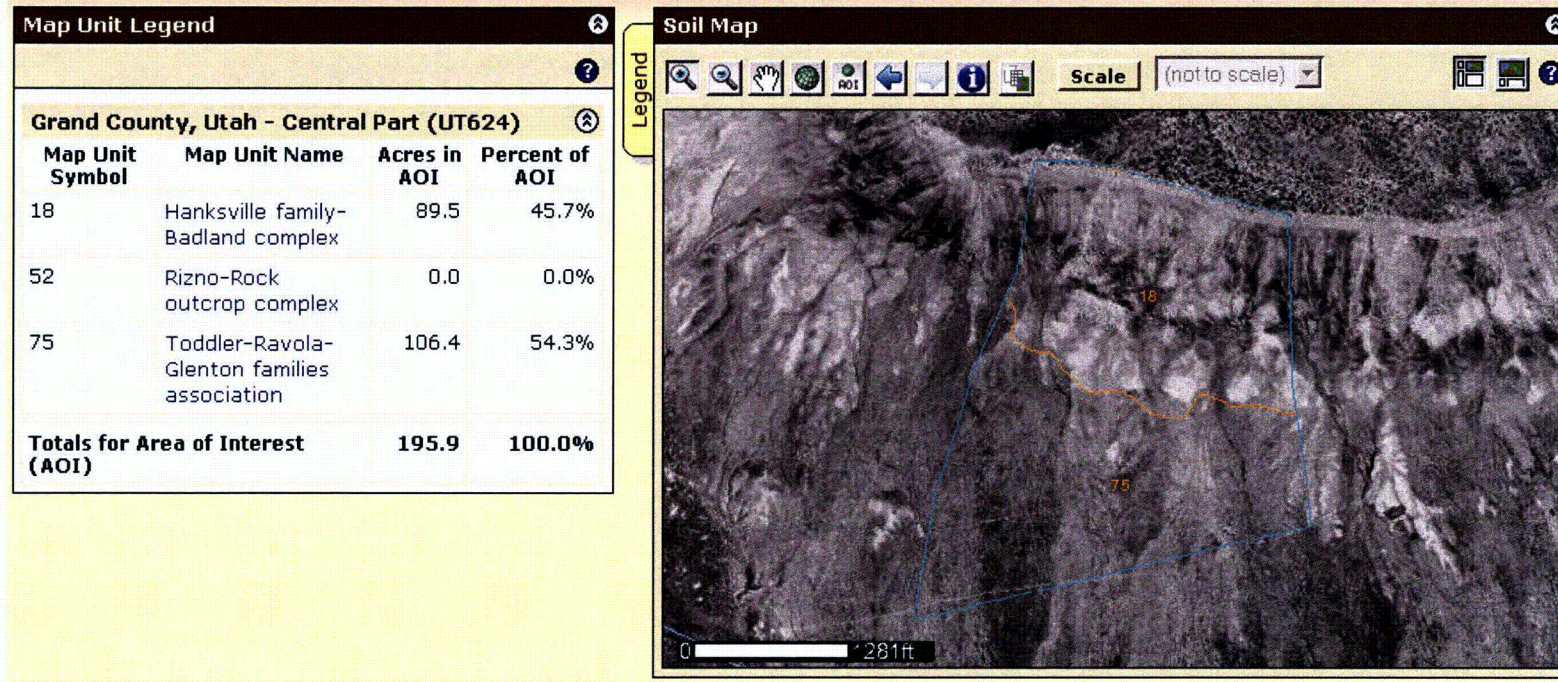
Typical profile

- 0 to 3 inches: Extremely bouldery silt loam
- 3 to 14 inches: Silty clay loam
- 14 to 23 inches: Silty clay
- 23 to 35 inches: Silty clay
- 35 to 39 inches: Weathered bedrock

Description of Badland

Setting

- Landform: Cuestas, mesas
- Down-slope shape: Linear
- Across-slope shape: Convex



Map Unit Legend			
Grand County, Utah - Central Part (UT624)			
Map Unit Symbol	Map Unit Name	Acres in AOI	Percent of AOI
11	Chipeta complex	9.9	0.8%
18	Hanksville family-Badland complex	224.6	19.1%
31	Mesa-Chipeta-Thedalund family complex	24.3	2.1%
52	Rizno-Rock outcrop complex	12.0	1.0%
75	Toddler-Ravola-Glenton families association	902.4	76.9%
Totals for Area of Interest (AOI)		1,173.3	100.0%



Appendix C
RUSLE2 Results

Worksheet: Crescent Junction Constant Slope

Tract #: Book Cliffs
 Owner name: Bob
 Field #: West

Info: RUSLE2 simulation of constant slope in the area between the wedge and the Book cliffs.

Compare management alternatives for a single hillslope profile | Compare individual hillslope profiles | Compute avg. soil loss for a field/watershed

Location: Utah\Crescent Junction
 Soil: CJ Glenton
 Length along slope, ft: 2600
 Avg. slope steepness, %: 3.5

Segment	Steepness, %	Length along slope, ft
1	3.5	1000
2	3.5	800
3	3.5	800

Temp. scenario	Base management	Residue burial level	General yield level	Contouring	Strips/barriers	Diversion/terrace, sediment ba	Surf. cov. values	Detachment on slope, t/ac/yr	Soil loss erod. portion, t/ac	Soil loss for cons. plan, t/ac/yr	Sediment delivery, t/ac/yr
Profile	Bare ground, smooth surface	Normal	Normal	Contour	(none)	(none)	cover	2.6	2.6	2.6	2.6

Worksheet: Crescent Junction Compound Slope

Tract #: Book Cliffs
 Owner name: Bob
 Field #: West

Info: RUSLE2 simulation of compound slope of area between the wedge and the Book cliffs.

Compare management alternatives for a single hillslope profile | Compare individual hillslope profiles | Compute avg. soil loss for a field/watershed

Location: Utah\Crescent Junction
 Soil: CJ Glenton
 Length along slope, ft: 2600
 Avg. slope steepness, %: 16

Segment	Steepness, %	Length along slope, ft
1	40	1000
2	3.5	800
3	2.5	800

Temp. scenario	Base management	Residue burial level	General yield level	Contouring	Strips/barriers	Diversion/terrace, sediment ba	Surf. cov. values	Detachment on slope, t/ac/yr	Soil loss erod. portion, t/ac	Soil loss for cons. plan, t/ac/yr	Sediment delivery, t/ac/yr
Profile	Bare ground, smooth surface	Normal	Normal	Contour	(none)	(none)	cover	27	28	13	9.1

Soil: CJ Glenton

Graphic: 

Rock cover, %: 0

Erodibility, US: 0.43

Texture: Loam

Hydrologic class: B - mod. low runoff

Hydrologic class with subsurface drain: B - mod. low runoff

Calculate consol. from precip?: No
 Nominal consolid. time, yr: 7.0
 T value, t/ac/yr:

Particle sizes	Nomograph Info	Volcanic Info	Detached particles	Info
Sand, %	45			
Silt, %	30			
Clay, %	25			

Climate: Utah\Crescent Junction

R Factor, US
 10 year EI, US

Standard EI distribution

In Req area?
 Use Req EI dist.?
 H Equiv, US
 EI dist. for Req condition
 Adjust for soil moisture?

Annual precip, in.

Vary soil Erod. with climate?

Monthly | Daily | Info

Monthly Climate			
Month	Avg. temp., deg C	Month precip., mm	
Jan	-3.1	25	
Feb	0.78	14	
Mar	5.0	26	
Apr	10.0	21	
May	15	25	
Jun	20	9.0	
Jul	25	20	
Aug	24	22	
Sep	18	26	
Oct	12	31	
Nov	4.1	17	
Dec	-0.31	16	

JACOBS

Calculation Cover Sheet

(Ref. FOWI 116 Design Calculations)

Calculation No:
C-04

Page 1 of 23 – Plus
Appendices 31 Pgs

Rev. No.: 2

Revision Date:
2/06/08

Previous Revision
Date: 01/30/08

Current Revision
Date: 2/06/08

Issuing Department:

Federal Operations Design Engineering

Supersedes:

Client: Energy solutions
Project Title: Moab UMTRA
Project Number: 35DJ2600
System:

Engineering Discipline: Civil

Calculation Title: Area between Cell and Wedge

Purpose:

Analyze the area between the wedge and the waste cell to determine.

1. Does the ditch between the south side of the wedge and the access road require erosion protection to prevent runoff from the south side slope of the wedge eroding the berm on which the access road is constructed?
2. The discharge rate of runoff from the north side of the cell and the area between the cell and the access road to determine the need for flow control at the northwest and northeast corners of the cell aprons. The size of rock required for erosion protection north of the berm that diverts this runoff to the spreaders.
3. The size of rock lining required to protect the ditches north of the access road (beyond the end of the road) carrying water to the outlet spreaders on the east and west.
4. The scour depth at the spreader outlets.
5. The size of rock armoring required for the spreaders.
6. The effect of erosion on the south side slope of the wedge on the integrity of the wedge including both sheet and rill erosion and gully formation.

Prepared by: Bob Yager

Robert E. Yager

Date: 02/06/08

Checked by: Bill Barton

Bill Barton

Date: 02/06/08

Engineering Managers Approval: Bill Barton

Bill Barton

Date: 02/06/08

C04_R2_Area_Between_Cell_and_Wedge_Calc_Pg01-23_Moab020608.doc The current applicable version of this publication resides on Jacobs' Intranet. All copies are considered to be uncontrolled. Copyright Jacobs Engineering Group Inc., 2007

Revision History:		
Pages Affected By Revision	Revised/Added/Deleted	Description of Revision
<u>Revision 1 Modifications</u>		
Page 3	Added	Inserted item 8 in bullet list under "Description of Calculation".
Page 8	Revised	Renumbered items in list under "Description of Calculation"
Page 8	Added	Inserted item 7 in bullet list under "Method of Solution".
Page 11	Added	Added <u>Spreader Rock and Scour.xls</u> under "Calculation Section"
Page 20	Revised	Revised last sentence of first paragraph under "Rock in Channels and on North Side of Berms"
Page 21	Revised	Changed heading from "Scour at Spreader Outlets" to "Rock and Scour at Spreader Outlets"
Page 21	Added	Added two rows to Table 8.
Page 22	Revised	Changed scour depth of 4.47' to 4.46 ft in item 5.
Page 22	Added	Added rock size calculation results to item 5.
<u>Revision 2 Modifications</u>		
Page 3	Revised	Revised first paragraph on page 20 to describe flow in channels instead of along north side of berms.
Page 8	Revised	Revised Table 7 on page 20 to be consistent with flow in channels.

Description of Calculation:

- Determine the runoff from the areas encompassing the south slope of the wedge for design storms with return intervals from 1 year to the PMP.
- Calculate the potential sediment transport in a hypothetical channel that routes the runoff along the south side of the wedge toward the east and toward the west using methods from Johnson, 2002.
- Calculate the sediment loss from the south slope of the wedge using the Modified Universal Soil Loss equation (MUSLE) (Nelson, et. al., 1986)
- Compare the potential sediment loss from the south slope of the wedge with the potential sediment transport in the ditches between the wedge and the access road to determine whether net erosion or sedimentation is expected to occur.
- Calculate the potential depth of gullies formed on the top and side slopes of the wedge using the methodology of Johnson, 2002 to determine whether the wedge may be breached by gullying.
- Calculate the size of rock protection required in the ditch south of the wedge beyond the east and west ends of the access road using the safety factor method.
- Calculate the expected depth of scour at the spreader outlets for the PMP storm using the methods of the Federal Highway Administration.
- Compute the rock size required for erosion protection from the flow in the spreaders.
- Compute the peak runoff from the PMP for the watersheds comprising the areas between the access road berm and the drainage divide on top the cell using SCS methods.
- Compute the rock size required for erosion protection for flow along the north side of the berms from the northwest and northeast corners of the cell using the safety factor method.

Assumptions:

- The 1-hour PMP event is estimated to be 8.2 inches, ("Site Drainage—Hydrology Parameters" calculation, Draft RAP Attachment 1, Appendix E).
- The rainfall frequency-depth-duration data were developed in the Draft RAP. The 1 year rainfall depth was taken from the NOAA Atlas 14 (http://hdsc.nws.noaa.gov/hdsc/pfds/sa/ut_pfds.html).
- Over a period of 1000 years 12.7% of the total rainfall will become runoff (Johnson, 2002).
- The unit weight of compacted soil in the wedge and the road berm is 103.5 pcf.

Design Inputs:

See following pages.

Software:

Title	Developer	Versions	Revision Level
EXCEL	Microsoft	2002	
HEC-HMS	USACE	3.1.0	

C04_R2_Area_Between_Cell_and_Wedge_Calc_Pg01-23_Moab020608.doc The current applicable version of this publication resides on Jacobs' Intranet. All copies are considered to be uncontrolled. Copyright Jacobs Engineering Group Inc., 2007

JACOBS

(Ref. FOWI 116 Design Calculations)

Calculation Sheet

Project: 35DJ2600
Calculation Number: C-04
Page 6 of 23 – Plus Appendices 31 Pgs

Calculation Section:

See following pages.

C04_R2_Area_Between_Cell_and_Wedge_Calc_Pg01-23_Moab020608.doc The current applicable version of this publication resides on Jacobs' Intranet. All copies are considered to be uncontrolled. Copyright Jacobs Engineering Group Inc., 2007

Conclusions/Recommendations:

See following pages.

Reference:

See following pages.

DESCRIPTION OF CALCULATION:

Analyze the area between the wedge and the waste cell to determine.

1. Does the ditch between the south side of the wedge and the access road require erosion protection to prevent runoff from the south side slope of the wedge eroding the berm on which the access road is constructed?
2. The discharge rate of runoff from the north side of the cell and the area between the cell and the access road to determine the need for flow control at the northwest and northeast corners of the cell aprons. The size of rock required for erosion protection north of the berm that diverts this runoff to the spreaders.
3. The size of rock lining required to protect the ditches north of the access road (beyond the end of the road) carrying water to the outlet spreaders on the east and west.
4. The scour depth at the spreader outlets.
5. The effect of erosion on the south side slope of the wedge on the integrity of the wedge including both sheet and rill erosion and gully formation.

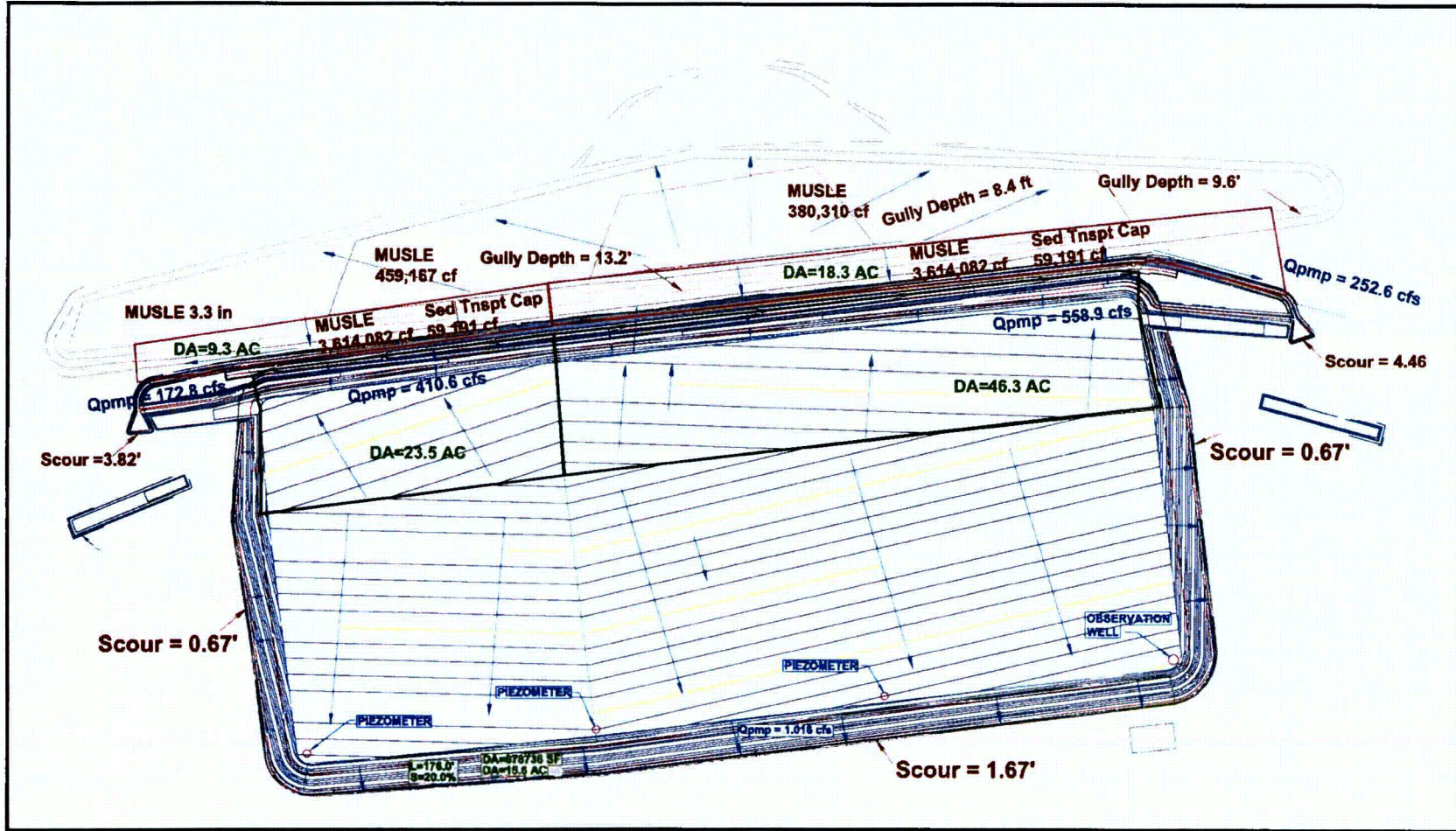
METHOD OF SOLUTION:

- Determine the runoff from the areas encompassing the south slope of the wedge for design storms with return intervals from 1 year to the PMP.
- Calculate the potential sediment transport in a hypothetical channel that routes the runoff along the south side of the wedge toward the east and toward the west using methods from Johnson, 2002.
- Calculate the sediment loss from the south slope of the wedge using the Modified Universal Soil Loss equation (MUSLE) (Nelson, et. al., 1986)
- Compare the potential sediment loss from the south slope of the wedge with the potential sediment transport in the ditches between the wedge and the access road to determine whether net erosion or sedimentation is expected to occur.
- Calculate the potential depth of gullies formed on the top and side slopes of the wedge using the methodology of Johnson, 2002 to determine whether the wedge may be breached by gulying.
- Calculate the size of rock protection required in the ditch south of the wedge beyond the east and west ends of the access road using the safety factor method.
- Calculate the size of rock protection required for flow in the spreaders.
- Calculate the expected depth of scour at the spreader outlets for the PMP storm using the methods of the Federal Highway Administration.
- Compute the peak runoff from the PMP for the watersheds comprising the areas between the access road berm and the drainage divide on top of the cell using SCS methods.
- Compute the rock size required for erosion protection for flow along the north side of the berms from the northwest and northeast corners of the cell using the safety factor method.

ASSUMPTIONS:

- The 1-hour PMP event is estimated to be 8.2 inches, ("Site Drainage—Hydrology Parameters" calculation, Draft RAP Attachment 1, Appendix E).
- The rainfall frequency-depth-duration data were developed in the Draft RAP. The 1 year rainfall depth was taken from the NOAA Atlas 14 (http://hdsc.nws.noaa.gov/hdsc/pfds/sa/ut_pfds.html).
- Over a period of 1000 years 12.7% of the total rainfall will become runoff (Johnson, 2002).
- The unit weight of compacted soil in the wedge and the road berm is 103.5 pcf.

Figure 1 Configuration of the Wedge and the Waste Cell



CALCULATION SECTION:

Calculations are performed in the spreadsheets RoadBermNE Erosion.xls RoadBermNW Erosion.xls.
WatershedParms.xls Channel Rock and Scour.xls Spreader Rock and Scour.xls.

Sediment Transport Capacity**Drainage Area Characteristics**

Two drainage areas were delineated between the wedge and the access road draining to the southeast and to the southwest. Two more were delineated between the watershed divide on top the cell and the access road to the northeast and the northwest. These drainage areas are shown in Figure 1. For all storms except the PMP, an initial abstraction of 0.3 inches was estimated for compacted NRCS Type B soil (<http://websoilsurvey.nrcs.usda.gov/app/WebSoilSurvey.aspx>) with a constant infiltration rate of 0.1inches/hour. For the PMP the initial abstraction was set equal to 0.0 inches. Figure 2 shows a cross section through the south side slope of wedge to the north slope of the waste cell.

Pertinent properties of the four drainage areas are computed in WaterShedParms.xls and listed in Table 1. The flow lengths are used to develop a unit hydrograph using the USBR methodology and the Lag time is used in the SCS unit hydrograph method. The time of concentration was computed as the time along the predominantly east-west flow paths plus the time along the steeper predominantly north-south flow paths.

Table 1. Drainage Area Characteristics

Drainage Area	Area (acres)	Max Flow Length (ft)	Time of Concentration (min)	Lag = 0.6 Tc
Southwest Wedge Side Slope	9.3	2062	23.38	14.0
Southeast Wedge Side Slope	18.3	3470	35.53	21.3
Northwest Portion of Cell	23.5	1471	25.38	15.2
Northeast Portion of Cell	46.3	2891	41.96	25.2

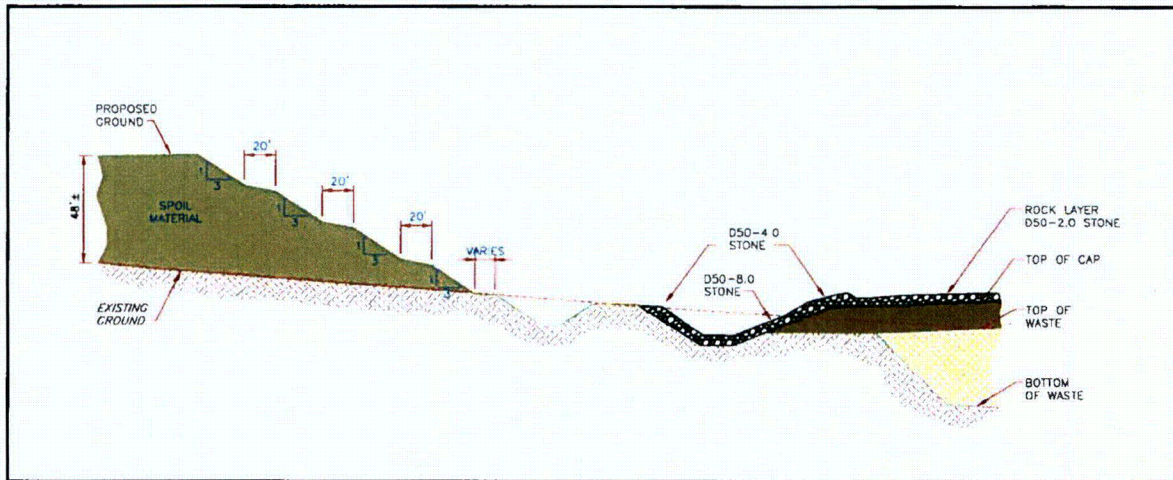


Figure 2 Cross Section of the Area between the Waste Cell and the Wedge.

Runoff Hydrograph Calculations

Since these drainage areas are constructed and not in a natural condition, the SCS unit hydrograph transform was used. The USBR method was developed for natural areas in the west and is not appropriate for the constructed wedge and cell. The runoff hydrographs were computed using the Computer Program HEC-HMS (USACE 2007).

Rainfall Depths Applied

The series of storms for the runoff calculations was developed from the Hydrology data in the draft RAP and NOAA Atlas 14. The number of storms of each depth was chosen conservatively as follows.

- A storm with rainfall depth equal to or greater than the 1000 year storm occurs on the average once every 1000 years. Since the rainfall depth may be any depth between the 1000 year storm and the PMP, the PMP was used for this storm.
- A storm with rainfall depth equal to or greater than the 500 year storm occurs on the average twice every 1000 years. Since the rainfall depth may be any depth between the 500 year storm and the 1000 year storm, the 1000 year rainfall depth was used for this storm. Since the PMP is one of these storms, one 1000 year storm was used.
- A storm with rainfall depth equal to or greater than the 200 year storm occurs on the average five times every 1000 years. Since the rainfall depth may be any depth between the 200 year storm and the 500 year storm, the 500 year rainfall depth was used for this storm. Since two larger storms have already been applied, three 500 year storms were used.

Following this logic through storms of all available return periods resulted in the distribution of rainfall depths and number of storms listed in Table 2. All storms represent 24 hour precipitation depth except for the PMP which is a 6 hour depth.

Table 2 Design Storms used in Sediment Transport Capacity Calculations.

Return Interval Represented (years)	Return Interval Employed (years)	Precipitation Depth (inches)	Number of Storms Equal or Greater than Interval Represented	Number of Storms of Depth Employed
1000	PMP (6 hour)	9.0	1	1
500	1000	3.73	2	1
200	500	3.15	5	3
100	200	2.58	10	5
50	100	2.35	20	10
25	50	2.12	40	20
10	25	1.91	100	60
5	10	1.63	200	100
2	5	1.42	500	300
1	2	1.16	1000	500
< 1	1	0.93	Unknown	1000

The runoff from each area was computed using HEC-HMS with the results from the wedge and from the book cliffs area flowing to the west combined into one hydrograph. A five minute time step was used.

Sediment Transport Capacity

The capacity of the flow to the east and the flow to the west along the north edge of the wedge was estimated using a procedure in NUREG 1823 (Johnson 2002). In this method the sediment transport capacity of a channel can be computed as

$$q_s = c_{s1} h^{c_{s2}} V^{c_{s3}}$$

where

q_s = unit sediment transport rate in ft^2/s (unbulked)

V = velocity in ft/s

h = flow depth in feet

NUREG 1623 gives the coefficient and exponents as a function of grain size distribution. Those that most closely correspond to the grain size distribution of the native soil are

$$C_{s1} = 3.3 \times 10^{-5}$$

$$C_{s2} = 0.715$$

$$C_{s3} = 3.30$$

Trapezoidal channels with a bottom width of 2 feet and a side slope of 3 horizontal to 1 vertical were assumed (See Figure 3). The slope of the channels were 0.007 to the east and 0.005 to the west as determined from the topography of the site and the location of the channels. A table was constructed of sediment transport in cfs as a function of discharge in each channel. The flow in each 5 minute period of a runoff hydrograph was then used to interpolate to find the sediment transport during each 5 minute increment of the hydrograph. The sediment transport of each hydrograph was then computed as the sum of these 5 minute contributions.

For the channel shown below with a discharge Q , a depth h , and a top width T , the volume of sediment transport capacity in a five minute period was calculated as follows. q_s was computed as above. Since this is

C04_R2_Area_Between_Cell_and_Wedge_Calc_Pg01-23_Moab020608.doc The current applicable version of this publication resides on Jacobs' Intranet. All copies are considered to be uncontrolled. Copyright Jacobs Engineering Group Inc., 2007

the unbulked volume transport rate the unit weight was assumed to be 165 pcf. The value of q_s will vary across the channel as it depends on both the velocity and depth of flow. As a conservative approach, the value q_s computed for the full depth, h , was applied throughout the channel. The total rate of sediment transport in cubic feet/sec (unbulked) was computed as

$$Q_s(\text{unbulked}) = q_s T$$

$q_s * T$ and the rate in cf/5 min (bulked) as

$$Q_s(5 \text{ min_bulked}) = Q_s(\text{unbulked}) * (300 \text{ sec}) * \frac{165 \text{ pcf}}{103.5 \text{ pcf}}$$

where the unit weight of compacted soil in the wedge and the road berm is 103.5 pcf.

These 5 minute contributions was summed for each of the 5 minute flow periods of a storm hydrograph to compute the total sediment transport potential in cf of the native soil from a single storm.

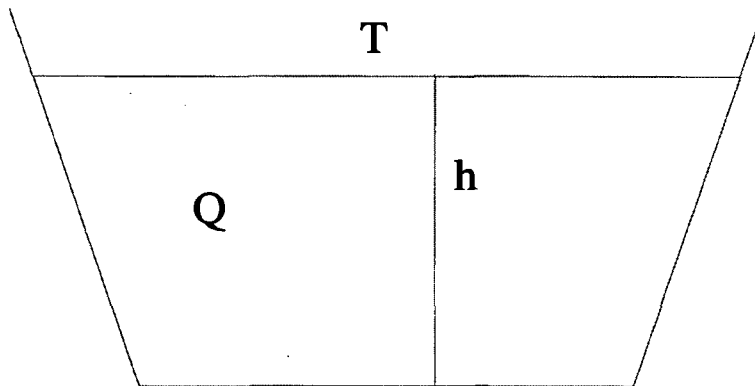


Figure 3 Assumed Cross Section of the Channel Carrying Runoff from the South Side of the Wedge.

This calculation was repeated for all the storms listed in Table 2 and the total potential sediment transport during 1000 years was computed. These calculations are performed in the files RoadBermNE Erosion.xls and RoadBermNW Erosion.xls.

Unaccounted for Runoff

The total runoff of water in the listed storms was also computed. Since the annual rainfall at Thompson during the period (1971-2000) was 9.97 inches(reference), and NUREG 1623 states that a reasonable estimate of the ratio of runoff to rainfall in the semi-arid regions of the western United States is 0.127, a volume of total expected runoff during 1000 years was computed. Comparing this volume with that computed from the listed storms indicated that 40% of the runoff had not been accounted for by the listed storms.

Assuming that the sediment concentration in this additional runoff will be equal to the average concentration in the runoff from the one year storm, an additional volume of sediment transport was added by multiplying this average concentration by the volume of additional runoff.

Sediment Supply from the Book Cliffs Area

The runoff from the south side of the wedge will transport sediment toward the ditch between the wedge and the road berm. The total sediment loss over a 1000 year period from the two watersheds on the south slope of the wedge can be estimated with the Modified Universal Soil Loss Equation (MUSLE).

The equation is

$$A = R \times K \times LS \times VM$$

where:

- A = soil loss in tons per acre per year,
- R = rainfall factor,
- K = soil erodibility factor,
- LS = topographic factor, and
- VM = dimensionless erosion control factor relating to vegetative and mechanical factors.

The rainfall factor is 25, as given in NUREG/CR-4620 (Nelson et al. 1986) for the eastern third of Utah. The soil erodibility factor was estimated using the nomograph given in NUREG/CR-4620 (Nelson et al. 1986).

The topographic factor is calculated by the following equation:

$$LS = \frac{650 + 450 \times s + 65 \times s^2}{10,000 + s^2} \times \left(\frac{L}{72.6} \right)^m$$

where:

- s = slope steepness in percent,
- L = slope length in ft, and
- m = exponent dependent upon slope steepness.

The dimensionless erosion control factor used for the undisturbed watersheds was 0.4, from Table 5.3 of NUREG/CR-4620 (Nelson et al. 1986), representing seedings of 0 to 60 days to mimic light vegetation in the area. Over an extended period of time, some vegetation can be expected to develop. Table 3 summarizes the results of the soil loss equation. Since the south side slope of the wedge varies from approximately 118 to 176 feet wide and 30 to 48 feet high, intermediate values of 160 feet wide and 40 feet high were used in this analysis. As the results will indicate, no further refinement was warranted.

Table 3. Results of Soil Loss Equation

Soil Cover	Western End of Side Slope	Eastern End of Side Slope
Rainfall factor, R	25	25
Silt and very fine sand (%)	60	60
Sand (%)	25	25
Organic matter (%)	2	2
Soil structure	Very fine granular	Very fine granular
Relative permeability	Moderate	Moderate
Erodibility factor	0.35	0.35
Topographic factor, LS	7.94	7.94
VM (low density seedings)	0.4	0.4
Soil loss (tons/acre/year)	27.8	27.8
Soil loss (feet)/1,000 years	12.3	12.3
Area of Side Slope (acres)	6.1	11.9
Total sediment loss in 1000 years (cf)	3,265,142	6,417,082

Sediment Budget

The calculated volumes of potential sediment transport from the ditch and sediment supply from the side slope of the wedge over a 1000 year period are summarized in Table 4.

Table 4 Sediment Budget for the Area between the Road Berm and the Wedge.

Area	Sediment Transport Capacity (cf)	Sediment Yield from MUSLE (cf)
Channel along south side of wedge to the west	22,792	
Channel along south side of the wedge to the east	59,191	
Western portion of the south side of the wedge		3,265,142
Eastern portion of the south side of the wedge		6,417,082
Ratio of sediment supply to transport capacity (west)	143	
Ratio of sediment supply to transport capacity (east)	108	
Volume of Ditch to the West	588,000 cf (18% of potential sediment supply)	
Volume of Ditch to the East	1,156,400 cf (18% of potential sediment supply)	

These results indicate that the water flowing in the ditch along the southern side of the wedge to the west and the east does not have sufficient sediment transport capacity to carry away the supply of sediment from the south side slope of the wedge. These results indicate a sufficient volume of sediment will erode from the south side slope of the wedge to completely fill the ditch in about 180 years. Because of the geometry of the wedge and the ditch, the flow in the ditch will increase from the high point near the east-west center of the wedge and carry increasingly more sediment as the flow proceeds downstream. The nearly uniform sediment supply along the length of the ditch and the increase in sediment transport capacity in a downstream direction will cause the bottom slope of the ditch to increase over time. This will increase the sediment transport capacity of the ditch, but it is not expected to increase enough to carry away the total sediment supply from the side slope of the wedge.

Erosion from Side Slope of the Wedge

The results presented in Table 3 indicate soil to a depth of approximately 12 feet will be lost from the south side slope of the wedge. Since the south side slope of the wedge will be 30 feet high at the east and west ends and 48 feet high in the center, this depth of erosion, while substantial, will not threaten the integrity of the wedge since the top of the wedge is over 230 feet wide at the west end and 150 feet at the east end.

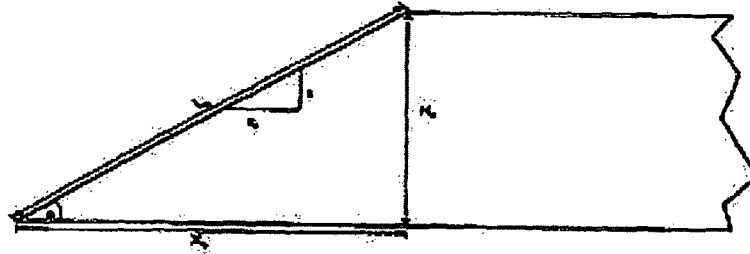
Gully Formation on the Side Slope of the Wedge

In addition to potential erosion of the wedge by sheet and rill erosion from precipitation directly on the south side slope of the wedge, the runoff from precipitation on the south side slope is expected to form gullies on these steep slopes. The potential depth of these gullies can be estimated with an approach detailed in NUREG 1623. The three types of embankment geometries analyzed in this guidance document as shown in Figure 4. Gullies forming on the steep side slope wedge are analyzed as a Type 3 slope. The effective tributary drainage area for a gully is computed as

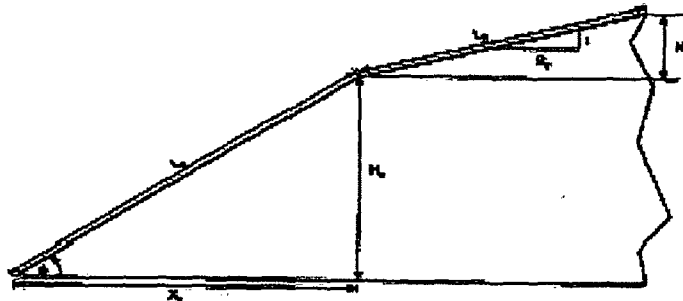
$$A = 0.276[L \cos(\theta)]^{1.636}$$

where L = total length of the flow path. A gully factor depending on the soil type, the height of the embankment and the volume of runoff to the toe of the embankment toe is

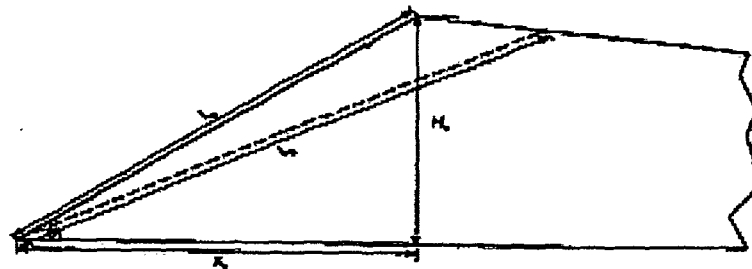
$$G_f = \frac{1}{2.80 + \left[0.197 \frac{V_r}{H_o^3} \right]^{-0.70}} \text{ for a clay content between 15 and 50\%}$$



Type 1 Embankment



Type 2 Embankment



Type 3 Embankment

Figure B-4. Three types of embankment geometry.

NUREG-1623

B-6

Figure 4 The Three Types of Embankment Geometry Analyzed in NUREG 1623 for Gully Formation.

The estimated maximum depth of gully incision is

$$D_{\max} = G_f L_{\text{total}} S$$

where S is the original slope of the embankment. The top width of the gully at its deepest point is

$$W = \left[\frac{D_{\max}}{0.61} \right]^{1.149}$$

and the location of the deepest incision measured in units of D_{\max} downslope from the crest of the embankment is

$$D_i = 0.713 \left[\frac{V_r S}{L_o^3} \right]^{-0.415}$$

The results of these calculations are summarized in Table 5. The calculations are performed in metric units and the results converted to English units.

Table 5 Data and Results of Calculations of Gully Depths.

Variable	Description	End of South Side Slope	Center of South Side Slope
H_o (ft)	Height of Embankment	30	48
X_o (ft)	Horizontal Length of Embankment	118	176
L_o (ft)	Length of Embankment along Slope	121.8	182.4
θ (radians)	Embankment Slope Angle	0.249	0.266
L_l (ft)	Long Term Embankment Slope Length	143	214
A (sq ft)	Effective Drainage Area	1,358	2,612
V_r (cf)	Rainfall Volume	143,310	275,637
G_f	Gully Factor	0.27	0.22
D_{\max} (ft)	Maximum Gully Depth	9.6	13.2
W (ft)	Gully Width at Maximum Depth	20	28.5
D_i (ft)	Distance of D_{\max} from Top of Slope	35	58

While the predicted depth of the gullies that will form on the south side slope of the wedge over a period of 1000 years are substantial, the gullies are not expected to threaten the ability of the wedge to route runoff from the Book Cliffs around the waste cell. In each case the height of the wedge is more than three times the calculated gully depth and the minimum north-south dimension of the wedge is 118 feet, much greater than the expected gully depth.

Rock in Channels and on North Side of Berms

The channels carrying runoff from the south side slope of the wedge to the east and to the west will not be armored for most of their lengths because of the excess sediment supply from the south side of the wedge. Beginning approximately 100 feet upstream of each end of the end of the access road, rock will be placed in the channels to protect them against erosion from that point to the spreaders that terminate the channels. If the channels fill with sediments, the flow will leave the channels and flow southward toward the berm shown in Figure 2. In addition, flow from the top of the cell and the area south of the access road and north of the cell will flow to the east and to the west in trapezoidal ditches with 3H to 1V side slopes and a bottom width of 20 feet. The flow in these ditches will continue along the north side of berms that extend from the cell side slopes to the spreaders.

The peak flows resulting from the PMP in each of these areas have been calculated using the SCS unit hydrograph technique with an initial abstraction of 0.0 inches and a constant infiltration rate of 0.1 inches/hour. The results of these calculations are included in Table 6. The time of concentration is calculated as the sum of the flow on each of the slopes in the drainage area. For example, the time of concentration for the flow from the cell toward the west is the sum of T_c (northward flow on the top slope of the cell) + T_c (northward flow on the side slope of the cell) + T_c (westward flow to the point where the channel turns south.) Except for flow on the cell as described in Cell_Rock.doc, the mean of the Kirpich and SCS time of concentration equations was used. Except for the peak flow, these data are copied from Table 1.

Table 6 Peak Flows from the Area between the Wedge and the Waste Cell for the PMP.

Peak flow from PMP	South Side of Wedge (West)	South Side of Wedge (East)	Flow from Cell (West)	Flow from Cell (East)
Drainage Area (acres)	9.3	18.3	23.5	46.3
Time of Concentration (min) (T_c)	23.4	35.5	25.4	42.0
Lag (min) = $0.8T_c$	14.0	21.3	15.2	25.2
Peak Flow (cfs)	172.8	252.6	410.6	558.9

The D50 of stone erosion protection was determined using the safety factor method. The results of these calculations are presented in Table 7. Each of the channels north of the road berm is assumed to have a bottom width of 10 feet and side slopes of 3H to 1V. The flow from the cell flows along the north of the berms with the side slope of the channel being 3H to 1V along the berm and 2.3% (the natural ground slope) on the opposite side.

Table 7 D50 of the Stone Required for Erosion Protection

D50 for Erosion Protection	South Side of Wedge (West)	South Side of Wedge (East)	Flow from Cell (West)	Flow from Cell (East)
Peak Flow (cfs)	172.8	252.6	410.6	558.9
Channel Slope	.0094	.0076	.0089	.0063
D50 (inches) on 3:1 Side of Channel	3.3	3.4	3.8	3.3
D50 (inches) on Bottom of Channel	2.6	2.6	2.9	2.5
Portion of Channel after it has Turned Southerly				
Channel Slope	.0175	.0175		
D50 (inches) on Side of Channel	5.8	7.2		
D50 (inches) on Bottom of Channel	4.5	5.6		

Rock and Scour at Spreader Outlets.

Flow from the channel north of the access road and from the top of the cell will combine at the spreader for discharge onto the natural ground. The peak flows from the PMP have been added to estimate the peak flow from each spreader. To obtain the flow per unit width, the peak flow has been spread over a width of 100 feet. To account for potential channelization in the rock of the spreaders, the unit flow has been multiplied by three for calculation of the required D50 of rock for erosion protection and potential scour depth at the outlet of each spreader. The D50 was calculated using the safety factor method assuming a channel with 3H to 1V side slopes, a 1 ft bottom width and a channel slope of 2.3%. The scour was calculated using the Federal Highway Administration culvert scour equations as described in Calculation C-02 assuming flow in a v-shaped ditch with 2H to 1V side slopes. The results are summarized in Table 8.

Table 8 Calculated Depth of Scour at Spreader Outlets.

	West Spreader	East Spreader
Peak Flow from Channel (cfs)	172.8	252.6
Peak Flow along Berm (cfs)	410.6	558.9
Combined Peak Flow (cfs)	583.4	811.5
Concentration Factor	3	3
Design Flow (cfs/ft)	17.50	24.35
Minimum Rock D50 (in)	4.5	5.2
Estimated Scour Depth (ft)	3.82	4.46

The spreaders should be constructed with rock armoring extending approximately 5 feet below ground level to protect against head cutting by scour from the discharge of the PMP runoff.

Summary

A wedge of spoil material consisting of approximately 3,000,000 cubic yards of soil excavated from the waste cell will be placed between the Book cliffs and the waste cell to divert runoff from the Book Cliffs area around the waste cell. These calculations have been performed to assess whether erosion protection is required for the ditch north of the access road and south of the wedge and to assess the sediment budget in that ditch. The erosion protection requirements of the broad channels that carry flow from the areas between the wedge and the cell to the outlet spreaders on the east and west have also been determined. Specific results/conclusions are summarized here.

1. Runoff from direct precipitation on the south slope of the wedge will be collected and carried to the east and west by ditches between the wedge and the access road. The sediment transport capacity of this runoff during the 1000 year design life has been assessed using equations from NUREG 1623. The supply of sediment by sediment yield from the south side slope of the wedge has been estimated by use of the Modified Universal Soil Loss Equation (MUSLE), as described in NUREG 4620 (Nelson et al. 1986). The results of these calculations indicate that the total sediment carrying capacity of the runoff as it flows to the east and west is approximately 5% of the volume of the access road berm over the 1000 year design life of the cell. The sediment supply to this area estimated from the MUSLE will be many times larger than the sediment transport capacity of the flow in these channels. The net sediment supply to these channel indicates that the channels may fill with sediment in somewhat less than 200 years. The sediment supply will be nearly uniform along the length of the ditch, but the flow will be very small at the high point of the channels and increase nearly uniformly toward the east and west. This will result in a greater sediment transport capacity in a downstream direction and cause the bottom slope of the ditch to increase over time. This will increase the sediment transport capacity of the ditch, but it is not expected to increase enough to carry away the

sediment supply to the channel. This will delay the filling of the ditches with sediment but probably not beyond the 1000 year design life of the waste cell. Some additional flow from the north side of the waste cell may run off over the access road and add to the flow and sediment transport capacity of these channels, but it will not be sufficient to keep them flushed of sediment.

2. Precipitation falling directly on the south side slope of the wedge will run off toward the south. This runoff will erode the side slope of the wedge. Application of the MUSLE to estimate the volume of sediment lost from the wedge through this mechanism indicate that the south side slope will be reduced in average height by approximately 12 feet. With a design height ranging from approximately 30 to 48 feet and a north-south dimension ranging from 150 to 490 feet, this loss of soil will not threaten the integrity of the wedge.
3. Runoff from the south side slope of the wedge will also concentrate and form gullies on the slope. The depth, width, and location of the deepest portions of these gullies has been estimated with techniques described in NUREG 1623 (Johnson 2002). The results are summarized in Table 5. While the predicted depth of the gullies that will form on the south side slope of the wedge over a period of 1000 years are substantial, the gullies are not expected to threaten the ability of the wedge to route runoff from the Book Cliffs around the waste cell. In each case the height of the wedge is more than three times the calculated gully depth and the minimum north-south dimension of the wedge is 118 feet, much greater than the expected gully depth or length. It should be noted that because of the time period over which gullies developed that were used in developing the equations, the NRC staff recommends that this method be used for a design cell life of 200 years. Since the gully depth increases with time, the calculation has been extrapolated to 1000 years as the best available estimate of the extent of potential gully formation over a 1000 design period.
4. Flow from the south side slope of the wedge and from the north portion of the cell top and side slopes will flow to the east and west. The flow from the cell will be carried in a channel south of the access road with the cell apron being the bottom of the channel, one side slope is the cell side slope of 5H to 1V, and the opposite side has a 3H to 1V side slope with rock armoring with a D50 of 4 inches. As this water reaches the east and west edges of the cell apron, it will continue to flow in a shallow channel formed by a berm to the south and the natural ground slope to the north. The north sides of the berms with a 3H to 1V side slope will be protected by stone armoring with a D50 of 4 inches. The broad north side of the channel with a nominal side slope of 2.3% will be protected by rock with a D50 of 3 inches. The channels carrying the flow from the side slope of the wedge will not be armored until 100 feet before the end of the access road berm. From that point the channels will be armored with rock with a D50 of 2.0 inches until they turn south. From that point to the spreader the rock D50 will be 4.5 inches on the bottom and 5.8 inches on the side for the channel to the west and 5.6 and 7.2 inches for the channel to east.
5. The two channels carrying flow in each direction (east and west) will both discharge into the spreaders and spread to a channel 100 feet wide. The calculated scour depth for the PMP is 3.82 feet for the spreader on the west and 4.46 feet for the spreader on the east. A concentration factor of three has been assumed for determining the design unit flow. The spreaders will each have rock armoring with a minimum D50 of 4.5 inches on the west and 5.2 inches on the east. This rock protection will extend to a depth of 5 feet at the outlets.

References:

- 10 CFR 40. U.S. Nuclear Regulatory Commission (NRC), "Domestic Licensing of Source Material," Appendix A, *Code of Federal Regulations*, February 2007.
- 40 CFR 192. U.S. Environmental Protection Agency (EPA) "Health and Environmental Protection Standards for Uranium and Thorium Mill Tailings," *Code of Federal Regulations*, February 2007.
- Abt, S.R., and T.L. Johnson, 1991. "Riprap Design for Overtopping Flow", *Journal of Hydraulic Engineering*, 117(8), pp. 959–972.
- Abt, S.R., T.L. Johnson, C.I. Thornton, and S.C. Trabant, 1998. "Riprap Sizing at Toe of Embankment Slopes", *Journal of Hydraulic Engineering*, 124(7), July.
- Abt, S.R., J.F. Ruff, and R.J. Wittler, 1991. "Estimating Flow Through Riprap", *Journal of Hydraulic Engineering*, 117(5), pp. 670–675.
- Chow, V.T., 1964. *Handbook of Applied Hydrology*, McGraw-Hill Book Company, New York, New York.
- DOE (U.S. Department of Energy), 1989. *Technical Approach Document, Revision II*, UMTRA-DOE/AL 050424.0002, December.
- DOT (U.S. Department of Transportation), 1983. *Hydraulic Design of Energy Dissipaters for Culverts and Channels*, Hydraulic Engineering Circular No. 14, September.
- Geotechnical Engineering Group, Inc. (GEG), 2005. Technical Testing, Crescent Junction, GEG Job No. 2165, December 22.
- Johnson, T.L., 2002 *Design of Erosion Protection for Long-Term Stabilization*, Final Report, NUREG-1623, U.S. Nuclear Regulatory Commission, September.
- Nelson, J.D., S.R. Abt, R.L. Volpe, D. van Zyl, N.E. Hinkle, W.P. Staub, 1986. *Methodologies for Evaluating Long-Term Stabilization Design of Uranium Mill Tailings Impoundments*, NUREG/CR-4620, U.S. Nuclear Regulatory Commission, June.
- Temple, D.M., K.M. Robinson, R.M. Ahring, and A.G. Davis, 1987. *Stability Design of Grass-Lined Open Channels*, U.S. Department of Agriculture Handbook No. 667, September.
- USDA (U.S. Department of Agriculture), 1994. "Gradation Design of Sand and Gravel Filters", *National Engineering Handbook*, Part 633, Chapter 26, October.

Appendix A
Reference Materials

in column 6 is given from the sediment rating curve, or Equation 6. For each interval, the water yield in column 5 is calculated from multiplying columns 2 and 6. Likewise, the annual sediment yield in column 7 is calculated from Equation E-5 given Δp , Q and C_s from columns 2, 4 and 6. The interannual total sediment yield is finally obtained from the sum of column 7.

2.5 Trap Efficiency

When sediment-laden water enters reservoirs, lakes, impoundments, and settling basins, the settling of sediment will cause aggradation of the bed. The trap efficiency is used to determine how much sediment is expected to settle in backwater areas. The trap efficiency is defined as the percentage of incoming sediment for a given size fraction (i) that will settle within a given reach. The trap efficiency can be calculated as follows:

$$T_{Ei} = 1 - e^{-\frac{Xw_i}{hV}} \quad (E-7)$$

where X is the reach length; w_i is the settling velocity for sediment fraction i from Table E-4; h is the mean flow depth; and V is the mean flow velocity. The exponent is dimensionless and any consistent system of units can be used in this equation.

The sediment load that settles within the reach is given by the product of the incoming sediment load and the trap efficiency. The outgoing sediment load is calculated by subtracting the settling load from the incoming load. The trap efficiency varies with sediment size through the settling velocity. Typically, the trap efficiency is approximately one for coarse sediment, e.g., gravels, and approaches zero for fine sediment, e.g., clays.

2.6 Sediment Transport Capacity of a Channel

Simons, Li, and Fullerton (1981) developed an efficient method of evaluating sediment discharge. The method is based on easy-to-apply power relationships that estimate sediment transport based on the flow depth h and velocity V . These power relationships were developed from a computer solution of the Meyer-Peter and Müller bedload transport equation and Einstein's integration of the suspended bed sediment discharge:

$$q_s = c_{s1} h^{c_{s2}} V^{c_{s3}} \quad (E-8)$$

The results of the total bed sediment discharge are presented in Table E-2. The large values of c_{s3} ($3.3 < c_{s3} < 3.9$) show the high level of dependence of sediment transport rates on velocity. Depth has comparatively less influence ($-0.34 < c_{s2} < 0.7$).

Table E-2. Power equations for total bed sediment discharge in sand- and fine-gravel-bed streams.

	$q_s = c_{s1} h^{c_{s2}} V^{c_{s3}}$							
	D_{50} (mm)							
	0.1	0.25	0.5	1.0	2.0	3.0	4.0	5.0
Gr = 1.0								
c_{s1}	3.30×10^{-5}	1.42×10^{-5}	7.6×10^{-6}	5.62×10^{-6}	5.64×10^{-6}	6.32×10^{-6}	7.10×10^{-6}	7.78×10^{-6}
c_{s2}	0.715	0.495	0.28	0.06	-0.14	-0.24	-0.30	-0.34
c_{s3}	3.30	3.61	3.82	3.93	3.95	3.92	3.89	3/87
Gr = 2.0								
c_{s1}		1.59×10^{-5}	9.8×10^{-6}	6.94×10^{-6}	6.32×10^{-6}	6.62×10^{-6}	6.94×10^{-6}	
c_{s2}		0.51	0.33	0.12	-0.09	-0.196	-0.27	
c_{s3}		3.55	3.73	3.86	3.91	3.91	3.90	
Gr = 3.0								
c_{s1}			1.21×10^{-5}	9.14×10^{-6}	7.44×10^{-6}			
c_{s2}			0.36	0.18	-0.02			
c_{s3}			3.66	3.76	3.86			
Gr = 4.0								
c_{s1}				1.05×10^{-5}				
c_{s2}				0.21				
c_{s3}				3.71				

Definitions: q_s , unit sediment transport rate in ft^2/s (unbulked); V , velocity in ft/s ; h , depth in ft ; $G_r = 0.5 [(D_{84}/D_{50}) + (D_{50}/D_{16})]$ gradation coefficient.

For flow conditions within the range outlined in Table E-3, the regression equations should be accurate within 10%. The equations were obtained for steep sand- and gravel-bed channels under supercritical flow. They do not apply to cohesive material.

The equations assume that all sediment sizes are transported by the flow without armoring. The sediment concentration $c_{mg/l}$ is calculated from

$$c_{mg/l} = 2.65 \times 10^6 \frac{q_s}{q} \quad (E-9)$$

where q_s is calculated from Equation E-8 and $q = V_h$ is the unit discharge in ft^2/s .

3 DESIGN AND ANALYSIS PROCEDURES

The following procedures may be used to determine: 1) sheet and rill erosion; 2) gully erosion; 3) calculated sediment yield; 4) measured sediment yield; 5) trap efficiency, and 6) sediment transport capacity of channels.

3.1 Sheet and Rill Erosion Procedure

The following sheet and rill erosion procedure based on the USLE may be used to determine soil erosion losses from upland erosion. If data are available, this approach should be supplemented with field measurements to properly calibrate and ascertain the accuracy of other procedures and/or computer models.

- Step A-1. Gather topographic, soil type and land use information. Subdivide the domain into sub-watersheds. For each sub-watershed, determine: drainage area, runoff length, average slope, soil type, percentage of canopy cover and ground cover and any particular method of soil conservation practice.
- Step A-2. Determine the mean annual rainfall erodibility factor R for the specific site location.
- Step A-3. Determine, for each sub-watershed, the soil erodibility factor K from soil samples.
- Step A-4. Determine the slope length-steepness factor LS from the runoff length and average slope.
- Step A-5. Determine the cropping-management factor C from the ground and canopy cover data.

Table E-3. Range of parameters for the Simons-Li-Fullerton method.

Parameter	Value range
Froude number	1 - 4
Velocity	6.5 - 26 ft/s
Manning coefficient n	0.015 - 0.025
Bed slope	0.005 - 0.040
Unit discharge	10 - 200 ft/s
Particle size	$D_{50} \geq 0.062 \text{ mm}$
	$D_{50} \leq 15 \text{ mm}$

APPENDIX B

METHOD FOR DETERMINING SACRIFICIAL SLOPE REQUIREMENTS

1 INTRODUCTION

In many cases where tailings extend over a large area, slope lengths may be so long that extremely gentle slopes will be needed to provide long-term stability. Such gentle slopes may necessitate the use of very large amounts of soil, such that some of these slopes (with no tailings directly under them) may extend greatly beyond the edge of the tailings pile.

In such cases, licensees may be able to demonstrate that it is impractical to provide stability for 1,000 years and may choose to show that stability for less than 1,000 years, but for at least 200 years, is a more cost-effective option. Such a design may incorporate tailings embankment "out slopes," where there are no tailings directly under the soil cover. Such slopes, designed for less than the 1,000-year stability period, may be acceptable if properly justified by the licensee.

It should be emphasized that the staff considers that a 200-year sacrificial slope design should be used only in a limited number of cases and only when a design life of 1,000 years cannot be reasonably achieved. However, it should not be assumed that the design period should immediately jump from 1,000 to 200 years. The staff concludes that the selection of a design period should proceed in a stepwise fashion, with consideration given to intermediate design periods from 200-1,000 years. In determining a minimum design, a 200-year sacrificial slope design, as presented below, may be used. However, such a design has a considerable amount of uncertainty associated with its use, due to its development by extrapolation of a relatively limited data base. Therefore, the staff considers that the procedure should be used only after other reclamation designs have been considered. The staff considers that the procedures for justifying a design period of less than 1,000 years, as discussed in Appendix C, should be carefully followed to document that a 200-year sacrificial slope design is the best design that can be reasonably provided.

2 TECHNICAL BASIS

The long-term gully erosion process has the potential to destabilize an earthen embankment or soil cover constructed to prevent waste material release to the environment. Figures B-1 and B-2 present photographs of earthen embankments damaged by gulying. It was apparent to the staff that little criteria were available that assisted the designer in predicting the potential impacts of gulying processes to long-term stability of the waste material. The NRC thereby supported a series of studies to expand the knowledge base on the potential impacts of gullies on reclaimed impoundments and provide guidance for assuring the long-term stability of the waste.

In 1985, Falk et al. conducted a pilot study in an attempt to develop a procedure to predict the maximum depth a gully may incise into a tailing slope as a function of time. Falk characterized 16 reclaimed mine and/or overburden sites in Colorado and Wyoming that demonstrated incision



Figure B-1. Damage caused by gullying.



Figure B-2. Damage caused by gullying.

on the side slope and in some cases extended into the top slope areas. Field measurements included gully length, slope length, pile height, pile age, maximum gully depth, and width, tributary drainage area, vegetative cover and soil composition. From these data, Falk et al. attempted to formulate a procedure for estimating the maximum depth of incision, width of gully, and location of the maximum incision from the crest. The estimation procedure had a limited application but indicated that an estimation procedure could potentially be developed.

Pauley (1993) performed a series of flume studies in which near prototype soil embankments were constructed simulating a reclaimed waste impoundment. Figure B-3 presents a photograph of the flume used in the study. A series of rainfall and subsequent runoff events were conducted resulting in gully incision into the embankment. The gulying processes were documented as a function of rainfall duration and volume, soil type, embankment slope and the maximum depth of incision. The results of the study indicated that the gully incision depth was a function of the clay content of the soil, volume of runoff to the gully, and the embankment height (Abt et al. 1994). The gully processes observed by Pauley and later documented by Abt et al. (1995b) in the flume study closely paralleled those observed in the field by Falk (1985) and others.

In an attempt to expand the Falk et al. (1985) data base, Abt et al. (1995a) conducted a study in which 11 field sites that demonstrated gulying on reclaimed impoundments were located, characterized, measured, and sampled in the Colorado and Wyoming region and each gully was characterized (Falk et al. 1985).

The information presented by Falk et al. (1985), Pauley (1993) and Abt et al. (1995a) was consolidated into a composite data base as reported by Abt et al. (1995b). A comprehensive procedure was presented to estimate the maximum depth of gully incision, top width of the gully, and location of the maximum incision from the crest. The procedure allows the designer to determine gully depths and to predict the location of maximum gully incision.

A review of existing waste and tailing reclamation designs in conjunction with extensive site experience indicates that three primary embankment/cover configurations are commonly proposed. The three embankment configurations or types have been proposed or constructed as presented in Figure B-4. It is important to recognize that although each embankment type is similar along the main embankment face, the top slope, and subsequent potential tributary drainage, significantly impact the maximum depth of gully incision, D_{max} , that may intrude into the main slope. Therefore, a different procedure was developed to estimate the potential tributary drainage area and volume of runoff for each embankment type.

An empirical gully incision estimation procedure is presented as a function of the embankment/cover geometry, hydrologic parameters, soil composition, and the design life. It is anticipated that the estimation procedure will provide the user the maximum depth of gully incision, the approximate location of the maximum depth of incision along the embankment slope, and the approximate top width of the gully at the point of maximum incision as schematically presented in Figure B-5. The user will need to insure that the gully incision does not expose the waste/tailings materials.

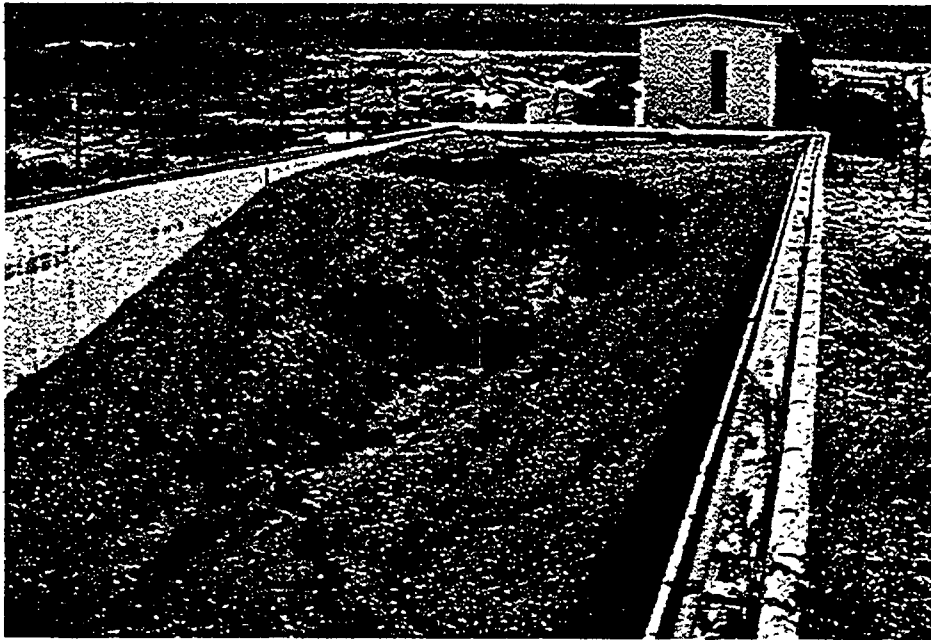
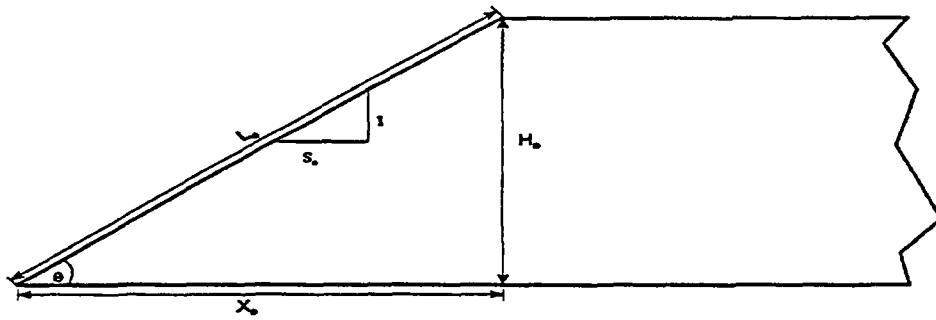
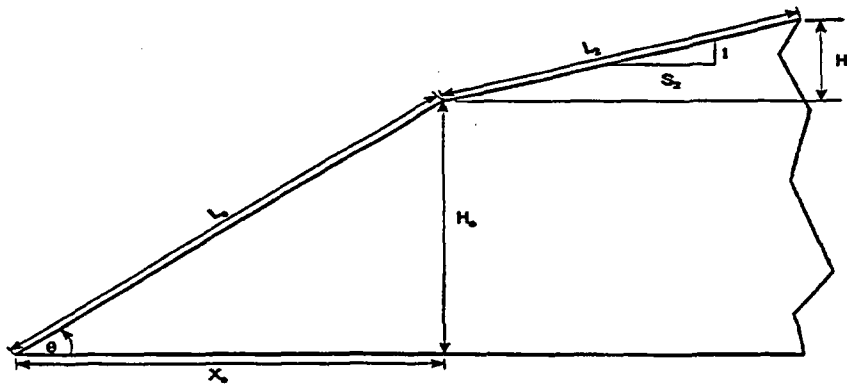


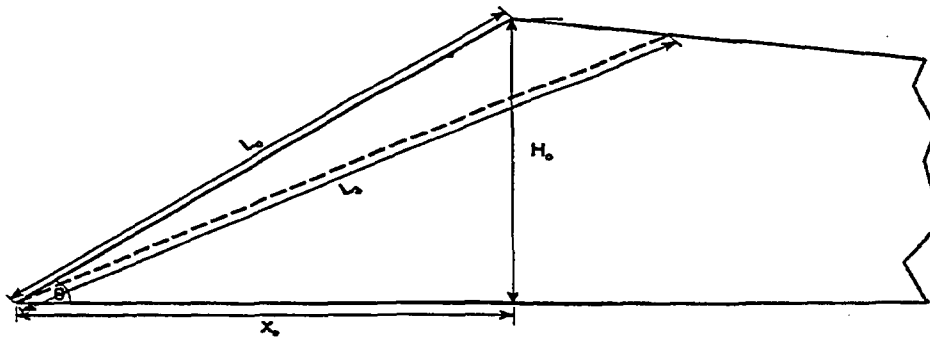
Figure B-3. Flume used by Pauley (1993).



Type 1 Embankment



Type 2 Embankment



Type 3 Embankment

Figure B-4. Three types of embankment geometry.

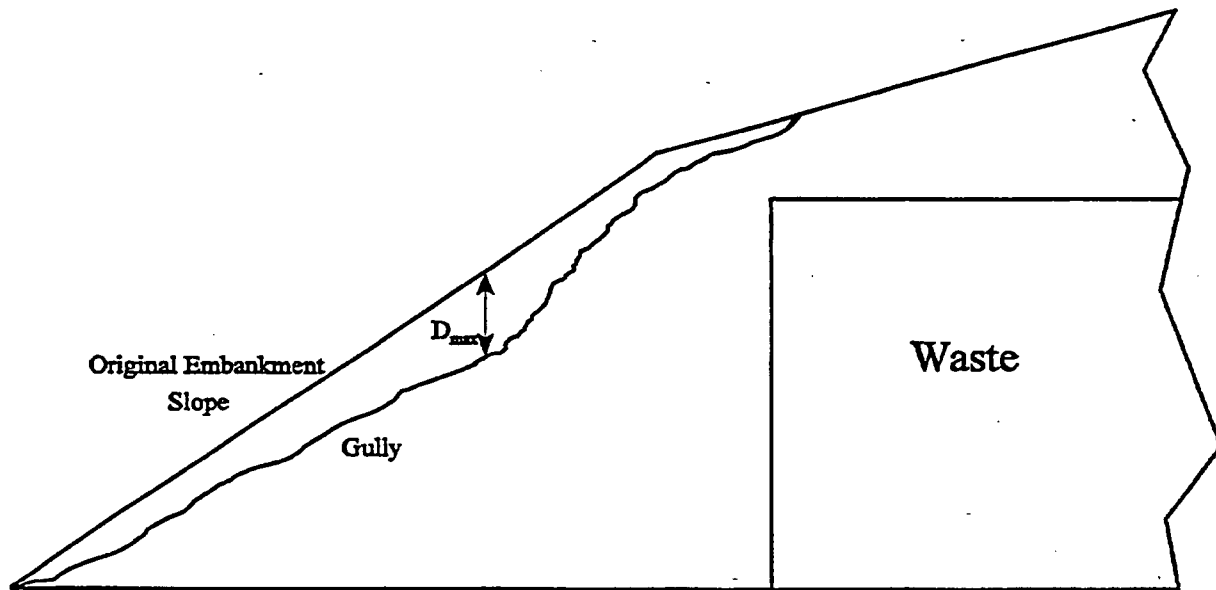


Figure B-5. Schematic of typical waste impoundment.

Staff review indicates that locating the depth of maximum gully incision is the most unpredictable part of the design procedure. The field data and flume data cannot be relied on totally to adequately describe the gully profile along the length of the slope. For example, the procedure may predict that the maximum gully depth will be 20 ft and will occur 500 ft from the embankment crest. However, not reflected in the design procedure is the possibility that the same gully could be 19 ft deep at the crest. The gully profile data available and staff experience suggest that gully depths approaching the maximum gully depth could occur near the crest. Thus, until more data are available, the staff recommends that the location of maximum gully be assumed to occur near the crest of the slope. In addition, because of the need for significant data extrapolation, the staff suggests that this procedure be used to determine sacrificial slope requirements for a 200-year period.

In situations where increasing the set back distance of waste with respect to the embankment crest is not feasible, the concept of embankment stabilization utilizing launching riprap may be examined. Abt et al. (1997) presents a preliminary approach to the stabilization technique. Figure B-6 presents a photograph of a laboratory simulation of embankment stabilization using launching riprap. Based upon the findings of the pilot test series, a set of preliminary guidelines and a design procedure is outlined by Abt et al. (1997). The procedure presented represents the pilot test series and its application has not been tested and verified under field or near prototype conditions. It is recommended that the procedures outlined by Abt et al. (1997) be applied with a high degree of engineering judgement.

3 PROCEDURES

A procedure has been developed to estimate the effects of gullying over time. The following steps outline the estimation procedure.

- Step 1. Determine the embankment design life as outlined in Appendix A. Stability of the embankment must be insured for periods ranging from 200 to 1,000 years.
- Step 2. Select the embankment type (Type 1, Type 2, or Type 3) and determine values of the appropriate design variables.

Embankment/cover variables applicable to all three types of embankments include the embankment height (H_o) (m), slope length (L_o) (m), slope angle (θ) (degrees), and horizontal distance from the embankment toe to the crest (X_o) (m) as presented in Figure B-4.
- Step 3. Determine the embankment/cover soil composition, expressed as a percentage of the sands, silts, and clays. Discriminating thresholds for gully intrusion potential for embankments are segmented into soils with clay content less than 15 percent, clay content between 15 and 50 percent, and clay content greater than 50 percent.
- Step 4. Determine the average annual precipitation (P), expressed in meters, for the embankment site. Estimates of precipitation can be obtained from U.S. Weather Bureau isohyetal maps, local climatological data, or other appropriate means.

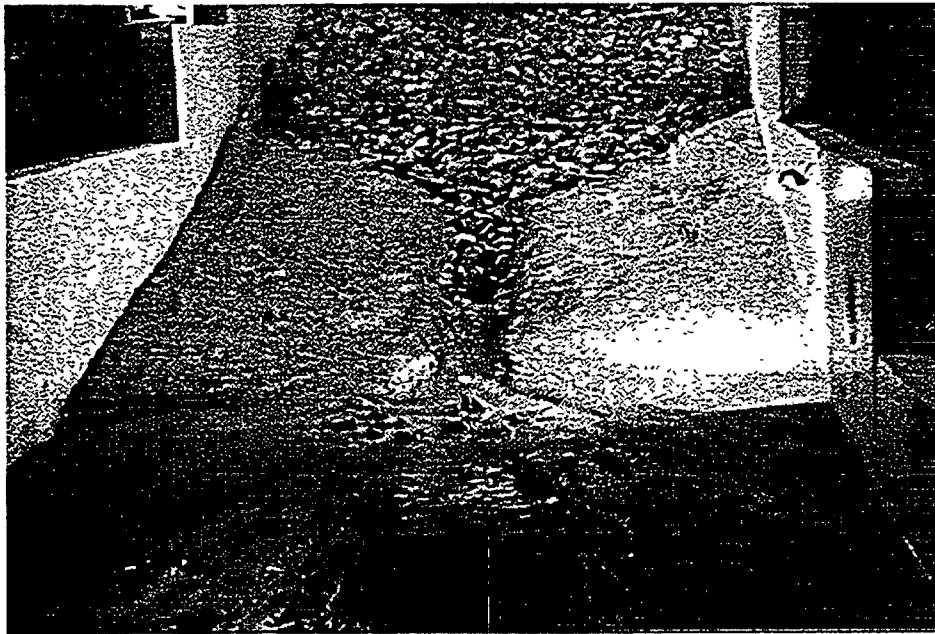


Figure B-6. Photograph of launching riprap flume test.

Step 5. Determine the drainage area tributary to the embankment to estimate the volume of runoff to which an embankment will be exposed in its design life. For embankments without external drainage basins, the tributary drainage area that forms on the face of the embankment will determine the total volume of runoff (Abt, Thornton, and Johnson, 1995b). The tributary drainage area that forms on the embankment face is a unique function of the type of embankment being evaluated.

Type 1 Embankment

The tributary drainage area for a Type 1 embankment may be estimated by

$$A = 0.276 * [L_o * \text{Cos}(\theta)]^{1.636} \quad (\text{B-1})$$

where: A = tributary drainage area (m²)
 L_o = original embankment length (m)
 θ = slope angle in degrees computed as Tan⁻¹(S_o)

Type 2 Embankment

The tributary drainage area for a Type 2 embankment is computed by summing the embankment face length (L_o) and the embankment top length (L_t). The resulting length (L_t) is then entered in Equation B-1 as:

$$A = 0.276 * [L_t * \text{Cos}(\theta)]^{1.636} \quad (\text{B-2})$$

where: A = tributary drainage area (m²)
 L_t = total length of embankment
 θ = slope angle in degrees computed as Tan⁻¹(S_o)

Type 3 Embankment

The tributary drainage area for a Type 3 embankment can be estimated using Equation B-1; however, an effective embankment length (L_e) must be determined. Flume and field observations indicate that a gully forming on a Type 3 embankment can extend past the crest and into the adverse slope. When this condition occurs, the effective length of the embankment is increased. To provide an estimate of the tributary drainage area at any point in time, the value of the effective embankment length is determined by estimating the final gully bottom slope. Abt et al. (1995b) reported that the gully bottom slope may be estimated as

$$S_b = [1.008 * S_o] - 0.063 \quad (\text{B-3})$$

where: S_b = gully bottom slope (rise/run)
 S_o = original embankment slope (rise/run)

The effective embankment length can then be computed as:

$$L_3 = 1.175 * L_o \quad (B-4)$$

where L_o and L_3 are expressed in meters. The tributary drainage area can then be computed using Equation B-1 where L_3 is substituted for L_o .

In situations where the embankment toe is exposed to runoff that develops on a tributary drainage area external to the embankment, the supplemental area (A_x) is added to the drainage area value computed using Equation B-1.

Step 6. The total depth of precipitation to which the site may be exposed to over the design life needs to be determined. In Step 1, the design life of the embankment was estimated. The average annual precipitation for the project site was then estimated based on Step 4. The expected depth of precipitation, in meters, is then calculated as:

$$D_t = \text{Average Precipitation Depth (m)} * \text{Design Life (years)} \quad (B-5)$$

Step 7. The runoff to rainfall ratio, R_r , is needed to convert the potential depth of precipitation for the embankment design life to potential runoff tributary to the developing gully. The U.S. Geological Survey (USGS) developed a runoff map method (Gebert et al., 1989) to determine the average annual runoff expected from any location in the United States. The USGS map provides the user the annual depth of runoff from a site specific location. The ratio of the runoff to rainfall is computed by dividing the runoff depth derived from Gebert et al. by the average annual precipitation for the appropriate locale. The average runoff-ratio using the USGS Average Annual Runoff Method is 0.127. The runoff-rainfall ratio of 0.127 provides a reasonable estimate for the arid and semi-arid regions of the western United States.

Step 8. The cumulative volume of runoff (V_r) tributary to the embankment toe, in cubic meters, is calculated as:

$$V_r = D_t * R_r * A \quad (B-6)$$

where A is the tributary drainage area, expressed in square meters, as determined in Step 5. It is acknowledged that a single storm event will significantly impact the development of the gully. Abt et al. (1995a) indicates that the total volume of runoff can serve as a predictor of the ultimate dimensions (i.e., maximum depth, width, etc.)

of the gully. The volume of runoff tributary to the gully for the embankment design life is the primary element reflecting the analysis period.

Step 9. The maximum depth of gully incision (D_{max}) can be estimated as a function of the cumulative volume of runoff, V_r , the embankment height, H_o , the embankment slope length, L_o , L_2 , or L_3 , the embankment slope, and the clay content of the soil composition. A gully factor, G_f , was developed from the analysis described by Abt et al. (1994) for varying clay content of the proposed construction material. The gully factor is defined as:

$$G_f = \frac{D_{max}}{L_i * S_o} \quad (B-7)$$

where L_i is L_o , L_2 , or L_3 as applicable and the embankment slope S_o , is H_o/X_o . The gully factor is computed as:

Clay content < 15%:

$$G_f = \frac{D_{max}}{L_o * S} = \frac{1}{2.25 + \left(0.789 * \frac{V_r}{H_o^3}\right)^{-0.55}} \quad (B-8)$$

Clay content > 15%, < 50%:

$$G_f = \frac{D_{max}}{L_o * S} = \frac{1}{2.80 + \left(0.197 * \frac{V_r}{H_o^3}\right)^{-0.70}} \quad (B-9)$$

Clay content > 50%:

$$G_f = \frac{D_{max}}{L_o * S} = \frac{1}{3.55 + \left(0.76 * \frac{V_r}{H_o^3}\right)^{-0.85}} \quad (B-10)$$

Step 10. The maximum depth of gully incision expected on the embankment slope may then be estimated as:

$$D_{\max} = G_f * L_i * S \quad (\text{B-11})$$

where D_{\max} is in meters.

Step 11. After the value of D_{\max} is determined, the top width of the gully at the deepest incision can be calculated as:

$$W = \left(\frac{D_{\max}}{0.61} \right)^{1.149} \quad (\text{B-12})$$

where: W = top width of gully (m)
 D_{\max} = depth of deepest gully incision (m)

Step 12. In some applications, it is important to estimate the location of the maximum gully incision to evaluate the stability of the embankment or the potential to penetrate into the waste storage area. The location of the maximum depth of incision, measured down slope from the crest, may be determined as:

$$D_i = 0.713 * \left(\frac{(V_r * S)}{L_i^3} \right)^{-0.415} \quad (\text{B-13})$$

where: D_i = location of D_{\max}
 V_r = cumulative volume of runoff (m^3)
 S_o = original embankment slope (rise/run)
 L_o = original embankment length (m)

Step 13. To provide a conservative estimate of the possible damage caused to an earthen embankment by a migrating gully, it is assumed that the maximum depth of gully intrusion occurs at the crest of the embankment. The embankment material is then assumed to erode, at the angle of repose of the embankment material, up slope of D_{\max} . The set back distance of the waste material is determined for each of the three types of embankments by assuming the embankment erodes at the angle of repose.

Step 14. If altering the set back distance is not feasible, protection may be examined utilizing launching riprap. A detailed explanation of the launching riprap application is

presented by Abt et al. (1997). The following preliminary guidelines should be followed in a launching riprap application:

- The minimum riprap size should be determined using accepted riprap sizing criteria for overtopping flow. A minimum median stone size (D_{50}) of 9 cm was found to work well in flume studies.
- The protective riprap layer should have adequate volume to provide slope coverage under maximum expected gully conditions. A layer thickness of approximately $3 D_{50}$ is recommended, depending on the volume requirements and the length of the riprap layer.

4 RECOMMENDATIONS

The stable slope should be determined using the procedures presented in Appendix A. Appropriately conservative values of input parameters should be used in the computation. Additional refinements can be made after the analysis of the sacrificial slope requirements.

In analyzing Type 2 Embankments, the top slope of the cover should be much flatter (less than or equal to 5%) than the slope of the embankment face. The gully would likely occur far upstream from the crest if the top slope were steep. The following example is presented to outline the stability assessment procedure, not to promote or compare any embankment types.

5 EXAMPLE OF PROCEDURE APPLICATION

The following example is used to outline the procedure of stability analysis of a Type 2 Embankment. Type 2 Embankments, presented in Figure B-4, are identified by an embankment slope that transitions into a flatter top slope. Embankments constructed with Type 2 geometry are evaluated by superimposing the total length of the embankment, L_1 , on the slope of the embankment face.

Step 1. Design Life

An embankment design life of 200 years will be evaluated.

Step 2. Embankment Geometry

Once the embankment type is determined, the initial design variables are required. It will be assumed that the embankment has the following physical dimensions:

H_o = embankment height	= 9 meters
L_o = embankment slope length	= 55 meters
S_o = embankment slope	= 0.15 rise/run
L_2 = top embankment length	= 100 meters
S_2 = top embankment slope	= 0.05 rise/run

Step 3. Soil Composition

It is assumed that a soil analysis has been conducted and that the embankment material is composed of 13 percent clay by volume, and has an angle of repose of 34 degrees.

Step 4. Precipitation

Local climatological data indicate an average annual precipitation of 0.20 meters for the site.

Step 5. Potential Tributary Drainage Area

The total potential tributary drainage area for a Type 2 Embankment is determined by computing the total embankment length as shown below

$$L_t = L_o + L_2 \quad (B-14)$$

where: L_t = total embankment length (m)

L_o = length of embankment face (m)

L_2 = length of embankment top slope (m)

The value determined for the total embankment length is then combined with the slope of the embankment face and entered into Equation B-2 as shown below

$$A = 0.276 * \{155 \text{ meters} * \cos(8.53)\}^{1.636} \quad (B-15)$$

$$A = 1038 \text{ meters}^2$$

Therefore, the total potential tributary drainage area for the Type 2 Embankment is 1038 square meters. It is assumed that there is no additional drainage area external to the embankment.

Step 6. Potential Depth of Precipitation

The first step in computing the total runoff volume for the site is to determine the potential depth of precipitation, D_p , that the site will be exposed to during the design life. As described in Step 6, the total depth of precipitation is the product of the average annual precipitation and the design life. Therefore,

$$D_t = 0.20 \text{ meters/year} * 200 \text{ years}$$

$$D_t = 40.0 \text{ meters of precipitation} \tag{B-16}$$

and a potential depth of precipitation of 40.0 meters is computed.

Step 7. Runoff to Rainfall Ratio

A value of 0.13 is assumed as the average runoff to rainfall ratio, R_r , for the embankment area.

Step 8. The cumulative volume of runoff, V_r , is defined as the product of the potential depth of precipitation, D_t , the runoff to rainfall ratio, R_r , and the potential tributary area, A_t . Substituting the values of D_t , R_r and A_t obtained above into Equation B-6 yields

$$V_r = 40.0 \text{ meters} * 0.13 * 1038 \text{ meters}^2$$

$$V_r = 5,400 \text{ meters}^3 \tag{B-17}$$

Therefore, the embankment slope will drain approximately 5,400 cubic meters of runoff during the 200 year design life.

Step 9. Determination of Gully Factor

The gully factor, G_f , for the embankment should be determined as outlined in Step 9. A clay content of 13 percent in the embankment material requires that Equation B-8 be used to calculate the gully factor. Substituting values for H_e and V_r into Equation B-8 gives

$$G_f = \frac{1}{2.25 + \left[0.789 * \left\{ \frac{5,399.97 \text{ meters}^3}{(9.0 \text{ meters})^3} \right\} \right]^{-0.55}}$$

$$G_f = 0.380 \tag{B-18}$$

Step 10. Maximum Depth of Gully Incision

A gully factor of 0.380 is entered into Equation B-8 to determine the maximum depth of gully incision as follows

$$D_{\max} = 0.380 * 55.0 \text{ meters} * 0.15$$

$$D_{\max} = 3.14 \text{ meters} \quad (\text{B-19})$$

Thus, after a 200 year period, a gully incision 3.14 meters deep would be expected on the face of the embankment.

Step 11. Gully Top Width

Equation B-12 presents an empirical relationship that can be used to predict gully top width, W, as a function of maximum gully incision, D_{\max} . Substituting the value of 3.14 meters computed for D_{\max} into Equation B-12 gives

$$W = \left(\frac{3.14 \text{ meters}}{0.61} \right)^{1.149}$$

$$W = 6.57 \text{ meters} \quad (\text{B-20})$$

therefore, 6.57 meters would be the estimated gully width at the point of deepest gully incision.

Step 12. Location of Maximum Depth

Equation B-13 presents an empirical relation predicting the location of D_{\max} as a function of the total volume of runoff, embankment length, and embankment slope. Substituting the values determined above into Equation B-13 gives

$$D_1 = 0.713 * \left\{ \frac{(5,399.97 \text{ meters}^3 * 0.15)}{(55 \text{ meters})^3} \right\}^{-0.415}$$

$$D_1 = 6.50 \quad (\text{B-21})$$

which represents the number of D_{\max} 's down slope from the crest the deepest incision is expected to occur. To determine the location in meters, multiply the value determined for D_1 by that determined for D_{\max} . For this example the deepest incision point will occur approximately 20.4 meters down slope from the embankment crest.

Summarizing the results obtained above yields

$$D_{\max} = 3.14 \text{ meters,}$$

$$W = 6.57 \text{ meters}$$

$$D_1 = 20.4 \text{ meters}$$

However, for long-term stability applications, the location of D_{\max} should be assumed to be at the crest of the slope.

Step 13. Set Back Distance

For conservatism, the maximum depth of incision is assumed to occur at the crest of the embankment and the material is assumed to erode at the angle of repose (34° for this example) upstream of the crest. For the conditions of this example, the set back distance would be 4.66 meters up slope from the crest of the embankment. Therefore, tailings should be located a minimum horizontal distance of 4.66 meters up slope and a vertical distance of 4.71 meters down from the embankment crest.

Step 14. Rock Launching Application

If providing adequate setback distance is not feasible, embankment stabilization with launching rock may be considered. For details and a preliminary application procedure, see Abt et al. (1997). The findings discussed by Abt et al. (1997) should be adapted to each specific site with engineering judgement. In general, a volume of rock should be provided to cover the collapsed slope with a rock layer of 1.5 times the D_{50} size, considering the depth of gully intrusion and the length. It is recommended that the required D_{50} size be specifically determined for a collapsed slope of 1V to 2H. Figure B-7 presents a schematic of the rock launching application concept.

The results of the example outlined above can then be checked with the original design of the soil cover, as described in Appendix A. Engineering judgment then determines if the design is adequate to provide the level of protection necessary throughout the design life.

6 COMPUTER APPLICATION

To aid in the analysis of the stability assessment, a computer program has been developed. The Windows™ application provides an automated method of evaluating the stability procedure described above (Thornton, 1996). The program is available from the U.S. Nuclear Regulatory

Two basic approaches exist for the design of suitable erosion-resistant covers for a tailings impoundment surface as originally described by Nelson et al. (1983). The first approach consists of providing a cover material that will resist material transport by flowing water using the concept of critical shear stress. The second approach is based on the Universal Soil Loss Equation, an empirical method originally developed during the 1930's. The methodologies involved with both of these methods are discussed below.

5.1.1 Critical Shear Stress Approach

The critical shear stress approach consists of providing a cover material with a d_{30} grain size (i.e., 70% of the material by weight is coarser than the d_{30}) that will resist movement when subjected to the sheet flow maximum permissible velocity resulting from the application of the PMP over the entire impoundment surface. Minimum d_{30} grain sizes should be determined using the critical shear stress approach similar to the procedures discussed in Simons and Senturk (1977) applicable to overland flow. A numerical solution for selecting an appropriate d_{30} to provide armoring has been developed by Shen and Lu (1983).

The design approach described above, in which the critical grain size is selected to resist the onset of sheet erosion, should evaluate the runoff from PMP storms of different durations, such as 0.5, 1, 2, 4, and 6 hours to select the maximum d_{30} required. Rainfall depths will usually be based on 2.5 to 15 minute durations for small drainage basins as presented in Section 2.1.2. Typically, the minimum construction layer thickness is specified to be at least two times the maximum particle size. If the above approach results in a cover thickness less than about 6 inches, then other considerations - such as nonuniform placement of cover and particle breakdown due to handling, placement and weathering - would suggest that a minimum cover thickness of 10 inches should be considered. If a self-armoring cover can be provided, and there is no major concern for weathering of the cover material, the design is independent of time and the cover should remain intact indefinitely.

5.1.2 Soil Loss Equation Approach

The concept of sheet erosion was recognized by early researchers and the Universal Soil Loss Equation (USLE) was developed in the late 1930's by the Agricultural Research Service to evaluate soil conservation practices for cropland throughout the United States. After its inception, the soil loss procedure was used and modified as field experience and data were obtained incorporating the basic parameters of field slope and length, precipitation, and crop management to estimate soil losses on an annual basis. Application of the USLE to non-cropland areas and specifically for construction sites became feasible when Wischmeier et al. (1971), using basic soil loss characteristics, developed and implemented a soil erodibility factor (K) in the soil loss computation. Subsequent efforts refined the parameters used in the USLE for mining and construction activities in the interior western United States.

The Modified Universal Soil Loss Equation (MUSLE) was developed by the Utah Water Research Laboratory in 1978 for the principal objective of estimating soil losses due to highway construction activities. Alterations were made to the USLE to accommodate unique or special conditions encountered in highway construction, including steep and deep cuts and fill slopes that could cause erosion affecting adjacent or nearby roadways, streams, lakes, or inhabited areas. It is apparent that the modifications made to the USLE extend to many construction and mining sites beyond the scope of highway construction.

The Modified Universal Soil Loss Equation (MUSLE) is a mathematical model based on field determined coefficients and provides the most rational approach to evaluate the long-term erosion potential from an upland area similar to that of the area covering a reclaimed tailings pond. Recent investigations into appropriate methods of modeling major types of sheet erosion (Abt and Ruff, 1978; Nelson et al. 1983; Nyhan and Lane, 1983; and NRC, 1983), indicate that although more rigorous mathematical models are available to simulate erosion as a function of time, the use of the USLE has a strong precedent because it has a 40-year history of runoff and soil loss data.

The MUSLE is used to evaluate average soil losses for certain types of slopes as a function of time. The MUSLE does not consider the potential for gully development or intrusion as discussed in Chapter 4 because the topographic features of the tailings area are assumed to remain constant with time. Also, the MUSLE does not incorporate the concept of the PMP but rather a rainfall factor based on historical rainfall values. The MUSLE is defined by Clyde et al. (1978) as follows:

$$A = R K (LS) (VM) \quad (5.1)$$

where,

A = the computed loss per unit area in tons per acre per year with the units selected for K and R properly selected;

R = the rainfall factor which is the number for rainfall erosion index units plus a factor for snowmelt, if applicable;

K = the soil erodibility factor, which is the soil loss rate per erosion index unit for a specified soil as measured on a unit plot that is defined as a 72.6-ft length of uniform 9% slope continuously maintained as clean tilled fallow;

LS = the topographic factor, which is the ratio of soil loss from the field slope length to that from a 72.6-ft length under otherwise identical conditions;

VM = the dimensionless erosion control factor relating to vegetative and mechanical factors. This factor replaces the cover management factor (C) and the support factor (P) of the original USLE.

5.1.2.1 The Rainfall and Runoff Factor (R)

As noted by previous research at Los Alamos National Laboratory (Nyhan and Lane, 1983), the R factor as used in the MUSLE is often misinterpreted only as a rainfall factor. In reality, it must quantify both the raindrop impact and provide information on the amount and rate of runoff likely to be associated with the rain. More specifically, the R factor is described in terms of a rainfall storm energy (E) and the maximum 30-minute rainfall intensity (I₃₀). Generalized R factors applicable to the interior western United States are given in Table 5.1. For R factors in specific areas of the United States, it is recommended that erosion index distribution curves be obtained from local SCS offices.

Table 5.1. Generalized Rainfall and Runoff (R) Values.

State	Eastern Third	Central Third	Western Third
N. Dakota	50 - 75	40 - 50	40
S. Dakota	75 - 100	50	40
Montana	30 - 40	20	20 - 50
Wyoming	30 - 50	15 - 30	15 - 25
Colorado	75 - 100	40 - 50	20 - 40
Utah	20 - 30	20 - 50	15 - 40
New Mexico	75 - 100	40 - 50	20 - 40
Arizona	20 - 50	20 - 50	25 - 40

5.1.2.2 The Soil Erodibility Factor (K)

The soil erodibility factor (K) recognized the fact that the erodibility potential of a given soil is dependent on its compositional makeup, which in turn reflects the grain size distribution of the soil. To predict soil erodibility, five soil characteristics that include the percent silt and fine sand, percent sand greater than 0.1 mm, percent organic material, general soil structure and general permeability are determined. The K factor is then found by using the Wischmeier nomograph presented in Figure 5.1.

The makeup of the various soil fractions presented in Figure 5.1 is based on separating sand and silt at the 0.1 mm size. This differs from the Unified Soil Classification System which uses the No. 200 sieve size (0.075 mm) for the separation between sand and silt. The value to enter Figure 5.1 with should be the percentage of material finer than 0.1 mm in size, not the percentage passing the No. 200 sieve. Also, the determination of the Soil Erodibility Factor (K) as shown on Figure 5.1 does not specifically reference the percentage of clay (finer than 0.002 mm) contained in the material. The percentage of silt plus very fine sand to be used for Figure 5.1, therefore, is the percentage of material contained between 0.002 mm and 0.1 mm.

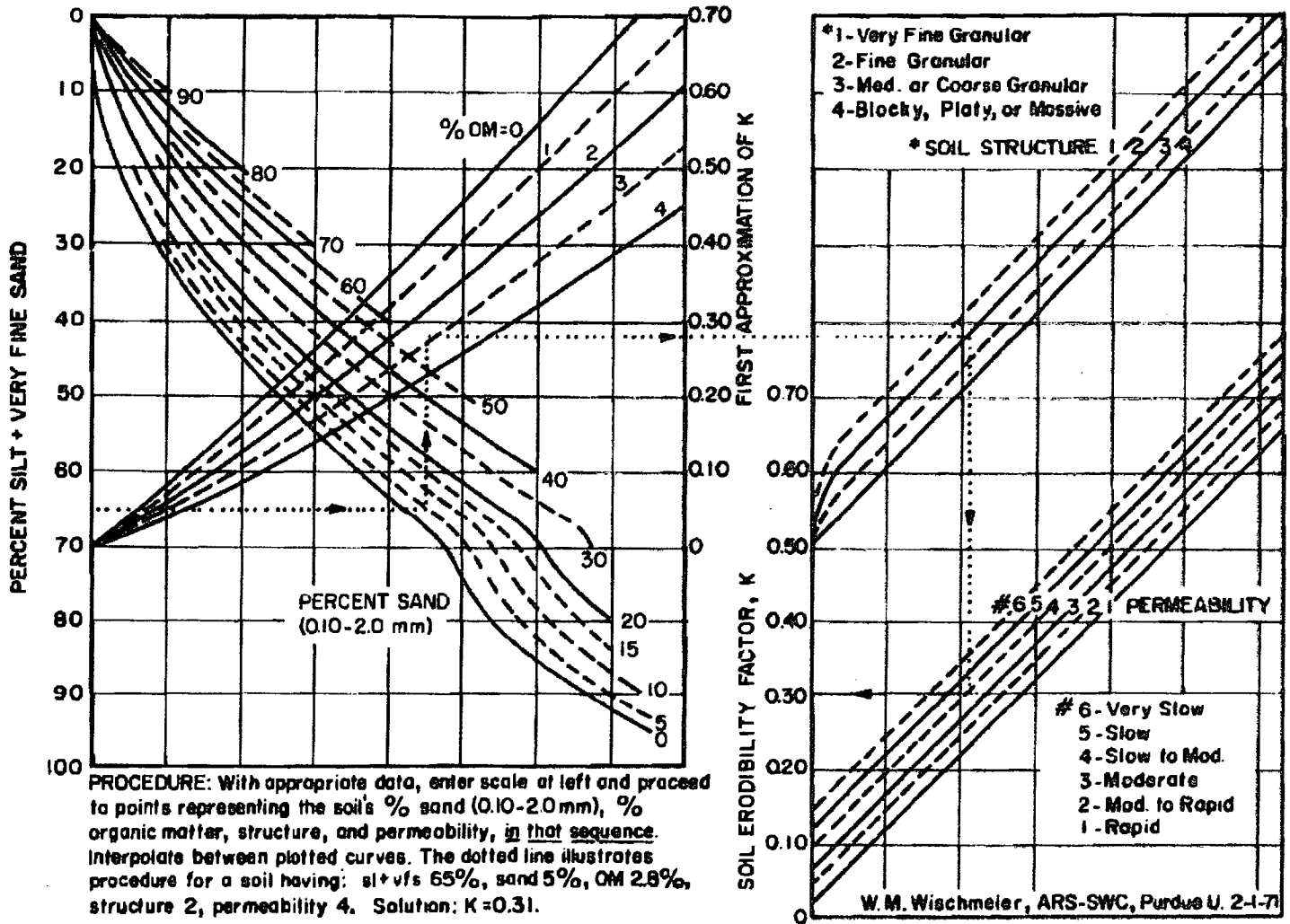


Fig. 5.1. Nomograph for determining soil erodibility factor K. Source: after Wischmeier et al., 1971.

5.1.2.3 The Topographic Factor (LS)

Although the effects of both length and steepness of slope have been investigated separately in different research efforts, it is more convenient for analytical purposes to combine the two into one topographic factor, LS. Wischmeier and Smith (1978) developed plots correlating the topographic factor for slopes up to 500 meters in length at slope inclinations from 0.5% up to 50%. Note that flat, short slopes will have less erosion than long, steep slopes and it is to the benefit of the design engineer to optimize slope length and gradients to fit the topography.

The equation to determine the LS factor is as follows:

$$LS = \frac{650 + 450s + 65s^2}{10,000 + s^2} \frac{L}{72.6}^m \quad (5.2)$$

- where LS = topographic factor
- L = slope length in feet
- s = slope steepness in percent
- m = exponent dependent upon slope steepness

The slope dependent exponent m is presented in Table 5.2.

Table 5.2 Slope Dependent Exponent

Slope (percent)	m
$s < 1.0$	0.2
$1.0 < s < 3.0$	0.3
$3.0 < s < 5.0$	0.4
$5.0 < s < 10.0$	0.5
$s > 10.0$	0.6

5.1.2.4 The VM Factor

The VM factor is the erosion control factor applied in place of the cover and erosion control factors found in the USLE. The erosion control factor accounts for measures implemented at the construction site to include vegetation, mulching, chemical treatments and sprayed emulsions to impede or reduce erosion due to the overland flow of water. Values of the VM factor relative to site-specific conditions are presented in Table 5.3.

The VM factor is perhaps the most sensitive factor to effect the computed erosion loss for a given site. As shown by the values presented

on Table 5.3, the development of a permanent vegetative cover can have a significant impact in reducing the computed erosion loss. However, the effectiveness of a vegetative cover over long-term periods should be questioned unless other protective schemes, such as armoring of the cover with the proper size material, are also included in the design.

5.1.2.5 Example Problem

An example problem in how to use the MUSLE is provided below.

Assumptions:

Site location: Western Colorado
Site description: Uncovered tailings pond
Pond size: 160 acres
Slope: 3%
Length: 2500 ft
Material: 42% sand greater than 0.10 mm;
58% fine sand and silt less than 0.10 mm;
5% clay less than 0.002 mm;
0% organics;
(53% silt plus fine sand less than 0.1 mm);
Consistency - fine granular;
Permeability - slow to moderate.

The following factors have been determined for use in Equation 5.1.

R = 20 from Table 5.1

K = 0.50 from Figure 5.1

LS = 0.747 from Equation 5.2 and Table 5.2

VM = 1.0 (average from Table 5.3 based on an undisturbed surface)

Using Equation 5.1, the annual soil loss (A) from the tailings pond due to sheet erosion caused by flowing water is computed to be 7.47 tons/acre/year, or 1195 tons/year from the facility. Therefore, the cover is estimated to erode at a rate of 0.003 ft per year, or 0.3 ft/century.

5.2 SUMMARY AND FUTURE STUDIES

The main application of the soil loss equation approach in the evaluation of cover integrity is to determine whether it is possible for sheet erosion to penetrate the tailings cover, thereby exposing bare tailings and constituting a failure of the cover. The followup study will concentrate

Table 5.3. Typical VM Factor Values Reported in the Literature.^a

Condition	VM Factor
1. Bare soil conditions	
freshly disked to 6-8 inches	1.00
after one rain	0.89
loose to 12 inches smooth	0.90
loose to 12 inches rough	0.80
compacted bulldozer scraped up and down	1.30
same except root raked	1.20
compacted bulldozer scraped across slope	1.20
same except root raked across	0.90
rough irregular tracked all directions	0.90
seed and fertilizer, fresh	0.64
same after six months	0.54
seed, fertilizer, and 12 months chemical	0.38
not tilled algae crusted	0.01
tilled algae crusted	0.02
compacted fill	1.24 - 1.71
undisturbed except scraped	0.66 - 1.30
scarified only	0.76 - 1.31
sawdust 2 inches deep, disked in	0.61
2. Asphalt emulsion on bare soil	
1250 gallons/acre	0.02
1210 gallons/acre	0.01 - 0.019
605 gallons/acre	0.14 - 0.57
302 gallons/acre	0.28 - 0.60
151 gallons/acre	0.65 - 0.70
3. Dust binder	
605 gallons/acre	1.05
1210 gallons/acre	0.29 - 0.78
4. Other chemicals	
1000 lb. fiber Glass Roving with 60-150 gallons asphalt emulsion/acre	0.01 - 0.05
Aquatain	0.68
Aerospray 70, 10 percent cover	0.94
Curasol AE	0.30 - 0.48
Petroset SB	0.40 - 0.66
PVA	0.71 - 0.90
Terra-Tack	0.66
Wood fiber slurry, 1000 lb/acre fresh ^b	0.05
Wood fiber slurry, 1400 lb/acre fresh ^b	0.01 - 0.02
Wood fiber slurry, 3500 lb/acre fresh ^b	0.10
5. Seedings	
temporary, 0 to 60 days	0.40
temporary, after 60 days	0.05
permanent, 0 to 60 days	0.40
permanent, 2 to 12 months	0.05
permanent, after 12 months	0.01
6. Brush	
7. Excelsior blanket with plastic net	
	0.04 - 0.10

^aNote the variation in values of VM factors reported by different researchers for the same measures. References containing details of research which produced these VM values are included in NCHRP Project 16-3 report, "Erosion Control During Highway Construction, Vol. III. Bibliography of Water and Wind Erosion Control References," Transportation Research Board, 2101 Constitution Avenue, Washington, DC 20418.

^bThis material is commonly referred to as hydromulch.

on using the MUSLE for several alternate cover designs in order to evaluate whether the proposed analytical approach can be successfully used to measure the long-term integrity of protective soil covers for uranium tailings reclamation. Alternative designs will be compared, both from a standpoint of overall integrity and construction difficulty. The covers will also be evaluated using the critical shear stress approach to determine, based on a given PMP, the minimum particle size necessary to protect the cover against long-term degradation.